Thesis

On

EXPLORATION OF SURFACE ROUGHNESS AND PROFILE ERROR IN SINGLE POINT DIAMOND TURNING OF MOLD INSERT MATERIAL - COPPER ALLOY C18000

Submitted in the partial fulfillment of requirement for the award of the

degree of

MASTER OF ENGINEERING

IN

PRODUCTION AND INDUSTRIAL ENGINEERING

Submitted by

ANIKATE GUPTA

ROLL NO: 801182002

Under the Guidance of

Dr. AJAY BATISH

Professor & Head

Mechanical Department

Dr. S V RAMAGOPAL

Chief Scientist

CSIR-CSIO

MECHANICAL ENGINEERING DEPARTMENT
THAPAR UNIVERSITY

PATIALA-147004

JULY 2013

CERTIFICATE

I hereby declare that the work being presented in this thesis entitled "**EXPLORATION OF SURFACE ROUGHNESS AND PROFILE ERROR IN SINGLE POINT DIAMOND TURNING OF MOLD INSERT MATERIAL - COPPER ALLOY C18000**" by "**Anikate Gupta**" in partial fulfillment of requirements for the award of degree of **MASTER OF ENGINEERING** in **PRODUCTION AND INDUSTRIAL ENGINEERING** is an authentic record of my own work carried out during January 2013 to July 2013 under the supervision of **Dr. Ajay Batish** refers other researcher's works which are duly listed in the reference section.

The matter presented in this work has not been submitted to any other university/institute for the award of any degree.

Anikate

Anikate Gupta

Roll No. 801182002

This is to certify that the above statement made by the candidate is correct and true to the best of my knowledge.

Dr. S V RAMAGOPAL
CHIEF SCIENTIST
CSIR-CSIO
Scientist
ral Scientific Instruments Organisation
Chandigarh

Dr. AJAY BATISH
PROFESSOR
DEPARTMENT OF MECHANICAL ENGINEERING
THAPAR UNVIERSITY, PATIALA

Countersigned by

DR. S.K. MAHAPATRA
DEAN (ACADEMIC AFFAIRS)
THAPAR UNIVERSITY,
PATIALA.

ACKNOWLEDGEMENT

I would like to express my sincere gratitude to **Dr. Ajay Batish**, Head of Department of Mechanical Engineering, Thapar University, Patiala, for his guidance and extended help at every stage of this project work. I am deeply indebted to him for giving me a definite direction and moral support to complete the project successfully.

With deep sense of gratitude, I wish to express my sincere thanks to my supervisor **Dr. S.V. RamaGopal**, Chief Scientist, CSIR-Central Scientific Instruments Organisation (CSIR-CSIO), Chandigarh for his excellent guidance and support throughout the project work. His unique inimitable styles have left an indelible impression on me. His constant encouragement, support and review during the course of my investigation are invaluable. He helped me to acquire as well develop some of the skills and intricacies of quality independent research. I is also benefited by learning some soft skills for industrial adaptability. In fact I availed of quality time from my supervisor during my project work, for which I am very thankful to him.

Special thanks goes to Director CSIR-CSIO for his valuable guidance and providing me with an opportunity to work at the Central Scientific Instruments Organisation (CSIR-CSIO), Chandigarh.

I would like to thanks to **Mr. Anirban Bhattacharya,** (Assistant professor) Department of Mechanical Engineering, Thapar University, Patiala for his constant encouragement, support and review during the course of my investigation.

Anikate

Anikate Gupta

Roll No. 801182002

ABSTRACT

Due to rapid development of science & technology, machining of different materials and polymers is the need of the day. Surface roughness being major parameter while machining, we make use of SPDT (Single point diamond tool) with that of the regular CNC machine tool. There is great requirement of ultra-precision components with micro-structured surfaces in the fields of mechanical, medical, optical, biological engineering. Single point diamond turning is certainly superior in machining precision and intricate micro-structured surfaces in nano-domains. General errors in the single point diamond turning cause form error to the machined micro-structured surfaces. This work describes a parametric analysis of nano-surface generation in single point diamond turning (SPDT). A series of face and profile cutting experiments are undertaken on a Copper Alloy "C18000" under different machining conditions using Taguchi Method L9 (Orthogonal array). The effects of various cutting parameters such as spindle speed , depth of cut, tool feed , tool rake angle, nose radius on the surface roughness and profile accuracies of the machined micro-structured surfaces (flat and curved) of thermally conductive, ductile material copper alloy C18000 are identified and analyzed. This study presents an optimization method of the machining parameters by using design of experiment technique of Taguchi and ANOVA methods. Results are analyzed for the optimization process using S/N ratio response analysis and Pareto analysis. The use of Grey Relational Analysis for optimizing the turning process parameters for the work-piece surface roughness and the Peak to Valley is also introduced.

Key words: *Turning, surface roughness, Taguchi method, Single crystal Diamond tool, Profile accuracy*

TABLE OF CONTENTS

ABBREVIATIONS

ANOVA: Analysis of Variance.

DF: Degree of Freedom.

DOC: Depth of Cut.

DOE: Design of Experiment.

RPM: Revolution per Minute.

SS: Spindle Speed.

S/N Ratio: Signal-to-noise Ratio.

SPDT: Single Point Diamond Turning.

SEM: Scanning Electron Microscope.

TNR: Tool Nose Radius.

TFR: Tool Feed Rate.

R_a: Arithmetic Average Roughness.

P_t: Peak to Valley height (Profile error).

GRA: Grey Relational Analysis.

DF: Degree of Freedom.

LVDT: Linear Variable Differential Transformer.

µm: Micron Meter, **nm**: Nano Meter.

LIST OF FIGURES

LIST OF TABLES

CHAPTER 1: INTRODUCTION

1 INTRODUCTION

1.1 CHARACTERISTICS OF ULTRA PRECISION MACHINING TECHNOLOGY

High precision finishing methods are of utmost importance and are the need of present manufacturing scenario. The need for high precision in manufacturing is felt by manufacturers worldwide to improve interchangeability of components, improve quality control and longer wear / fatigue life **(Mc Keown 1987).** In Fig.1.1, the machining processes are classifieds into three categories on the basis of achievable accuracy viz. Conventional machining, precision machining and ultra precision machining. Ultra precision machining are the processes by which the highest possible dimensional accuracy has been achieved at a given point of time. Machining accuracies in conventional processes would reach 1μm, while in precision and ultra precision machining would reach 0.01μm (10 nm) and 0.001μm (1 nm) respectively **(Taniguchi 1983).**

Ultra precision manufacturing has become a powerful tool for controlling surface properties and sub-surface integrity of parts being manufactured. Ultra precision machining has provided different methods for the generation of freeform surfaces and complex micro-structured surfaces with unique accuracy and cost effectiveness. Application of ultra precision manufacturing ranges from automotive to medical, illumination, astronomy, optics and metrology.

In ultra precision diamond turning, the quality of a surface plays an essential role in the functional performance of a product, especially in mechanical applications. **(Sata *et al* 1985)** pointed out that the quality of surface is influenced by tool geometry, feed rate, material properties, spindle rotational errors and by the displacement between the tool and work piece (i.e. relative tool-work vibration).

One of the remarkable achievements of modern manufacturing techniques is the ability to achieve nanometer surface finish. (**Corbett *et al* 2000)** the need for superior surface finish

and close dimensional tolerances is increasing rapidly in the fields of die and moulds, semiconductors, biomedical devices, laser applications and precise machine parts. Single Point Diamond Turning (SPDT) is the most important technique used in the manufacturing of high-precision components where surface finish is critical. In this context, single point diamond turning (SPDT) offers a practicable option for surface generation with numerous degrees of freedom in terms of machinable materials, machining parameters, precision tool kinetics and machine dynamics for precision curved surface generation.

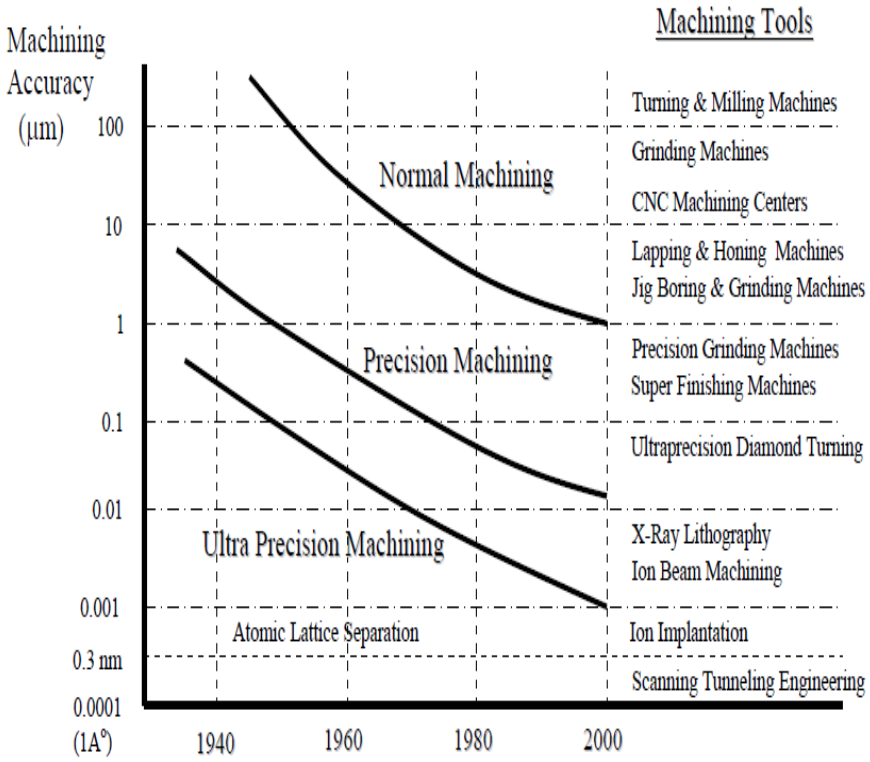

Fig.1.1: Achievable machining accuracy; (Keown, Precision Engineering, Tata McGraw-hill), (2001)

1.2 MOTIVATION

Ultra-precision machining is considered as a leading technology for the machining of advanced components. With ultra-precision machining, it is possible to achieve a form accuracy of 1µm or better and a surface finish of 10nm or lower. With the increasing demand for more advanced instruments and devices, it is obvious that more complex parts

are necessary for their fabrication. Thus, it is a great challenge for me to meet this requirement with a technology rather than the traditional machining processes. To meet this demand, ultra-precision machining is the most appropriate technology to produce complicated and intricate shapes. Apart from the ability to make complex shapes, this machining is much faster and more accurate.

1.3 SINGLE POINT DIAMOND TURNING (SPDT)

The use of special machine tools with single-crystal diamond-cutting tools to produce surfaces with nano level of accuracy is called diamond turning. This process make use of monocrystal diamond cutting tool which possesses nanometric edge sharpness and wear resistance to generate mirror-like surface of ultra-precision components. Ultra precision single point diamond turning (SPDT) is one of the most important and successful technologies in the field of precision engineering in the past several decades. SPDT is a process of very accurately cutting away a thin chip or layer of the surface under precisely controlled conditions **(Saito 1978)**. SPDT technology has already been applied in a broad range of fields from advanced science and technology for defense, energy, electronics applications to commercial and consumer products. Owing to the fast growing demand the production of different components for mechanical application, ultra-precision machining, including single-point diamond turning is employed frequently for fabrication of implicated surfaces. Diamond turning enables to control the process parameters accurately and to generate geometry of the components to a very high level of accuracy. Diamond turning is a well established process, which is used in manufacturing of high-precision components with surface roughness of few nanometers and form accuracy in the sub micron range **(Dornfeld *et al* 2008).** It has been improved to an ultra machining technology for mass production of precision part of ductile materials. The SPDT is an expensive process at the beginning of its appearance and is suitable for single piece or small volume production. When combining with mass production process such as injection molding and compression molding, the SPDT became appropriate for high quality low cost consumer products and quickly popularized among related industries.

Precision and ultra-precision machining, also termed nano and micro machining, is a new technological field which enables production of the high accuracy components, thus is tremendously important technologically and economically in modern society. High form accuracy and low surface roughness of mechanical, optical and optoelectronic components can significantly improve the quality, the range and ability of functions, and increases the intrinsic value of the final products. Ultra precision machining with diamond tool has been rapidly growing in the manufacturing of high precision machined parts for advance industrial applications **(Shimada *et al.* 1995).** The outstanding hardness and crystalline structure of diamond make it possible to fabricate components with sub micron form accuracy and surface roughness in nanometer range due to its extreme hardness and high resistance to wear. Although diamond turning technology has been established to produce components with high degree of surface finish and dimensional accuracy **(Jacob *et al.* 2005)** it is however limited by a number of materials that can be produced by diamond turning, especially in the fabrication of molds of optical components. Therefore, diamond turning of this material is a viable option for producing high quality optical surfaces without any post machining process such as polishing. This feature makes the technique economical and advantageous by reducing the overall production time for machining compared to other techniques such as grinding **(Blackley *et al.* 1991)** .Single point diamond turning is an ultra-precision techniques which is used to produce optical surfaces like (e.g. spherical and aspherical). It is frequently used for obtaining very fine surfaces on the soft materials such as Aluminium, Copper, Electroless Nickel. SPDT, however, can give optical quality together with damage-free surfaces on these brittle materials using fewer manufacturing steps than the traditional grinding and polishing methods. Several researchers have produced components with submicron form accuracy and nano level surface roughness on the variety of brittle and non ferrous materials **(Saito 1978).** The cutting tools used in single point diamond turning are very different from traditional turning ones; they must possess a nanometer edge radius. The limits of diamond turning for both figure and surface finish accuracy have not yet been reached. There are several important advantages of using diamond turning, including the ability to produce good optical surfaces to the edge of the element, to fabricate soft ductile materials difficult to polish, to eliminate alignment in some systems, and to fabricate shapes difficult to do by

other methods. Several components are manufactured with submicron form accuracy and nanometer levels surface roughness on a variety of brittle and nonferrous materials with the help of diamond turning. **(Uchindas *et al.* 1991).**

1.4 MICROMACHINING

Micromachining deals with machining of very small (micro) components. Micromachining is removal of material in the form of chips of debris having size in the range of micron. It can be considered as machining of micro components having intricate features or creating surface characteristics (especially surface finish) in the micro/ nano level **(Jain 2010).** Micromachining is a precision machining in which the machining error is extremely less in comparison to conventional machining.

1.5 DIAMOND TURNING PROCESS

Diamond turning is a preferred method for producing high-precision reflective surfaces on metals **(Zhong *et al.* 2003).** Thus, it is generally applicable to machining of ductile materials rather than to hard brittle materials. In diamond turning, both the figure and surface finish are largely determined by the machine tool and the cutting process. Single crystal diamond cutting tools and specialized machinery are used to create flat or curved surfaces with high profile accuracy, good surface finish and low sub surface damage on a variety of materials. The tool has to be very accurately moved over the profile to be generated and the edge of the diamond tool has to be extremely sharp and free of defects. The surface finish quality is measured as the peak-to-valley distance of the grooves left by the lathe. The form accuracy is measured as a mean deviation from the ideal target form.

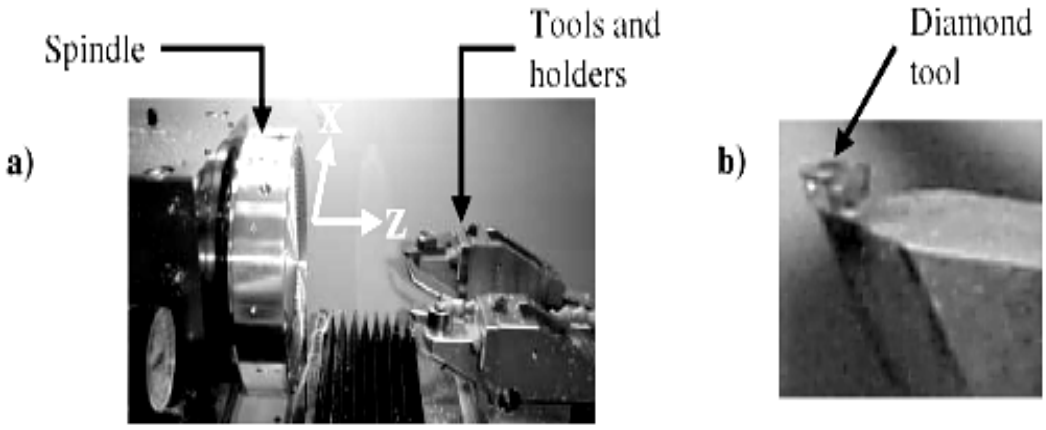

Fig.1.2: Diamond turning in progress, a) spindle and tools, b) enlarge image of the diamond tool; (Jain V.K. Introduction to Micromachining, (2010)

A schematic presentation of the diamond turning operation is shown in Fig.1.2. The material removal in SPDT is realized by the relative movement between the work piece and the cutting tool, that is, the linear movement of the machine tables and the rotation of the work piece.

1.6 OPERATING PARAMETERS OF SPDT

The operating parameters of a precision machining process on a given piece of material will vary considerably depending on the production rates required, work piece and machine characteristics, and all other process variables such as coolant, tool condition, depth of cut, tool feed rate (TFR), tool nose radius (TNR), cutting speeds, and depths of cut are typically much lower in diamond turning process compared to turning with conventional machining tools **(Sanger 1987)**. For a given material, under different combinations of machining parameters (within their optimum range), similar surface figure and finish results can often be obtained. It is most common to use the distance per revolution as it is directly related to the theoretical surface finish. For a given TFR, larger the tool nose radius, the better the optical surface finish. Surface quality depends to a great extent on the material characteristics like: grain size, microstructure of crystal boundary, crystal uniformity, annealing procedures etc.

1.7 TOOLS FOR SPDT

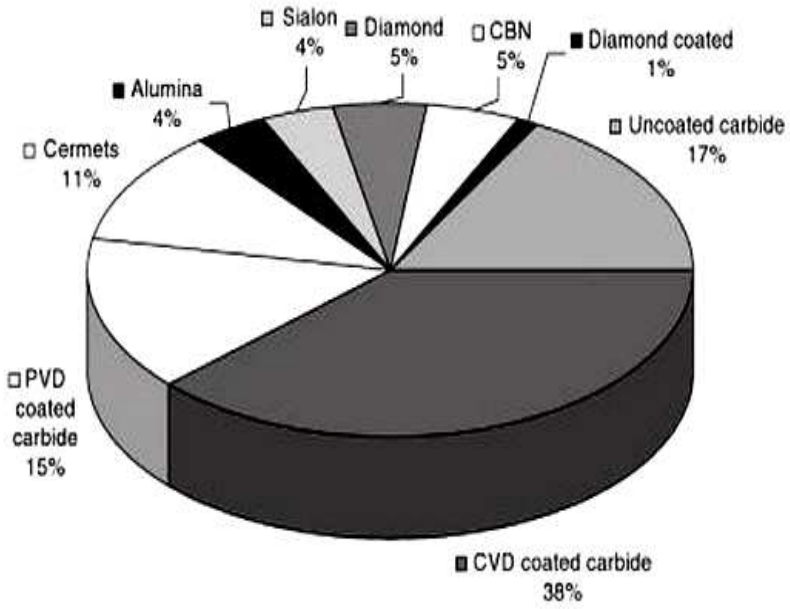

Fig.1.3: Tools used in SPDT Machine; (Mc Keown, Precision Engineering, Tata McGraw-hill), (2001)

SPDT utilizes a solid, flawless diamond as the cutting edge. The single crystalline diamond can be natural or synthetic, and is sharpened to the desired dimensions by mechanical grinding and polishing.

SPDT is a very accurate machining process used to create finished curvatures without the need for further polishing after completion. The generation of optical quality surfaces with high degree of form accuracy and surface finish depends on the three major factors viz. accuracy and rigidity of the machine, dynamics of machining and quality of cutting tool.

1.8 REQUIREMENTS OF SPDT TOOLS

Tool acts as wedge and penetrates into the work piece removing some material, providing the desired shape and surface quality. Tools material much harder than the work piece material is the prerequisite; by employing proper relative motion between the work piece and cutting edge, the desired shape of the component is obtained.

The critical requirements of the material processing tools are:

a. Strength
b. Hardness and hot hardness
c. Heat conduction
d. Wear resistance
e. Toughness

Table 1.1: Properties of diamond

Property	Value	Remarks
Hardness	8200-8500 Knoop	Hardest
Thermal conductivity	9-26W/cm/c at 20^0C	High
Coefficient of friction	0.08 in air	Low and high varies with direction of polishing
Thermal expansion	$0.8\pm 0.1* 10^{-4}$ at 20^0C	low
Density	3.15-3.53 gm/cc	High

The crystalline structure of single crystal diamond enables sharp cutting edge to the tune of 5 nm; its high conductivity, its ability to retain high strength at high temperatures leading to very less wear and high elastic and shear modulus which reduce deformation during machining make it suitable for SPDT applications. Due to high hardness, low thermal expansion and low frictional values make the diamond one of the most suitable for SPDT.

1.9 DIAMOND TURNING – CONVENTIONAL FABRICATION

In diamond turning, the final shape and surface of the component produced depends on the machine tool accuracy, whereas, in traditional optical fabrication, the final shape and surface of the optical element are produced by lapping and polishing. Feeds, speeds, and depth of cut are typically much lower in diamond turning than conventional machining, thus giving lower forces **Rhorer *et al.* (2010).**

Table 1.2: A Comparison between Conventional and Ultra-precision machining; (Cheung 2000)

Types of Process		Conventional Machining		Ultra-precision machining	
		Rough cut	**Finish cut**	**Rough cut**	**Finish cut**
Cutting conditions	**TFR (mm/rev)**	0.1-1	0.01-0.05	0.01-0.05	0.005 - 0.001
	SS (rev/min)	100-300	200-300	1000-2000	2000-3000
	DOC	0.1mm – 1mm	0.01mm – 0.1mm	10µm-50µm	1µm-5µm
	Tooling	HSS Carbide tool Ceramic tool		Single crystal diamond tool	
Part Quality	**Roughness (µm)**	10µm - 100µm	1µm -10µm	0.02µm-0.03µm	Less than 0.01µm
	Form Accuracy	1mm -0.5mm	0.01mm-0.005mm	1µm -2µm	0.3µm-0.5µm

Table 1.3: Comparison of diamond turning and traditional optical fabrication Rhorer *et al.* (2010)

CONVENTIONAL METHOD	SPDT
Force-controlled-process.	Displacement controlled process
Final shape and finish depend on lap &polish time, slurry composition.	Final shape & surface accuracy depend On M/c & tool Accuracy, RPM, depth of cut, tool feed rate & rake angle, job hardness, tool control mechanism etc.
Force is distributed over the whole area.	Force is concentrated over turning groove.
Surface roughness is in terms of scratches	Surface roughness is periodic.

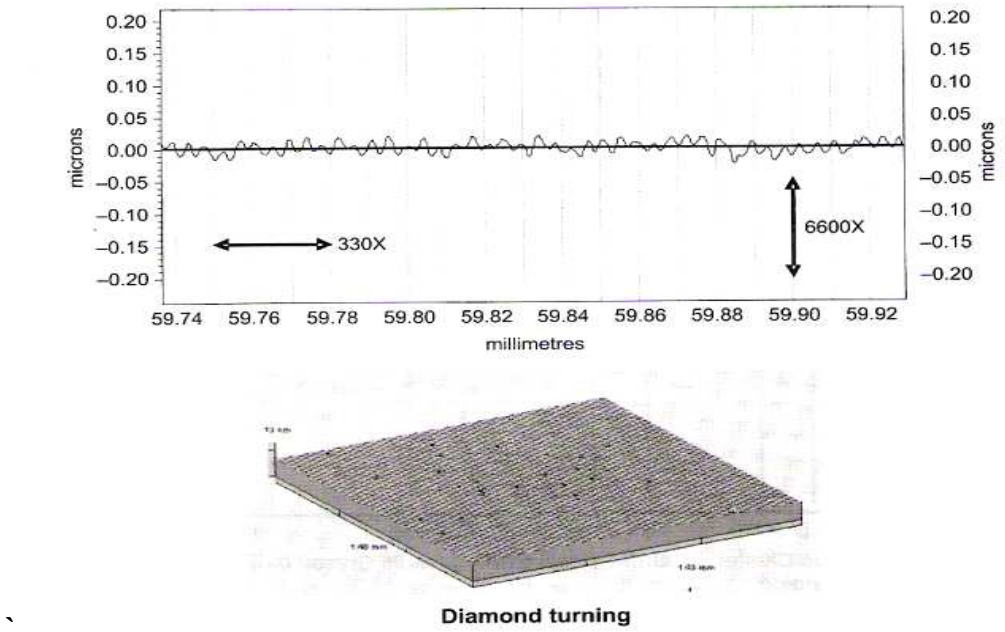

Fig.1.4: 2-D micro graphs and 3-D topography of the surface generated by SPDT (Jain V.K. (2010), Introduction to Micromachining)

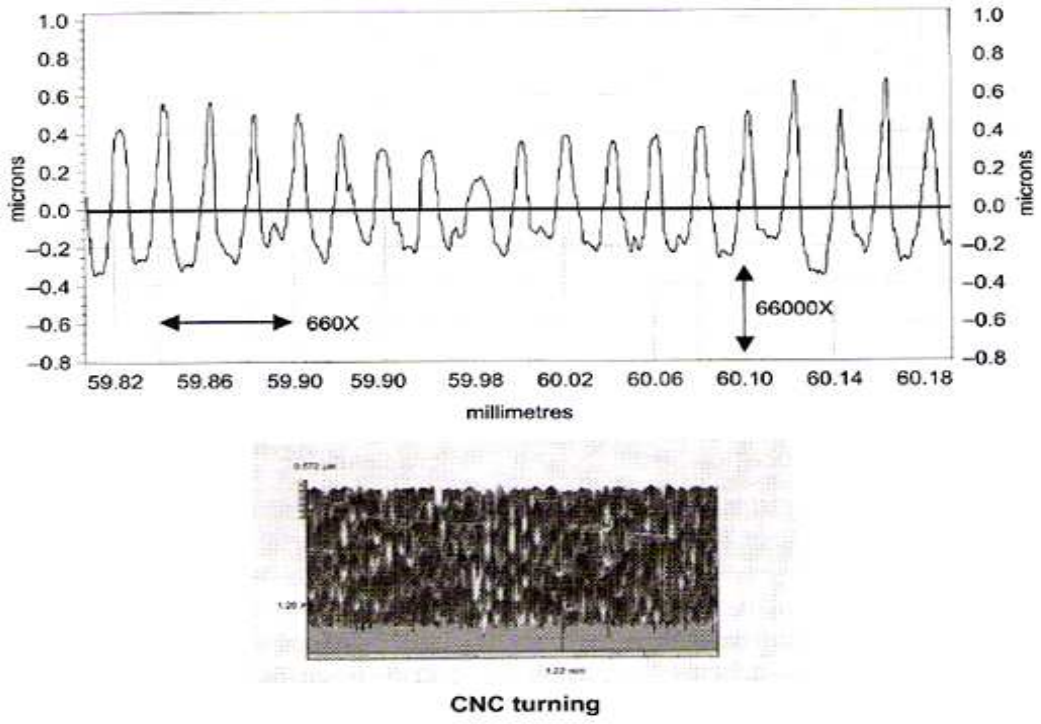

Fig.1.5: 2-D micro graphs and 3-D topography of the surface generated by CNC; (Jain V.K. Introduction to Micromachining), (2010)

1.10 DIAMOND - TURNABLE MATERIALS

Some materials just wear out the diamond-turning tools at a much faster rate than other materials do. For example, it is commonly known that ferrous materials rapidly wear diamond tools. Some tests have been made using different methods of diamond-turning ferrous materials to decrease wear rate that show some encouraging results. These methods include operating at:

1. Cryogenic temperatures.

2. In methane and acetylene environments.

3. And by ultrasonic vibration of the tool.

Many non-ferrous materials such as aluminum, copper, electro less nickel can be machined by diamond turning. Additionally, several polymers and crystals are also suitable for diamond turning. Polymers/plastics, the common diamond turnable materials are polycarbonate, poly methyl meth acrylate, polystyrene and nylon. The crystalline materials which can be successfully diamonds turned are: germanium, zinc solenoid, lithium niobate and silicon.

Table 1.4: Diamond tunable materials

METALS	POLYMERS	CRYSTALS
Aluminum alloys	Acrylic	Germanium
1100,2011,2107,2024,3003,	PMMA	Zinc sulfide
5086, 5186, 6061, 7075, A201	Polycarbonate	Zinc selenide
Cast.	Lexan	Calcium fluoride
Copper(OFCH, electroplated)	Polystyrene	Barium fluoride
Beryllium copper	Copolymers	Silicon
Brass	NAS	Cadmium telluride
Sliver	SAN	
Gold	CR-39	
Zinc	TPX	
Nickel (electro less plate)		

1.11 ADVANTAGES OF DIAMOND TURNING

There are several important advantages of using diamond turning, including the ability to fabricate soft ductile materials difficult to polish such as off-axis parabolas, to eliminate alignment requirement in some systems, and to fabricate shapes difficult to generate by other methods **Riedl (2001).** Other developments include application of fast tool servo and free form machining to generate complicated 3-dimensional surfaces.

1.12 DIAMOND TURNING – APPLICATIONS

The superior surface finish and form accuracy of SPDT allow the technology to be widely applied for manufacturing a variety of dedicated mechanical and optical parts. Applications are now seen in the manufacturing of inserts for injection-moulding plastic lenses of camera, scanner mirrors, photoconductor drums in copiers and substrates for memory disks ,metal mirrors for optical welding monitor systems, motor scanners for the inspection of printed circuit boards etc. Some applications of diamond turned components are listed in Table 1.5 most of them fall under the category of optics **(Smith *et al.* 1988)**. Some diamond turned components as shown in Fig.1.6. The application area of DTM ranges from drum for photocopy machine to metallic mirrors for astronomical telescopes missile cone to optical elements for night vision camera.

The current precision and ultra precision machining is widely used (from micron to submicron and even nano-regions) in automobile industry, constructions appliances, electronics, strategic sector, civilian applications. Similarly, precision and ultra precision machining technology has also contributed to the critical modules in multiple S&T areas, sensors and measurement technology and metal processing industries. Ultra-precision machining techniques are successfully adopted for the manufacture of computer memory discs used in hard drives, and also photoreceptor components used in many photocopier machine and printer applications. Such applications required extremely high geometrical accuracies to be achieved, in combination with super smooth surfaces. These surfaces are found to be most effectively manufactured by single point diamond turning,

Service Areas

- Freeform design
- Prototype manufacture
- Precision mould design and manufacturing
- Injection moulding of plastic optics
- Surface quality evaluation

Examples of applications of SPDT are found in the manufacturing of: **(Riedl 2001)**

- Inserts for injection-moulding plastic lenses of box cameras;
- Ultra-precision moulds in electroless nickel plated, brass and other non-ferrous metals;
- Free-form surfaces;
- Complex s infrared lenses and domes in germanium, silicon, zinc sulfide, zinc selenide and other crystals;
- Reflective mirrors in copper, gold, silver, electroless nickel and aluminium alloys;
- Scanner mirror, photoconductor drums in copiers and substrates for memory disks;
- Lenses, windows and prisms in an assortment of polymers (e.g. PMMA);

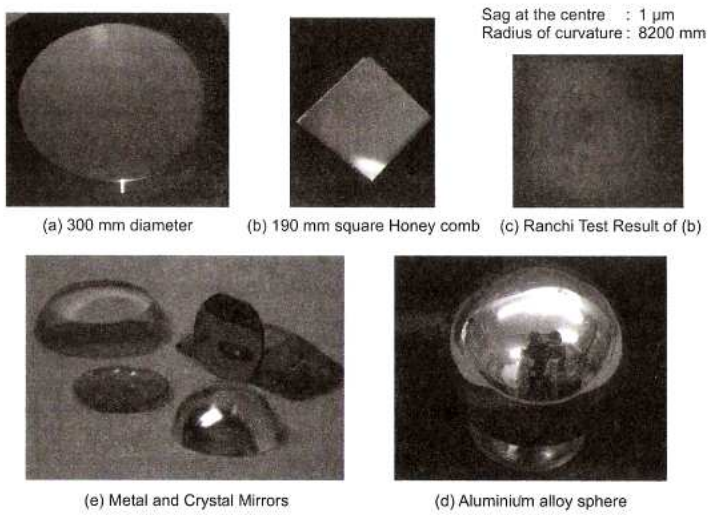

Fig.1.6: Diamond Turned Components; (Jain V.K. (2010), Introduction to Micromachining)

Table 1.5: Applications of diamond turning

Aspheric lenses and mirrors Cylindrical lenses Fresnel surfaces Diffractive optics Off –axis paraboloids Axicons Polygonal mirrors	Aluminum substrate for compact discs Projection TV lenses Molds for lens manufacturing Injection molds Faceted optics Missile cone Contact lenses

1.13 LIMITATIONS OF SPDT

There are always limitations for any manufacturing process, and SPDT is no exception. SPDT is not a perfect solution. As already mentioned, there are materials that cannot be diamond turned, for example, iron, steel, glass, silicon carbide, and tungsten. For compatible materials, however, diamond-turning technology continues to improve. There are, of course, many more applications suitable for SPDT, but the material presented here indicates clearly how powerful and cost-effective this technology can be if fully exploited.

1.14 FACTORS AFFECTING SURFACE ROUGHNESS

Many researchers have investigates the factors which significantly affect the surface quality. Most of the research work on surface generation in metal cutting is focused on geometrical and process aspects. The factors affecting the quality of the machined surface can be categorized into process factors and material factors as described in Table 1.6.

TABLE 1.6: Parameters for different material using diamond tool; (Cheung *et al* 2001)

<table>
<tr><td rowspan="3">Process factors</td><td rowspan="3">Can be minimized/eliminated through a proper selection of operational setting and better control of the dynamic characteristics of the machine</td><td rowspan="3">Cutting geometry and dynamic features of a cutting system</td><td>Cutting conditions(e.g. spindle speed, feed rate, Doc)</td></tr>
<tr><td>Tool geometry</td></tr>
<tr><td>Relative tool-work vibration</td></tr>
<tr><td rowspan="3">Material factors</td><td rowspan="3">Cannot be minimized solely by the optimization of process parameters and machine design</td><td colspan="2">Material anisotropy</td></tr>
<tr><td colspan="2">Material swelling</td></tr>
<tr><td colspan="2">Crystallographic orientation</td></tr>
</table>

1.15 STATISTICAL PARAMETERS FOR ROUGHNESS EVALUATION

If the surface is measured with an instrument that produces a profile such as by mechanical profiler, several different statistical methods can be used to describe the surface. Historically, the most common method of surface measurement has been to mechanically measure the variation of height of the surface along the line across the surface **(Whitehouse 1988).**

1.16 SURFACE ROUGHNESS

Surface finish is the allowable deviation from a perfectly flat surface that is made by some manufacturing process. All machining processes will produces some roughness on the surface. This roughness can be caused by a cutting tool, cutting rate and environmental conditions and the type of material. Texture produced by a machining process covers the whole surface, so ideally it should be assessed over the total area. Random scratches or marks may be present on any surface even if not part of the manufacturing process; these could be caused by bad control of swarf or handling afterwards.

Roughness average Ra is the arithmetic average of the absolute values of the roughness profile ordinates.

$$Ra = \frac{1}{l}\int_0^l |z(x)|\,dx$$

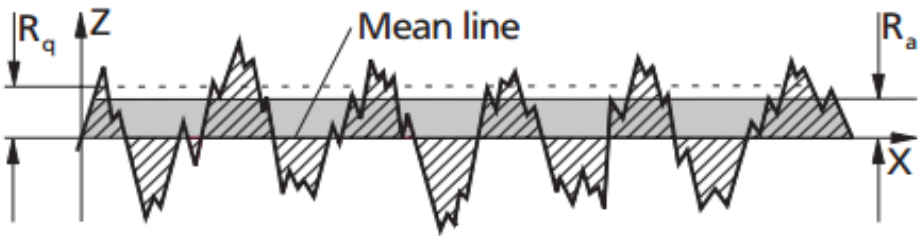

Fig.1.7: Surface characteristics

Profile depth Pt (total height of P-profile) is the sum of the largest profile peak height and the largest profile valley depth of the P-profile within the evaluation length ln (reference length). The reference length has to be stated.

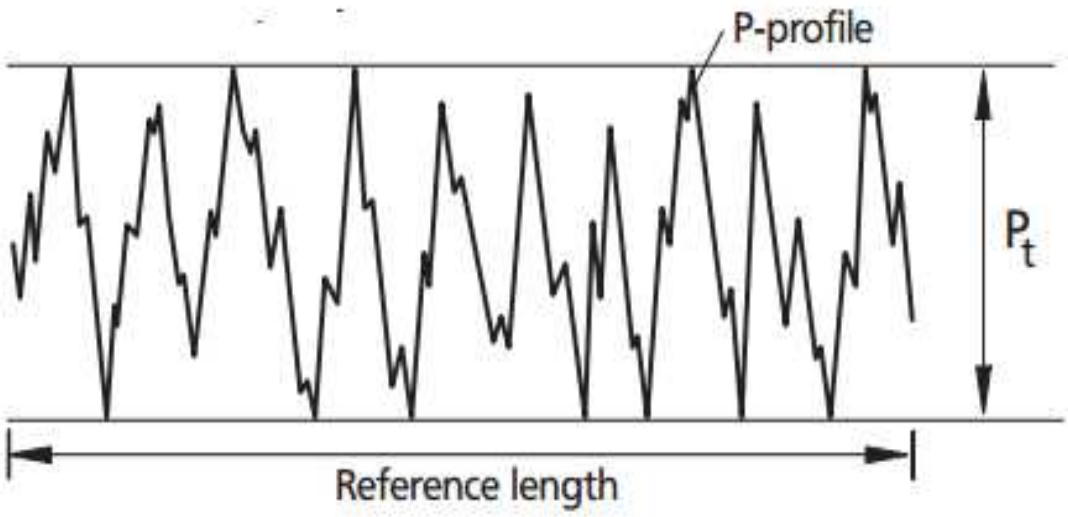

.

Fig.1.8: Surface characteristics

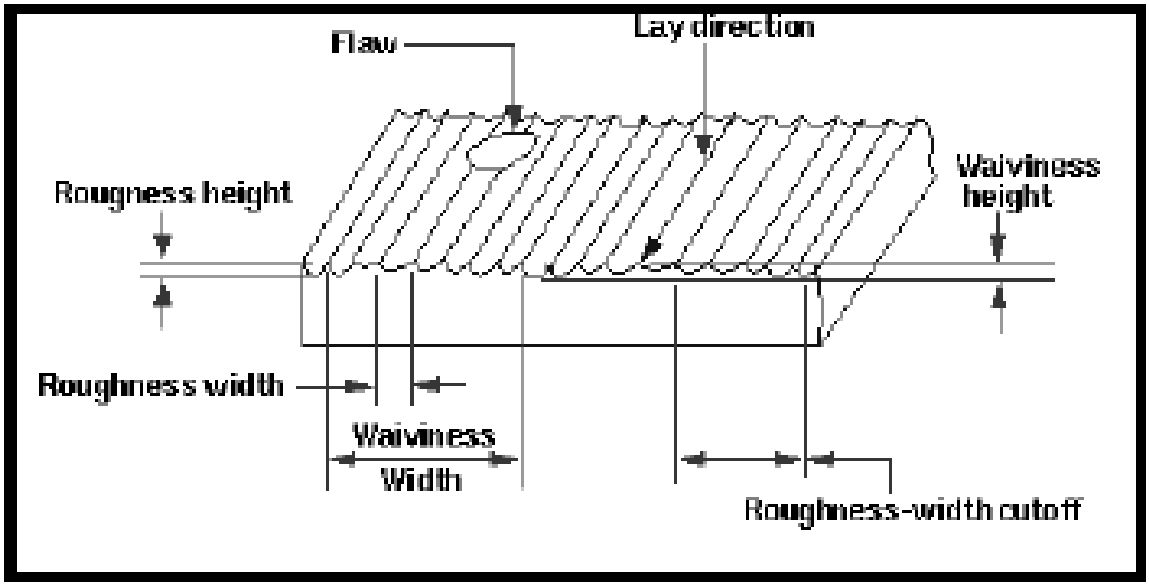

Fig.1.9: Surface texture

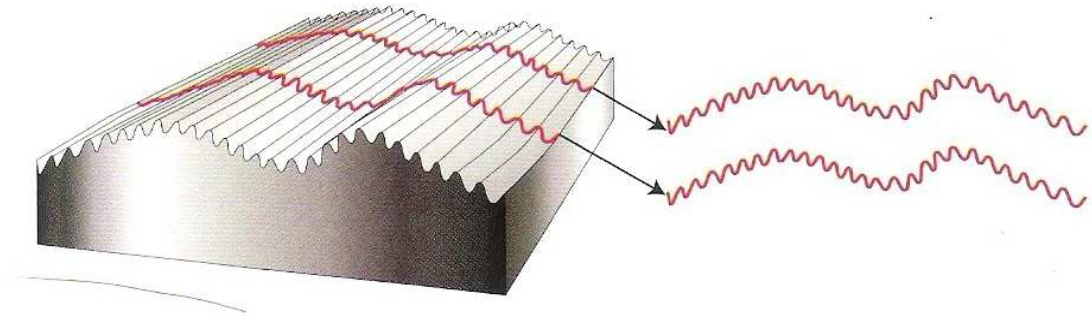

Fig.1.10: Parallel traces across a turned surface; (Mc Keown, Precision Engineering, Tata McGraw-hill), (2001)

1.17 THEORETICAL SURFACE TOPOGRAPHY

In single-point diamond turning, there are two types of generated surface that are well described. One is the tool-edge cut surface caused by the tool edge; another one is the tool-nose cut surface caused by the tool nose. Fig.1.11 demonstrates both the ideal tool-edge cut profile and the ideal tool-nose cut profile. These are similar to that of conventional turning as shown in Fig.1.11. The primary cutting edge surface in conventional turning is

like the tool-edge cut surface in SPDT while the secondary edge surface in conventional turning looks like the tool nose cut surface in SPDT.

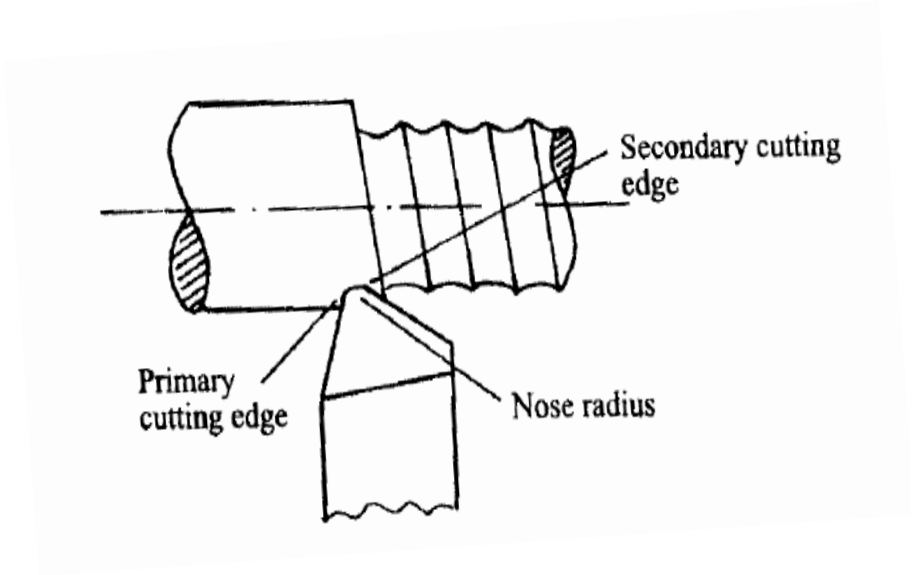

Fig.1.11 (A): Conventional axial turning indicating primary and secondary cutting edges; (Cheung 2003)

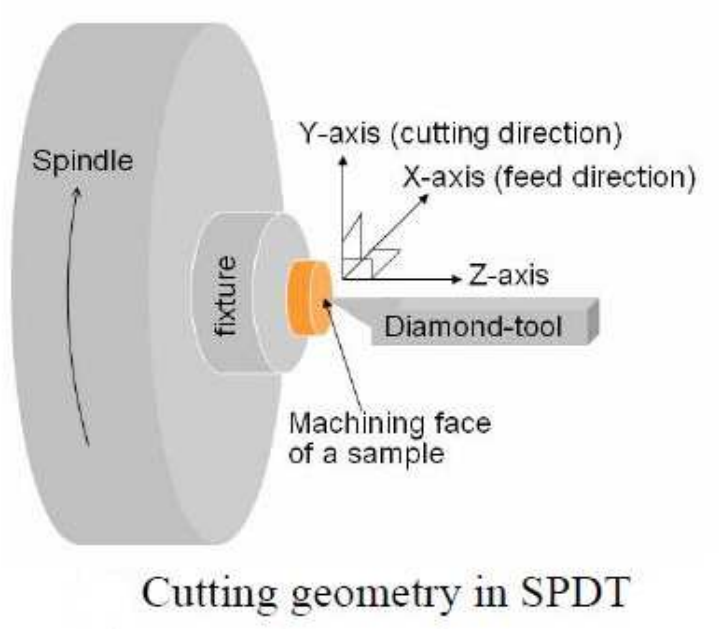

Fig.1.11 (B): Cutting geometry in single-point diamond turning; (Cheung 2003)

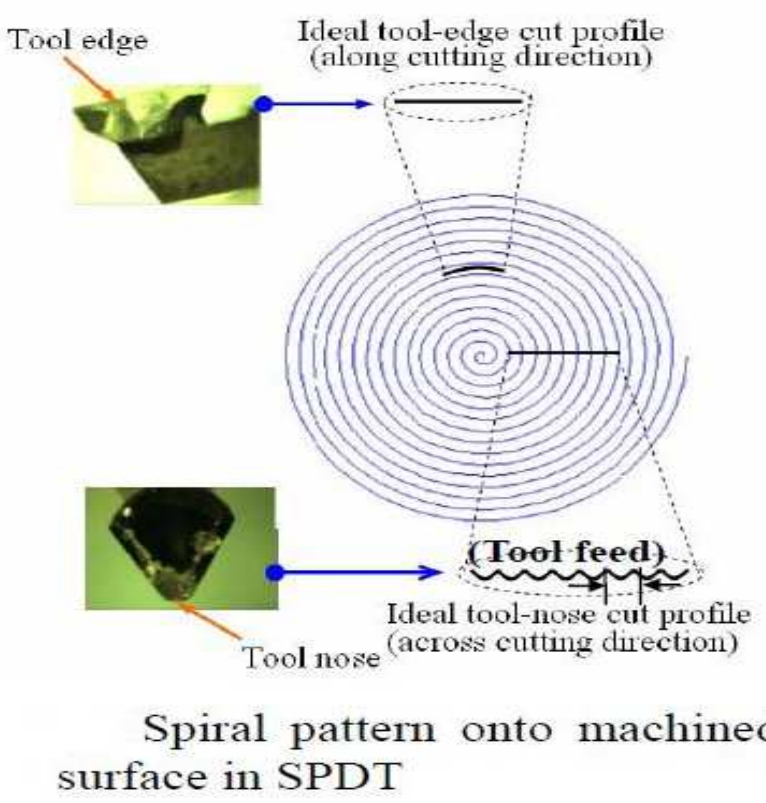

Fig.1.12: Illustration of theoretical tool-edge cut and tool-nose cut surface in SPDT; (Cheung 2003)

In diamond turning cutting is done at a very high speed in a range of thousands (usually 1000 rev min^{-1} to 5000 rev min^{-1}). Thus no build –up edge (BUE) occurs **(Cheung *et al* 2002).**

The SPDT process creates a periodic grooved surface being machined. Figure 1.13a is a greatly magnified schematic view of a localized contour of the turned surface in a machine functioning in a facing operation. Figure 1.13 illustrates this operation. The inherent roughness of the substrates surface before SPDT is depicted at left in Fig.1.13 a. The diamond tool has small curved nose of radius R. the motion of the tool across the surface creates parallel grooves as indicated on the right of that figure. The theoretical P-V height *h* of the resulting cusps is given by the following equation involving the parameters designation in Fig.1.13 b.

$$h = f^2/8R$$

Where f is the transverse linear feed of the tool per revolution of the surface

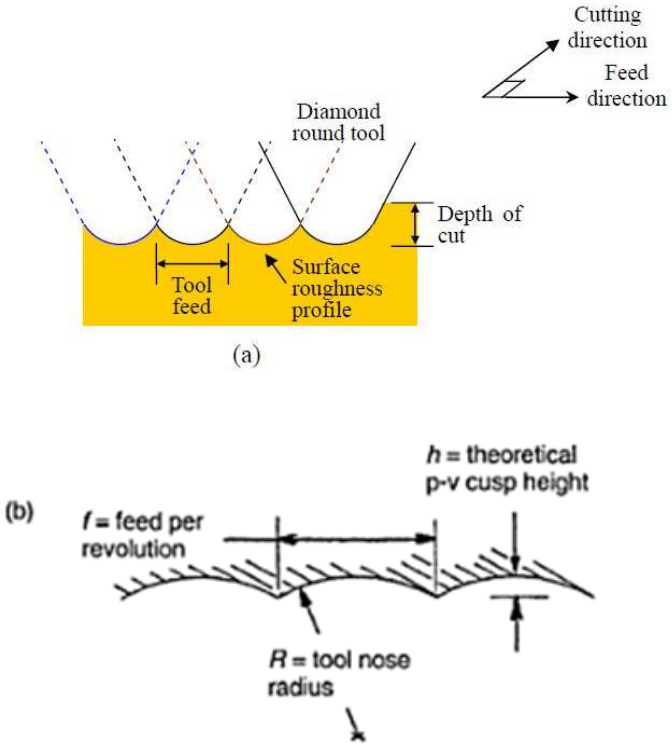

Fig.1.13: Schematic diagrams of (a) a single point diamond tool advancing from right to left across the surface of a substrate and (b) the geometry of the surface before (left side) and after (right side) passage of the tool on the SPDT process; (Cheung 2003)

1.18 SURFACE CHARACTERIZATION

Surface characteristics can be complex as one can see in Fig.1.14 roughness; waviness and form can exist in combination. Very few surfaces are molecularly smooth. In metals, grains areas will produce troughs and ridges in the order of 0.01µm. These irregularities are extremely fine compared with the texture form machining and some instruments with lesser sensitivity will not detect them.

This complex texture is the main reason why so many parameters have been proposed to quantify the various features **(Whitehouse 1994).** Surface finish is generally broken up

into three components such as roughness, waviness, and form. All three surface finish components exist simultaneously. They simply overlap one another.

It is impossible to say, at what point does finish error becomes figure error. It is better to separate finish, figure and form error according to their cause, as this relates to the performance factors. Roughness is due to the irregularities which are inherent in the production process (e.g. cutting tool, and feed rates). The roughness also depends on the material composition and heat treatment. Figure error or waviness may result from vibrations, chatter or work piece deflections and strains in the material. Form error is the general shape deviation of the surface from the intended shape, neglecting variations due to roughness and figure error.

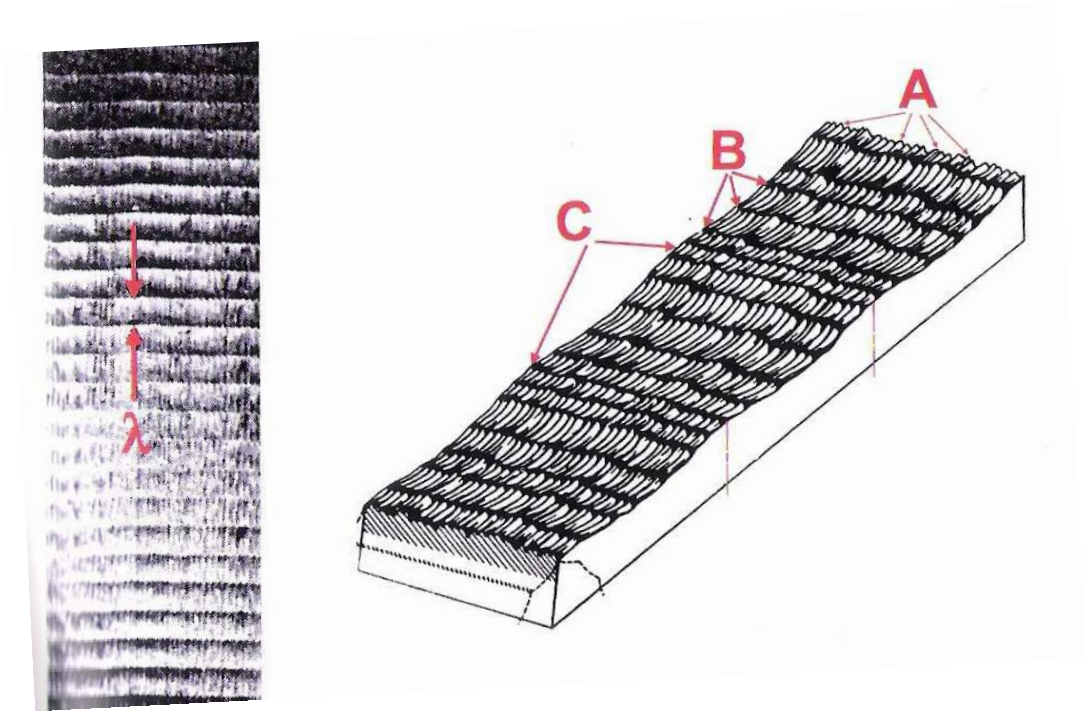

Fig.1.14: Milled surface

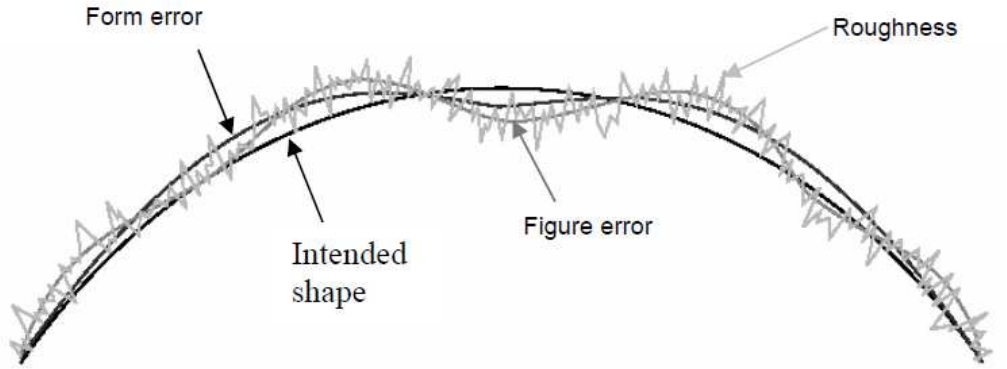

Fig.1.15: A surface profile represents the combined effects of roughness, waviness and form; (Whitehouse 1994)

In ultra-precision contour machining with a round nose tool, the profile accuracy of the cutting edge is a prime factor affecting the form accuracy of the machined surface.Surface metrology is the measure of deviation of work piece from its intended shape (the shape specified on the drawing). Profile error is explored by DIFFSYS software to generate a new tool path to reduce the error.

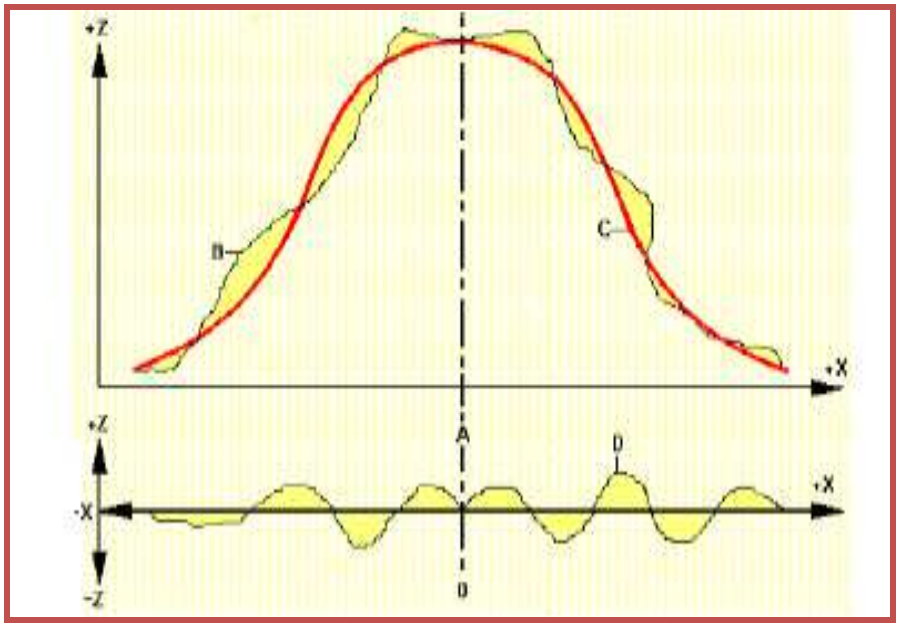

a – actual profile obtained **c – desired profile**

Fig.1.16: Analysis of Profilometers

1.19 SOURCES OF ERROR IN THE SPDT PROCESS

Surface figure errors in SPDT-generated surfaces are typically caused by a number of different setup and process errors. Error sources include: **(Richard *et al.* 2003)**

1. Misalignments between the cutting tool or the machine slides with respect to the spindle,
2. Thermal effects from the fabrication process,
3. Uneven tool wear,
4. Centripetal Distortion

TOOL DECENTRE ERROR

If at the vertex of the generating curve the tool is not coincident with the rotational axis of the work piece, then a tool setup error is present. The horizontal component of tool decentration with respect to the spindle axis or axis of rotation is usually called tool offset and the vertical component is generally referred to as tool height error. If tool offset exists, an aberration known as Ogive error is generated in the turned spherical surfaces. Figure 1.17 shows two forms of Ogive error generated on convex spherical surfaces.

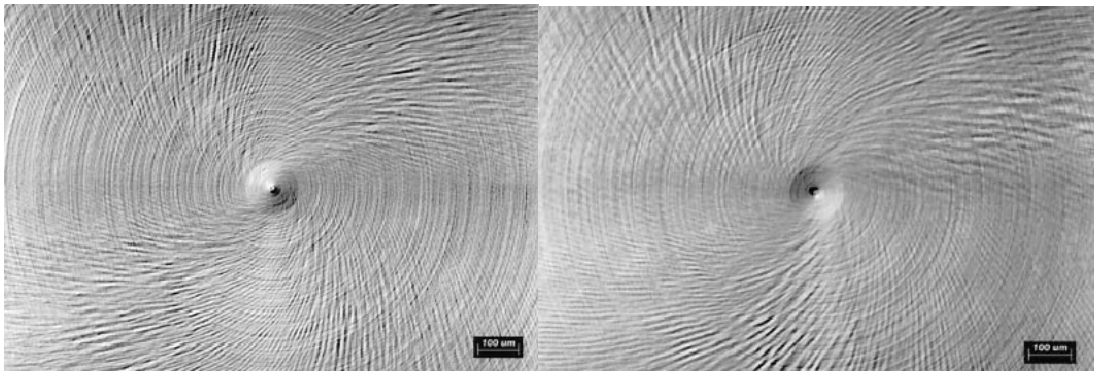

(A) **(B)**

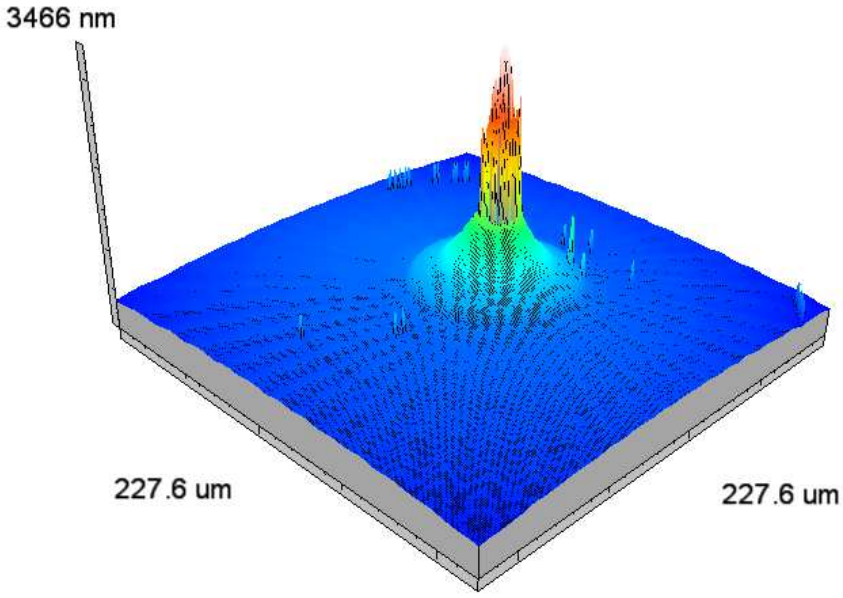

(C)

Fig.1.17: Decentring error: A) X- Offset; B) Z-offset (Richard *et al.* 2003), C) CCI image - tool

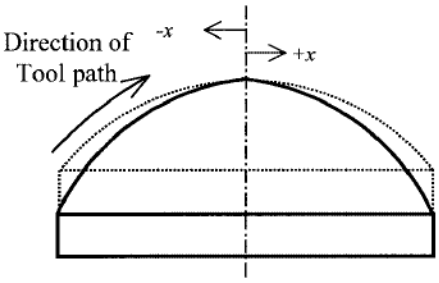

(a) Tool Offset +*x* µm

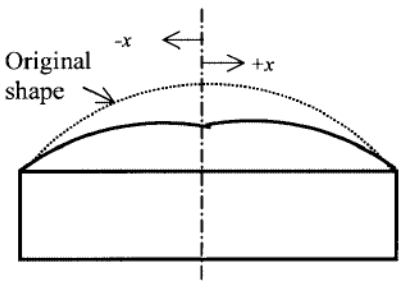

(b) Tool offset -*x* µm

Fig.1.18: Ogive error generated on convex spherical surfaces. (Richard *et al* 2003)

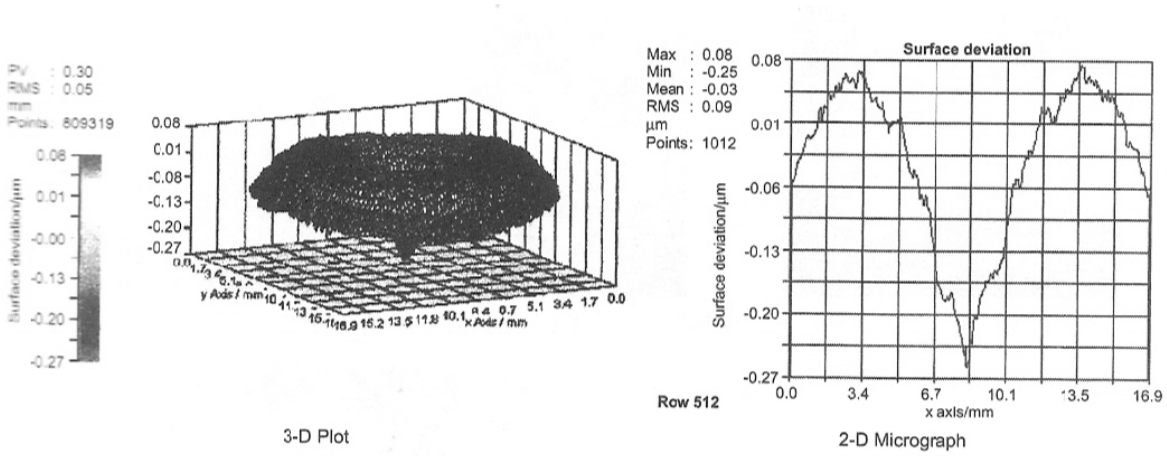

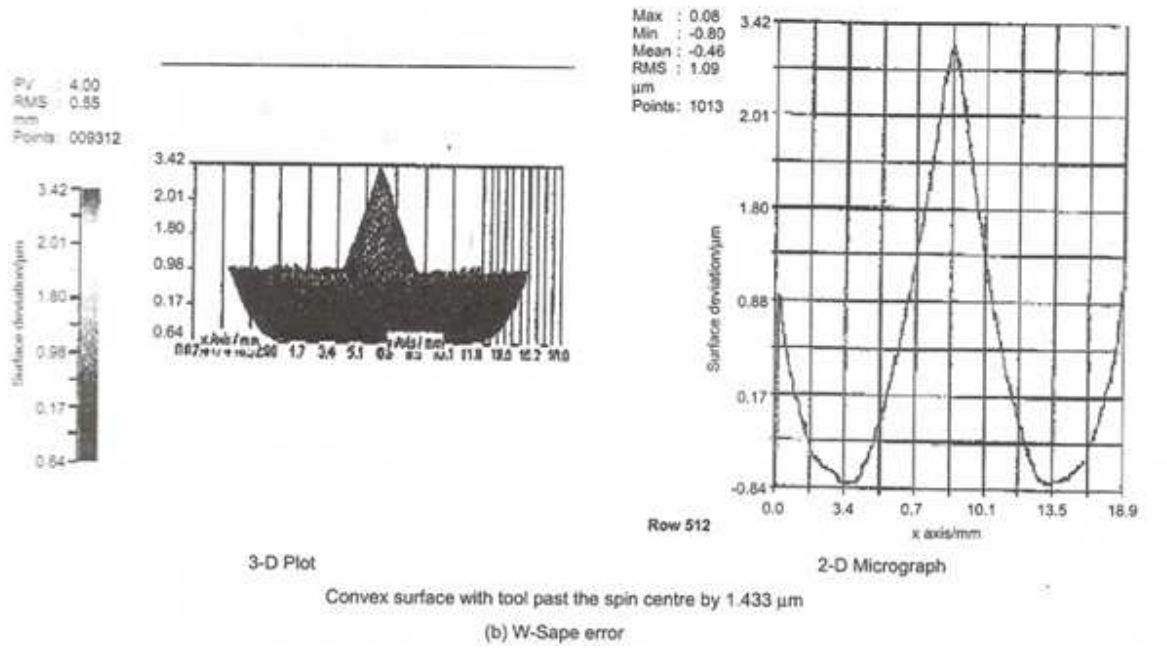

Fig.1.19: M and W- shape errors due to X- centering errors; (Richard *et al.* 2003)

UNEVEN TOOL WEAR

During the cutting process of curved profile the cutting point of tool changes continuously. In this case, the cutting edge roundness will govern the achievable form accuracy of machined surfaces. It is easy to understand that tool wear will also cause the loss of the original profile accuracy of the cutting edge unless the wear rate is even within the

working range of the cutting edge. The loss of original cutting-edge accuracy and the fluctuation in cutting force will degrade the machining accuracy. The peak-to valley (PV) value of the surface generated by a new tool is 0.14µm. However, this value changed to 0.26µm after 10km is cut by the tool. The surface roughness is found to be little affected by tool wear under the cutting conditions used in this test the profile accuracy of the cutting edge is a prime factor affecting the form accuracy of the machined surface.

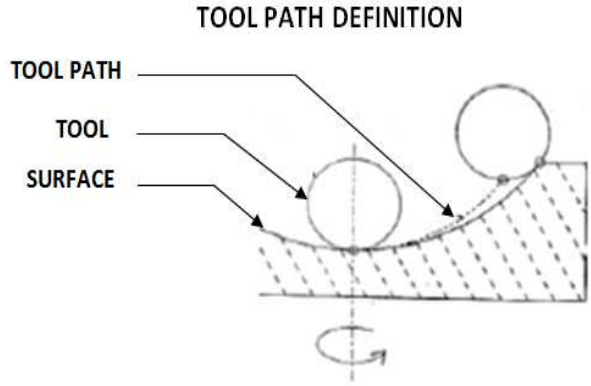

Fig.1.20: Generation of form error; (Richard *et al.* 2003)

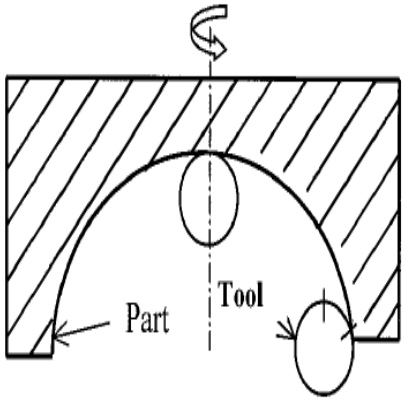

Fig.1.21: Changing of cutting point along tool edge; (Richard *et al.* 2003)

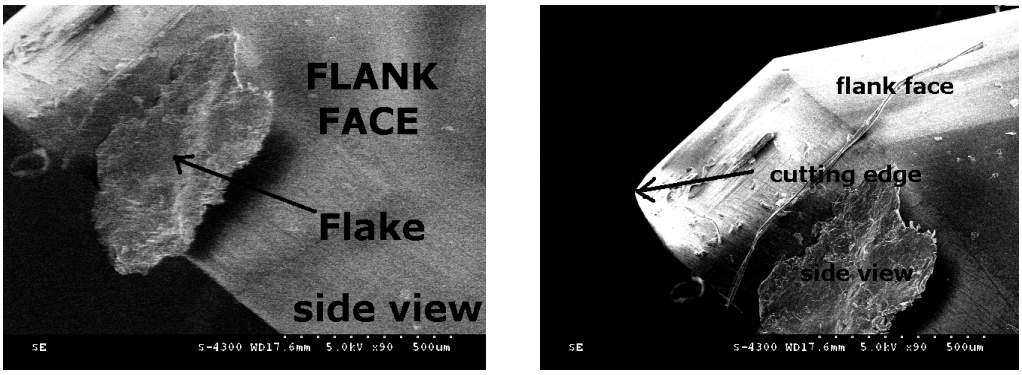

Fig.1.22: SEM photograph of tool wear; (Richard *et al.* 2003)

Tools employed on standard machines have cutting edges with few microns of waviness and sharpness. When such tools travels on the work piece, the errors in the cutting edge and the wear of the tool are transferred to the contour being machined and reduce tool sharpness results-in ploughed surfaces.

SLIDE TILT ERROR

If the machine slides are tilted with respect to the spindle, a figure error resembling a cone will be created on aspheric surfaces (if the surface is spherical, slide tilt error takes on the same form as tool Decentre error). The effect of this is shown in Fig.1.23, the figure on the left is the interferometric representation of this error; the figure on the right is the surface error.

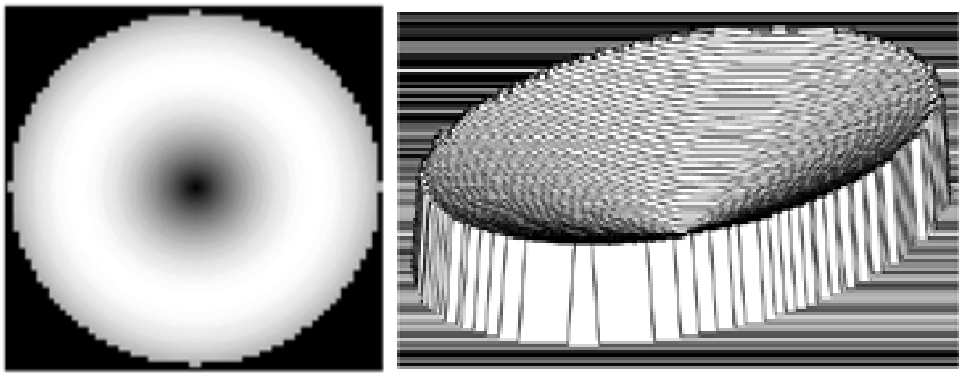

Fig.1.23: Surface error caused by slide tilt; (Richard *et al.* 2003)

THERMAL EFFECTS

Uneven cooling of the machine tool or part during fabrication can cause rotationally symmetric ripples across the surface. This is shown in Fig.1.24. The figure shows the surface error.

Fig.1.24: Surface error caused by uneven cooling of the machine or the part during fabrication; **(Richard *et al.* 2003)**

SPINDLE VIBRATION

Small vibrations in the spindle during fabrication can create azimuthally ripples on the surface. This is sometimes referred to as “Spindle star.” It can also be caused by imbalance of the work piece on the machine; this is more often seen on older spindles than on newer ones.

A properly designed spindle generally produces little or no spindle star. The size and location of the air bearing orifices can cause axial oscillations of the spindle; however, newer spindles all have continuous air slots that virtually eliminate this source of error. Spindle star is shown in Fig.1.25.

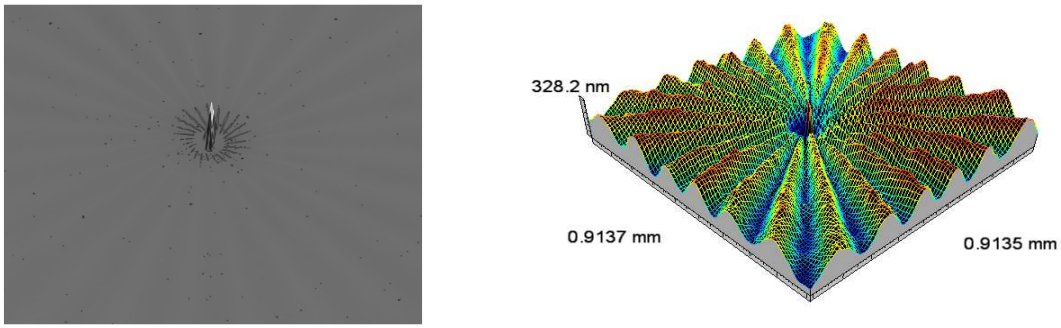

Fig.1.25: Surface error caused by spindle vibration (Spindle Star)

CENTRIPETAL DISTORTION

Centripetal distortion is caused by the rotation of the part on the machine. The rotation of the part can cause the outer portions of the surface to flatten out during the cutting process. When the rotation is stopped, the part springs back and the result is like the reverse of a rolled edge. This is most likely to happen to larger parts that are relatively thin, such as mirrors, or on off-axis parts where the segment being fabricated is only the off-axis part rather than the whole parent surface. The amount of centripetal distortion that occurs is a function of the rotation speed, the thickness of the part, the stiffness of the material, and the mounting technique of the part on the SPDT machine.

CHAPTER 2: LITERATURE SURVEY

SPDT (Single point diamond turning) is a deterministic machining process for the generation of the high quality surface texture. Diamond tools are used on SPDT for the machining of non ferrous materials. The major criterion for the acceptance of the work material is the surface texture values e.g. Ra (Surface roughness), Pt (Peak To valley) Form error etc to be within the tolerance limits. In this chapter, the research paper has been classified into three different categories, i.e. (i) papers related to the diamond tool requirement, (ii) surface finish improvement and (iii) Profile error minimization.

2.1 Overview Based on Tool Geometry on SPDT

Weck *et al.* (1988) investigated that the tool geometry is determined primarily by the shape of the profile being machined. When profiling operation is carried out, the cutting point on the tool cutting edge which is on contact with the surface being machined continuously changes. The machine controllers are programmed for components profiles and necessary tool path is calculated considering the tool nose radius. In case of any deviation in the tool nose radius, it is not considered by the controller and error in tool path is generated. The inaccuracies on the cutting edge profile (waviness) are also transferred to the component. Sharpness of the cutting edge plays a significant role on the quality of the surface being machined. Sharper tools results in better surface integrity including higher surface finish, lesser residual stresses, lesser sub surface damages, etc. Single crystal diamond can be sharpened to the theoretically minimum of 5nm.

Meng *et al.* (2004) investigated the effects of tool nose radius and tool wear on residual stress distribution in hard turning of bearing steel JIS SUJ2. Three types of CBN tools with different nose radius (0.4, 0.8 and 1.2 mm) were used and result revealed that the increase of the tool nose radius leads to an increase of the thrust force greatly. The ratio of the thrust force to cutting force and the ratio of the thrust force to feed force increase with the increase of the tool nose radius. There exists a tendency that the residual stresses induced at the machined surface shift from compressive stress to tensile stress as the nose

radius increases in the cutting condition of this study. The effect of the nose radius on the residual stress distribution decreases greatly with the increase of the tool wear.

Rahman *et al.* (2003) observed that the geometry and size of the surface to be machines and the quality of the surface dictates the size of the tool nose radius. Smaller tool nose radius makes lesser contact length on the component during machining; when smaller tool nose radius is used, the concave geometry on the component permits tool travel over a shorter cutting edge length whereas larger tool nose radius permits longer cutting edge length of too. Application of larger tool nose radius in such situation leads to transfer of larger error to the machines surface unlike smaller tool nose radius. Larger tool nose radius results in larger chip width and subsequently larger cutting forces resulting-in chatter and vibration effects deteriorating the quality of the machined surface.

Ramesh *et al.* (2005) observed that the inaccuracy of the tool is directly reflected on the components; when extremely accurate and rigid machines are used with better process control, inaccuracies of the tool significantly affects the quality of the surface generated. Hence, factors like quality of the tool, its ability to retain sharpness over a long period of time, its interaction with the work piece and tool setting accuracy need special attention while selecting tools for DTM. Performance of the diamond tool depends primarily on the strength and quality of the cutting edge. Single crystal diamond tool having (110) as the rake surface which is parallel to the top surface of the shank and (100) perpendicular to the shank top surface, this is the most common orientation used for large nose radius tools.

Turkes *et al.* (2011) investigated the influence of tool geometry on the surface finish in turning of AISI 1040 steel. In order to find out the effect of tool geometry parameters on the surface roughness during turning, response surface methodology (RSM) was used and a prediction model was developed related to average surface roughness (Ra) using experimental data. The results indicated that the tool nose radius was the dominant factor on the surface roughness. In addition, a good agreement between the predicted and measured surface roughness was observed.

2.2 Overview Based on Surface Finish on SPDT process

Wilks (1980) conducted study on the influence of the process parameters on turning process. It was found that feed rate and tool nose radius exerted a significant influence upon surface roughness. Thus, for a fixed tool nose radius, roughness deteriorates with an increase in feed rate, this effect being more pronounced as tool nose radius decreases. On the other hand, for a given feed rate, roughness increases with decreasing tool radius, this being more marked for higher feed rates. Mutual effects of crystallographic and change in cutting velocity during machining of Al 6061 are believed to be the main reason causing uneven wear along the cutting edge.

Lee *et al.* (1997) investigated the effect of the crystallographic orientation on the chip formation, cutting forces and surface micro topography in the single point diamond turning of aluminum single crystal. Continuous chips were formed under all cutting conditions for all of the crystals examined. However, differently orientated crystals exhibit differences in the cutting force and in the quality of the machined surface. Cutting force was found to increase with the depth of cut, but the cutting force did not increase or decrease monotonically with the feed rate. Turning (001) plane produces a high surface finish but that a poor surface finish is obtained when turning is done on the (110) plane.

Cheung *et al.* (2000) studied that the quality of surface is influenced by two main factors, process factors and material factors. The process factors include tool geometry, cutting conditions such as spindle rotational speed and feed rate, and relative vibration between the tool and work piece; while material factors include material anisotropy, swelling and crystallographic orientation of the material being cut. Process factors can be controlled but material factors cannot be minimized. The mechanism of surface generation differs from that of conventional machining .The diamond cutting process was usually carried out at very high cutting speeds so that the problems associated with the built-up-edge (BUE) do not arise.

Cheung *et al.* (2002) investigated that the tool interference inevitably affects the surface quality of a diamond turned surface. A surface topography simulation model was

proposed for the prediction of the effect of tool interference on surface generation in SPDT. The model takes into account both the kinematic and the dynamic factors which affect surface generation in diamond face turning. The former includes the machine parameters such as spindle speed, feed rate, depth of cut, and tool nose radius, whereas the latter considers the relative vibration between the tool and the workpiece caused by spindle error motions and machine vibration.

Jasinevicius *et al.* (2005) performed a study on machining of mono-crystalline silicon with (111) orientation by single point diamond turning machine. The cutting applications were performed under different conditions that result the ductile and brittle mode machining of silicon. When depth of cut was 5 μm, tool has 0.65 mm nose radius and -25^{o} rake angle, ductile mode machining resulted 1.6 nm Ra roughness where feed rate was 2.5μm/rev. When the feed rate of the process was increased to 8μm/rev, brittle mode of machining prevailed. So, the roughness of the machined surface increased up to 91.25 nm Ra and micro-cracks formed. Three dimensional views were obtained by atomic force microscope. In ductile mode machining, the surface is smooth and the cut grooves formed by tool can be seen. Surface prevailed by brittle mode machining was not smooth; pitting can be seen all over the surface and micro-cracks were formed on it.

Zhou *et al.* (2001) investigated the influence of applied loads on the deformation characteristics of silicon single crystal by conducting micro indentation and scribing tests. The transition of material removal from brittle to ductile was observed by continuously changing the cutting depth. The effect of tool rake angle on the machined surface quality was studied by actual diamond turning. A mirror surface, with a roughness of 5 nm *R*a, was produced using a tool with a - 25° rake angle. The surface quality generated with a tool of -25° rake angle is much better than that produced with a tool of 0° rake angle. This difference is believed to be because a large negative rake angle can provide the needed hydrostatic pressure to cause plastic deformation under the tool.

Zhong *et al.* (2002) studied, super-smooth surfaces of oxygen-free high-conductivity (OFHC) copper mirrors obtained by SPDT were characterized with an atomic force

microscope (AFM) from the 3D point of view. The machining conditions were also investigated. Two experiments were conducted; the feed rate was changed from 0.2 to 2.0µm per revolution and 0.3 to 3.0µm per revolution, respectively. To distinguish 3D and 2D parameters, the letter S is used in 3D instead of letter R in 2D. By 3D roughness characterization of these surfaces, the optimal feed rate was found to be 1.4µm per revolution when cutting depth was 1mm or 0.9 - 1.2µm per revolution at a cutting depth of 2µm, where an Sq of 2.6 and 2.3 nm could be obtained, respectively.

Pramanik *et al.* (2003) investigated that tool wear was not so significant although some defects on rake face were observed after cutting 15.6 km while machining of electroless nickel. Further cutting showed that the surface roughness increases with cutting distance, and that the cutting forces were larger than thrust force at the beginning of cutting, but after cutting 130 km, thrust force became larger and increased rapidly. It was also observed that forces increase with the increase of depth of cut, spindle speed and feed rate, and decrease with the increase of phosphorus content of the plating. Depth of cut has no significant effect on surface roughness, while it increases with increase of feed rate and decreases with the increase of percentage of phosphorus content in the work-pieces. In case of spindle speed, surface roughness decreases with the increase of spindle speed up to a certain value and then starts to increase with the increase of spindle speed.

Hocheng *et al.* (2004) studied the surface roughness obtained from the diamond turning of a phosphor–bronze lens mold with various tool nose radii, spindle speeds, feed rates and cutting depths. the tool geometry, low-frequency vibration and the measuring instrument were identified as the main influencing factors of the generated surface roughness. The intensities associated with the latter two vary little with the cutting conditions and are thus considered constant. The intensity of the tool geometry varies with the feed rate, the spindle speed and the radius of the tool nose. A relationship between the root-mean-square summation of the surface roughness and cutting conditions was found. The model agrees well with the experimental results.

Yan *et al.* (2004) investigated the nanometric machining characteristics of CaF_2. The effects of tool feed, tool rake angle, workpiece crystal orientation and cutting fluid were examined. Two major types of micro fractures were found to occur during wet cutting, namely, Type A and Type B. The A-type micro fracture is one to 10 microns in size and occurs under high tool feed conditions, whereas the B-type micro fracture is on the order of 100 microns in size and occurs under extremely low tool feed conditions. A-type micro fracture is due to crystallographic effect, while the B-type micro fracture results probably from the thermal effect. The <112>orientations correspond to the largest fracture depth while the <101>orientations are most easily to be ductile cut. Dry cutting can eliminate B-type micro fracturing.

Yan *et al.* (1995) investigated that pre-sintered (1300^0C/30min) ceramics can be machines with carbide tool and ceramic tools, the tools sustain significant levels of tool wear after a very short period of machining. The PCD tool sustains the least flank wear, due to extreme hardness. CBN is next to hardness to diamond, therefore the flank wear is next to that of PCD. Pure alumina ceramic tool and K10 are found to be very unsatisfactory and sustain the most severe flank wear. It is found that PCD tool is superior to the other tools, whilst the carbide tool and the ceramic tool are unsuitable for machining ceramics materials. It is also found that turning ceramics with a sucker in cool and highly humid weather moistens the tool face and promotes tool wear. However, when turning with hot blowing and sucking, the tool wear has considerable improvement, due to improvement in chip discharge.

Davim *et al.* (2010) presented a study about the Chemical Vapour Deposition (CVD) diamond coated tool performance when compared with Polycrystalline Diamond (PCD) and cemented carbide (K10) tools in machining unreinforced polyamide PA 6 and composite PA 66GF Cemented carbide (K10) tool presents the worse behavior for machining these materials, especially in terms of cutting forces. Two parameters must be considered: the maximum peak-to-valley height (R_t) and the arithmetic mean roughness (Ra). Surface roughness increases with the feed rate and reinforced PA 66GF presents

greater values compared with unreinforced PA 6. K10 presents great values of surface roughness with respect to CVD diamond and PCD.

Revel *et al*. (2006) experimental study of pure aluminum and aluminum alloys in terms of roughness and structural surface evolution was proposed. Both metals and alloys were machined in single point diamond turning. Moreover, a complementary study on optimization of turning parameters for different aluminum alloys was also undertaken. Surface characterizations were carried out using two powerful techniques: interferometry microscopy and grazing incidence X-ray diffraction. These non-destructive methods allow determining the evolution of mechanical and physical properties of materials, before and after turning.

Biddut *et al*. (2007) The effect of tool rake angle on the performance of single crystal diamond tools in micro-machining of BeCu, Diamond tools with rake angles of 0^0, $+5^0$ and -5^0 were studied. For a cutting distance of up to 11.69 km, 0^0 rake angle has superior performance in terms of tool wear, cutting forces, and machined surface roughness. Rake, $+5^0$ and -5^0 angles suffered from progressive wear with a corresponding increase in cutting forces. despite the increase in wear on tools with ,$+5^0$ and -5^0 rake angles, and cutting forces on the diamond tools with all three different rake angles did not significantly affect the surface roughness. The effects of various cutting parameters such as spindle speed and feed rate on the cutting forces and surface roughness were also presented in this study. Cutting forces increase proportionately with spindle speed and feed rate without any significant variation of surface roughness. Surface quality of up to 3 nm Ra was achieved during micromachining of BeCu.

Palanikumar (2008) discussed the use of Taguchi and response surface methodologies for minimizing the surface roughness in machining polycarbonate with a polycrystalline diamond (PCD) tool. The effect of cutting parameters on surface roughness is evaluated and the optimum cutting condition for minimizing the surface roughness is determined. A second-order model has been established between the cutting parameters and surface roughness using response surface methodology. The experimental results reveal that the

most significant machining parameter for surface roughness is feed followed by cutting speed. The predicted values and measured values are fairly close, which indicates that the developed model can be effectively used to predict the surface roughness in the machining of polycarbonate. For achieving good surface finish on the polycarbonate work piece, high cutting speed, high depth of cut and lower feeds are preferred.

Palanikumar *et al.* (2008) presented the experimental investigation on machining of fabricated silicon carbide particle reinforced aluminum metal matrix (A356/SiC/20p) composites by poly crystalline diamond (PCD) inserts. The parameters considered for the experiments were cutting speed, feed and depth of cut. The response considered for the analysis was surface roughness. An empirical model has been developed for predicting the surface roughness in machining of A356/SiC/20p composites. Response surface regression and analysis of variance (ANOVA) are used in order to study the effects of machining parameters. Optimum machining condition for minimizing the surface roughness is determined using desirability function approach. The surface plots are drawn using developed RSM model by varying the two different parameters by keeping the third parameter at the middle level. The chip formation mechanism in machining of Al/SiC composites is different than the conventional materials and it produce discontinuous chips. The increase in cutting speed reduces the surface roughness and vice versa. The surface roughness at 175m/min is better than the surface roughness at 75m/min. The increase in feed increases the surface roughness. During machining, if feed is increased, the normal loads on the tool also increase and it will generate a heat which in turn increases the surface roughness. The influence of cutting speed with respect to depth of cut by keeping feed at middle level. The increase in depth of cut does not show any appreciable change in surface roughness in machining of A356/SiC/20p composites

Osmer *et al.* (2010) presented the results for the machining of materials typically applied in ultra precision machining in comparison to a nitrocarburized tool steel. The influence of feed, depth of cut and cutting speed on surface quality, resulting cutting forces and tool wear have been investigated. The results show that the decisive factor for the ultra precision machining of nitrocarburized tool steel are the significantly higher cutting

forces. In some cases the high cutting forces lead to vibrations during the turning process deteriorating the surface integrity. Therefore, tool nose radius and depth of cut have to be reduced to minimize the cutting forces and avoid the vibrations. Pure aluminum and the OFHC-copper the anisotropy of the grain structure leads to unsteady surface topography The amorphous electro less nickel plating and the fine grained RSA-905 aluminum alloy show a very regular surface topography. Surface roughness values for the nitro carburized tool steel are slightly higher compared to the other investigated materials.

Abhang *et al.* (2011) *utilized* the regression modelling in turning process of En31 using response surface methodology (RSM) with factorial design of experiments. A first-order and second-order surface roughness predicting models were developed by using the experimental data and analysis of the relationship between the cutting conditions and response (surface roughness). In the development of predictive models, cutting parameters of cutting velocity, feed rate, depth of cut, tool nose radius and concentration of lubricants were considered as model variables, surface roughness were considered as response variable. Further, the analysis of variance (ANOVA) was used to analyze the influence of process parameters and their interaction during machining. From the analysis, it was observed that feed rate is the most significant factor on the surface roughness followed by cutting speed and depth of cut at 95% confidence level. Tool nose radius and concentration of lubricants seem to be statistically less significant at 95% confidence level. Furthermore, the interaction of cutting velocity/feed rate, cutting velocity/ nose radius and depth of cut/nose radius were found to be statistically significant on the surface finish because their p-values are smaller than 5%. The predicted surface roughness values of the samples have been found to lie close to that of the experimentally observed values. The surface roughness increases with increase feed rate followed by depth of cut but decreases with increase in the cutting velocity, tool nose radius and optimum concentration of solid-liquid lubricants respectively.

Patten *et al.* (2009) demonstrated that ductile regime single point diamond turning is possible on these materials to improve the surface quality without imparting sub surface damage. Machining parameters, such as depth of cut and feed, used to carry out ductile

regime machining will be discussed. A single crystal diamond tool with a 3mm nose radius, -45^0 rake angle and 5^0 clearance angles was used for the cutting test. The single point diamond turning experiments were successful in reducing the surface roughness of a CVD coated silicon carbide and Quartz. The Ra was brought down by two orders of magnitude (from 1.23μm to 88nm*)* for SiC and from 110nm to 41nm for Quartz. The best surface finish was obtained with the lowest feed rate attempted (1μm/rev) but initially a higher feed rate was used (30μm/rev for SiC) to maximize the material removal rate and minimize tool wear. The tool wear can be reduced by using suitable cutting fluids to reduce frictional effects and also by reducing the feed rates once the surface becomes smooth.

Yingfei *et al.* (2010) The wear pattern and its mechanisms of single crystal diamond (SCD) and polycrystalline diamond (PCD) tools have been investigated experimentally and theoretically during ultra-precision turning of SiC particle-reinforced 2009 aluminum matrix composite under wet machining conditions. The results showed that microwear, chipping, cleavage, abrasive wear and chemical wear were the dominating wear patterns of SCD tools, and PCD tools mainly suffered from abrasive wear on the rake face and adhesive wear on the flank face. The combined effects of abrasive wear of SiC particles and catalysis of copper in the aluminum matrix caused the severe graphitization of SCD tool with (rake face 1 1 0-flank 1 1 0) crystal orientation. The adhesive wear on PCD tool was induced by the intermittent growth and breaking off behavior of build-up-edge. SCD tool with the crystal orientation of (rake face 1 1 0, flank 1 0 0) had the best cutting performance among the three types of tools, by which the machined surface roughness Ra was less than 49nmafter cutting for over 9 km. PCD tool had a steady and favorable cutting performance and could produce acceptable surface quality when the cutting distance was less than 6 km, during which the value of Ra was less than 46nm and varied in the range of 12–15 nm.

Zhimin *et al.* (2011) investigated the process factors affecting the surface roughness in ultra-precision diamond turning with ultrasonic vibration. Stainless steel was turned by diamond tools with ultra- sonic vibration applied in the feed direction with an auto-

resonant control system. Surface roughness was measured and compared along with the change of the cutting parameters. The relation curves between the cutting parameters and surface roughness were achieved by comparing the experimental results with different cutting speeds, feed rates, cutting depths. Experimental results indicate that cutting parameters have an obvious effect on the surface roughness. The conclusions are draw in given conditions, the smaller amplitude of the vibration, the worse the surface quality and the higher vibrating frequency, the better surface quality, and the deeper the cutting depth and the more the feed rate, the worse the surface quality. Among these parameters, the feed rate was the most important factor on surface quality.

Chen *et al.* (2011) investigated that the cutting forces and surface roughness vary greatly with different crystallographic orientations of KDP crystal, and that amplitude variation of cutting forces and surface finish is closely related with the cutting parameters of the maximum undeformed chip thickness. With the maximum undeformed chip thickness below 30nm, the amplitude variation of cutting forces and surface roughness in minimized, and a super-smooth surface with consistent surface finish in all the crystallographic orientations can be achieved. The surface roughness is 2.698 nm (Ra) measured by Atomic Force Microscope (AFM).

Zhong *et al.* (2011) in this study, a rapidly solidified aluminum alloy was compared with beryllium copper and 6061 aluminum alloys in terms of their wear rates, hardness and performance as mold insert materials. The investigation results indicated that the BeCu alloy has the lowest wear rate, while aluminum 6061-T6 has the highest wear rate. The rapidly solidified aluminum alloy performs much better than aluminum 6061-T6 in molding of plastic lenses and is comparable to the BeCu alloy. It is able to attain finer surfaces of the molded plastic lenses. rapidly solidified aluminum alloy can replace the BeCu alloy as a good mold insert material, because beryllium (Be) is a toxic element. single-point diamond turning using an ultra-precision turning machine at a depth of cut of 6 µm, a work piece rotational-speed of 2000 rpm, and a feed rate of 5 µm/rev. rapidly solidified aluminium (RSA) alloy had the best surface texture, followed by the surfaces of

the beryllium copper alloy and the aluminum alloy 6061-T6. Dimples could be seen on the insert surface of 6061-T6.

Cheung *et al.* (2000) investigation of the mach inability of copper single crystals in terms of chip and surface roughness generation was performed under various cutting conditions. Based on the findings, the relationship between the cutting conditions on the anisotropy of surface roughness was explored. The implications of these findings on the improvement of the surface finish of a diamond turned surface are discussed. The surface roughness was found to vary systematically with the crystallographic orientation of the materials being cut. Greater variation is observed for (110) crystal than (111) crystal while that is the smallest for (001) crystal. As feed rate increase, the arithmetic roughness for the diamond turned crystals is found to increase. Considerable variation in the chip thickness affords evidence that the shear angle varies with the changing crystallographic orientation of materials being cut.

Yaldiz *et al.* (2011) the application of response surface methodology on the turning of Al 6061 T6 with single crystal diamond tool was carried out to develop the mathematical model of the surface roughness (Ra) so as to investigate the influences of cutting tool geometry parameters. For finding optimum value of geometry parameters, the quadratic model of response surface methodology was utilized. The result of ANOVA proved that the quadratic mathematical models allow prediction of surface roughness parameter with a 96% confident interval. Tool nose radius is the most significant factor on surface roughness with 51.45% contribution in the total variability of model. Also, approach angle and rake angle are significant factors on surface roughness with 18.24% and 17.74% contribution in the total variability of model, respectively. It can be said that the interaction between all factors has no significant effect on surface roughness. Using response optimization show that the optimal combination of machining parameters are (0.4 mm, 60^0, - 3^0) for tool nose radius, approach angle and rake angle, respectively.

Tanju *et al.* (2011) experimental investigation on surface roughness, cutting temperature and cutting forces in turning of aluminum 7075 alloy using diamond cutting tools was

presented. The effects of the feed rate, cutting speed and depth of cut on surface roughness, cutting temperature and cutting force were examined. In order to optimize the experimental results, Taguchi optimization method was employed. The effect of each parameter on the obtained results was determined by the use of analysis of variance (ANOVA). The relationship between dependent and independent parameters was modelled with regression analysis. The most effective control factor on the surface roughness value on the machined surface is feed rate. It has also been observed that feed is the most serviceable factor, still depth of cut and cutting speed play a role as well. The heat generation during the chip removal is in the direct proportion with feed. The feed with a proportion of 92.47% was the most effective factor in the formation of the roughness on the machined surfaces. Taguchi method is beneficial for the experimental design of the mach inability of Al 7075 alloy material

Patten *et al.* (2011) investigated the improvement the surface quality of Quartz to be used as an optic device (mirrors and windows) via single point diamond turning (SPDT). Sub-surface damage analysis was carried out on the machined sample using Scanning Acoustic Microscopy (SAcM). Surface roughness (Ra) values of less than 45 nm without sub surface damage were obtained. Tool wear was also investigated. The results show that ductile mode machining (using SPDT) is possible for the Spectrosil 2000 Quartz material. The surface roughness of the Spectrosil 2000 had been reduced from 110nm (Ra) to 40nm (Ra) and 1050nm Rz) to 300nm (Rz) in two machining passes. From the surface images and subsurface investigation, it is evident that there were no signs of brittle fracture. The single crystal diamond tools held up for both passes and only slight wear was observed on the tool used in pass 1 (1 mm programmed depth of cut). It has been observed that the surface finish tends to worsen if the depth of cut is larger than the peak-to-valley value as a deeper cut results in more valleys (feed marks or grooves) on the work piece surface.

Ding *et al.* (2012) investigated the crystallographic effects on the performance of cutting polycrystalline oxygen free copper C10200 (OFC) with single crystalline diamond (SCD) micro-tools. At both large cutting depth and cross-feed rate, as the micro-tool traversed a

grain with a crystallographic orientation less favorable for a stable machining process, the work material in front of the rake face was found to be severely deformed. This may lead to a reduced shear angle, thick chip, strsiation at the back of the chip, high cutting forces, degraded machined surface and the possibility of burr formation. The results showed minimal variations in the machined surface integrity and cutting forces compared to cut amorphous NiP plating with micro-tools. For a high cutting depth, burrs were also observed due to material deformation and pile-up occurring at the groove edges since the localized stress probably built up in front of the rake face. Cutting strategies were demonstrated to improve the performance of cutting OFC with micro-tools and to generate high aspect ratio micro-pillar arrays. When the cutting depth approached or exceeded 0.4μm, burrs due to material pile-up and deformation were formed at the groove edges. The cause of formation of deformation or pile-up may be attributed to the localized stress in front of the rake face building up. Cutting with a reduced cutting depth could minimize the burr size or prevent the burr formation; however, it could not avoid the crystallographic effects on the changes both in roughness Ra on the machined surface and the cutting forces.

2.3 Overview Based on Profile Error on SPDT process

Ngoi *et al.* (2001) investigated the effects of cutting tool conditions and tool set-up error on the surface distortion. Controlled cutting tests were performed on a two-axis diamond turning machine. Spherical mirrors with preset tool offset values and tool height values were turned. The relationship among machined form accuracy, tool offset, and tool height was investigated based on experimental and analytical results. The influence of tool wear on the machined surface quality was studied. Factors governing uneven wear along the cutting edge in contour machining were analyzed. A spherical surface with form accuracy better than λ/10 was produced. Methods for minimizing the effect of tool wear are also discussed.

Lee *et al.* (2000) observed that the form accuracy of the machined surface is seriously affected by the residual form errors. These errors might be caused by residual stress induced in the surface layers of the work pieces during cutting, wear of the diamond tool

and tool decentring. The errors arising from residual stress can be minimised or even eliminated by imposing a heat-treatment (stress-relief annealing) stage between successive cutting passes there is significant improvement of the residual form errors with the use of the compensation process. For deep-sag Curvature profiles, the tool has to be tilted, and also rotated in some cases to avoid the tool-part interference.

Fang *et al.* (2002) investigated that the tool path compensation procedure is very effective in correcting the tool nose curvature which result in form error. The tool has to be tilted and also rotated in some cases to avoid the tool-part interference. The centre cone form error, increases with an increase in the tilt angle, rotated angle and the tool nose radius. The tool radius has the most dominant effect, followed by the tilt angle and the rotated angle. The centre cone form error can be eliminated by selecting the smaller tool radius or rotating the tool to the right side, provided the tool arc angle is big enough.

Zhou *et al.* (2003) the errors cause defects on the machines surface and generates significant amount of form error on the component. Centre height error can results in significant damage near the region of spin axis on the brittle materials like single crystal silicon and germanium. In general, the centre height error must be less than one micron to minimize the cosmetic errors in these materials. The accuracy to which the tool is centered in X-direction affects the form accuracy of the component. OGIVE form errors are generated due to X-direction centering error

Sarepaka *et al.* (2012) Optical grade polycarbonate was explored for its single-point diamond turning (SPDT) features and its profile characteristics. This study focused on the optimization of SPDT machining parameters viz: tool feed rate, depth of cut, spindle speed for a given tool nose radius. In this study, the machining sensitivity in terms of surface roughness and profile error (Pt) was investigated. It is found that machining parameters play a major role in surface quality optimization in terms of roughness and profile. Tool feed is the dominant parameter for surface roughness followed by the spindle rotational speed. Depth of cut shows minimal effect. Depth of cut is the leading parameter for peak to valley error. Lower depth of cut is preferred for achieving good

optical surface on the polycarbonate work piece. Spindle rotational speed of 2000rpm, tool feed rate of1μm/rev and depth of cut of 2μm are selected for precise machining of polycarbonate.

2.4 Conclusion and Research Objective

Based on the above literature review it seen that only few work has been done related to surface roughness and Profile error minimization for both flat and spherical profile on Copper alloy material during SPDT, so this research are one step ahead for SPDT. Single point diamond turning is being used with increasing frequency to fabricate precision surfaces. However the process introduces its own peculiar form of errors that can compromise performance. These errors include misalignment error, thermal effects, low frequency surface ripples and mounting effects. Such errors affect the surface finish and profile of the final work piece. Thus, to achieve the best surface quality with minimum surface roughness and minimum profile error the process parameters are to be optimized by using S/N response and Pareto ANOVA techniques.

Project planning includes mainly two types of experiments for two different profiles viz: Flat and Curved (Spherical). In 1st experiment, a series of facing (machining) operations are conducted on Copper alloy C18000 to generate Flat Profile. In 2nd experiment, contour (concave) machining operations are conducted on Copper alloy C18000. These two experiments are carried under same machining conditions with different machining conditions as suggested by standard orthogonal array L9. Finally Grey relational analysis technique is use for the optimization of two responses. This effort provides an optimum Parameter for multiple responses for both the profiles.

This work undertaken in this project helps to find optimum processing parameters to optimize machining experiments and to improve productivity in single point diamond turning (while meeting desired surface quality), during the generation of both flat and curved surfaces.

CHAPTER 3: PROBLEM FORMULATION AND DESIGN OF STUDY

3.1 PROBLEM FORMULATION

Single point diamond turning involves complex physical process including machine tool vibration. Tool Nose Radius (TNR), Tool feed Rate (TFR), Depth of Cut (DOC), Spindle Speed (SS) will determine the surface roughness and waviness which in turn will influence the overall surface quality. Hence these process parameters should be chosen properly so that a better performance in the surface quality can be achieved. Over the past decade, there has been much research into the process and material factors affecting the surface roughness in machining operations. Hence to achieve an optical grade of surface quality these process parameters should be chosen properly. Moreover, each material has its own property and each material needs different sets of optimum combination of process parameters to set to achieve the better surface quality.

Single point diamond turning is being used increasingly for the fabrication of flat and curvature profiles on non ferrous materials with ease. However the process introduces its own peculiar form of errors that can compromise performance. These errors include misalignment error, thermal effects, low frequency surface ripples and mounting effects. These errors and machining parameters will affect the surface finish (Ra) and profile accuracy (Pt) of the final work-piece, which further deteriorates the performance of the final product. Minimization of these errors and optimization of machining parameters will tend to produce the optical grade of surface characteristics. The process is shown schematically in a step by step approach in Fig.3.1.

In the work presented in this thesis, the effect of each parameter over the surface roughness and profile error for Copper Chromium silicon nickel C18000 material is to be explored for both the Flat and Spherical profiles.

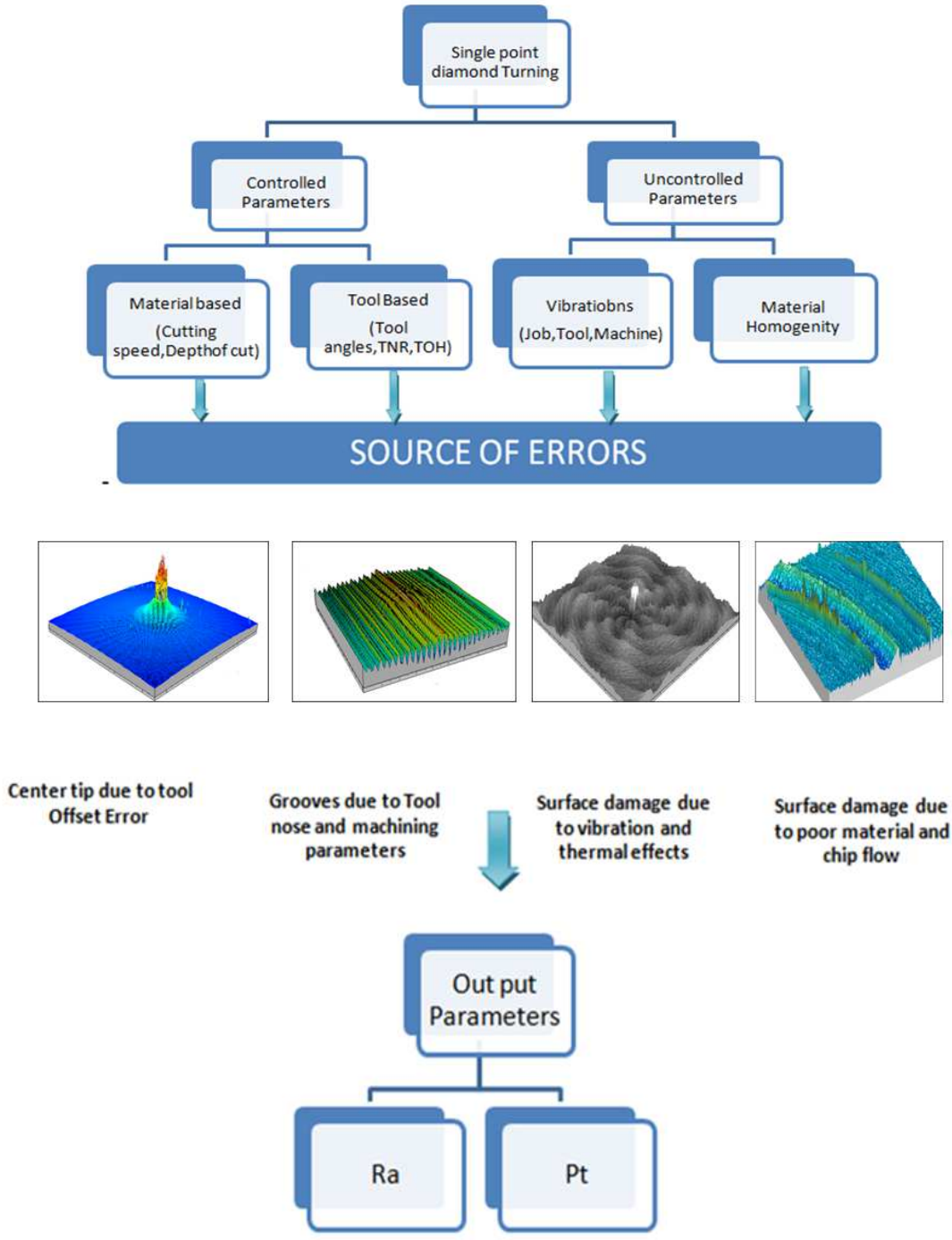

Fig.3.1 Problem Formulation

3.2 PARAMETERS FOR OPTIMIZATION

A good surface finish can only be achieved by proper combination of process parameters. Factors which affect the surface quality are basically differentiated into two major types:

Controllable and uncontrollable parameters. Machine tool vibration, ambience and metrology practice are considered to be the uncontrollable parameters and the cutting speed, feed rate, tool nose radius, coolant, depth of cut are considered to be the controllable parameters. Uncontrollable parameters cannot be controlled properly. One has to pay attention in selecting the best combination which fails would result in very rough surfaces. Thus the greatest challenge lies in one selecting the optimum combination of the process parameters to get the best surface quality. The parameters chosen for optimization are as follows:

- Spindle speed (SS)
- Feed rate (TFR)
- Depth of cut (DOC)
- Tool nose radius (TNR)
- Rake angle (α)

In this study, 0^0 rake angle tool insert is taken (kept constant), due to non availability of different type of rake angle (α) diamond stool in CSIR-CSIO.

3.3 PROCESS FLOW

The SPDT has a wide spectrum of operating parameters which needs attention to be set before the beginning of operations. The pre work for SPDT is of main concern, as it may result in bad results. The tool setting, tool nose radius compensation, job centering, spindle alignment are the main things which needs operator's keen attention. The flowchart of complete SPDT process is given in the Fig.3.2 (a). This flow chart provides a step by step approach followed by the operator before start of machining operation. The two main steps which are to be followed before working over SPDT are design and fabrication of Fixture for holding the work piece and tool setting with minimum error. The X-offset and tool height can be adjusted by performing machining operation (iterations) on the stud which is made of aluminum 6061 material. The tool height and X-offset should always kept minimum, to minimize the profile error. The flowchart of complete SPDT process is given in the Fig.3.2 (b). This flow chart provides the brief overview of the thesis work presented in this work.

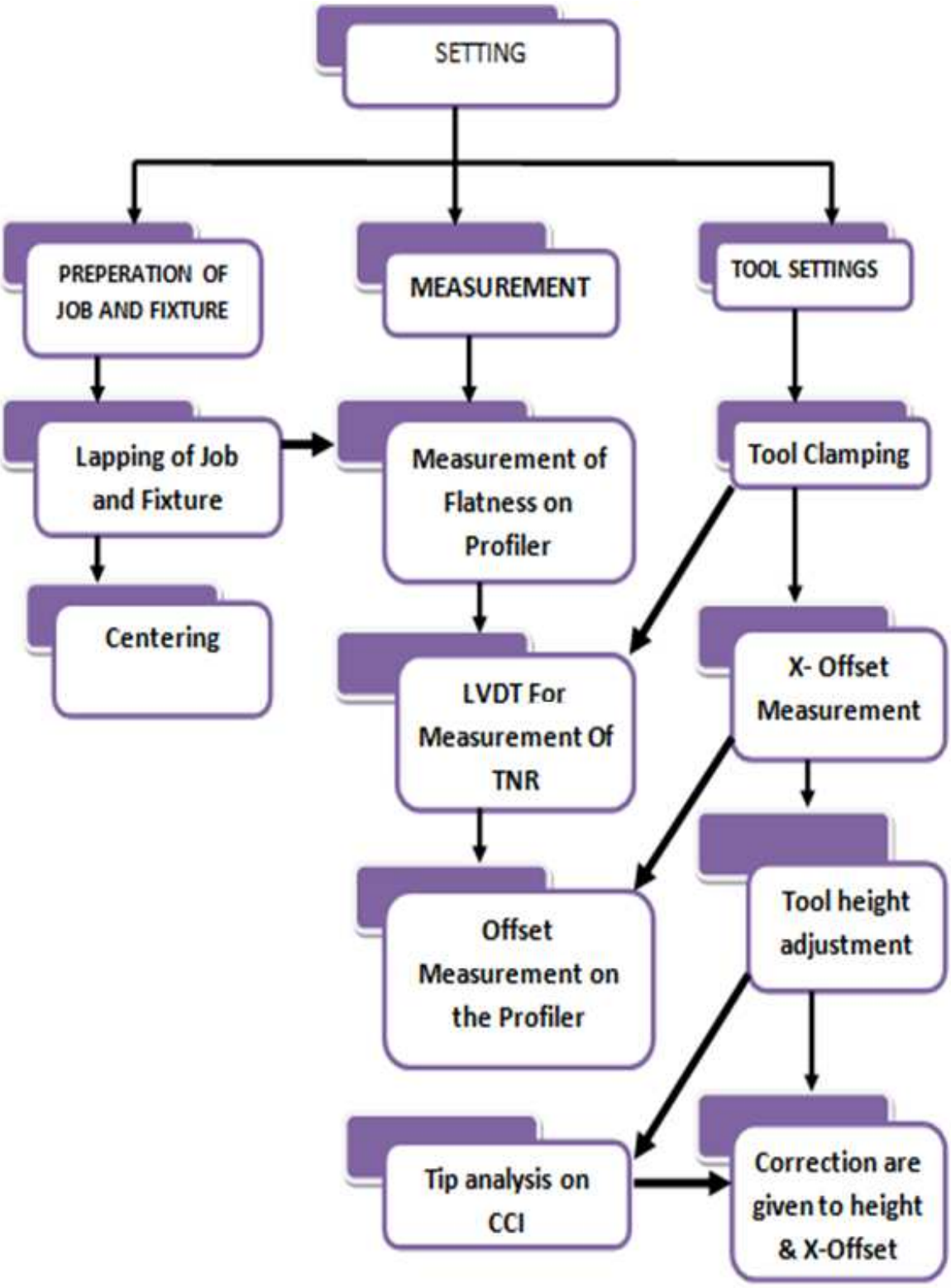

Fig.3.2 (a): Tool setting Process flow of the SPDT exercise

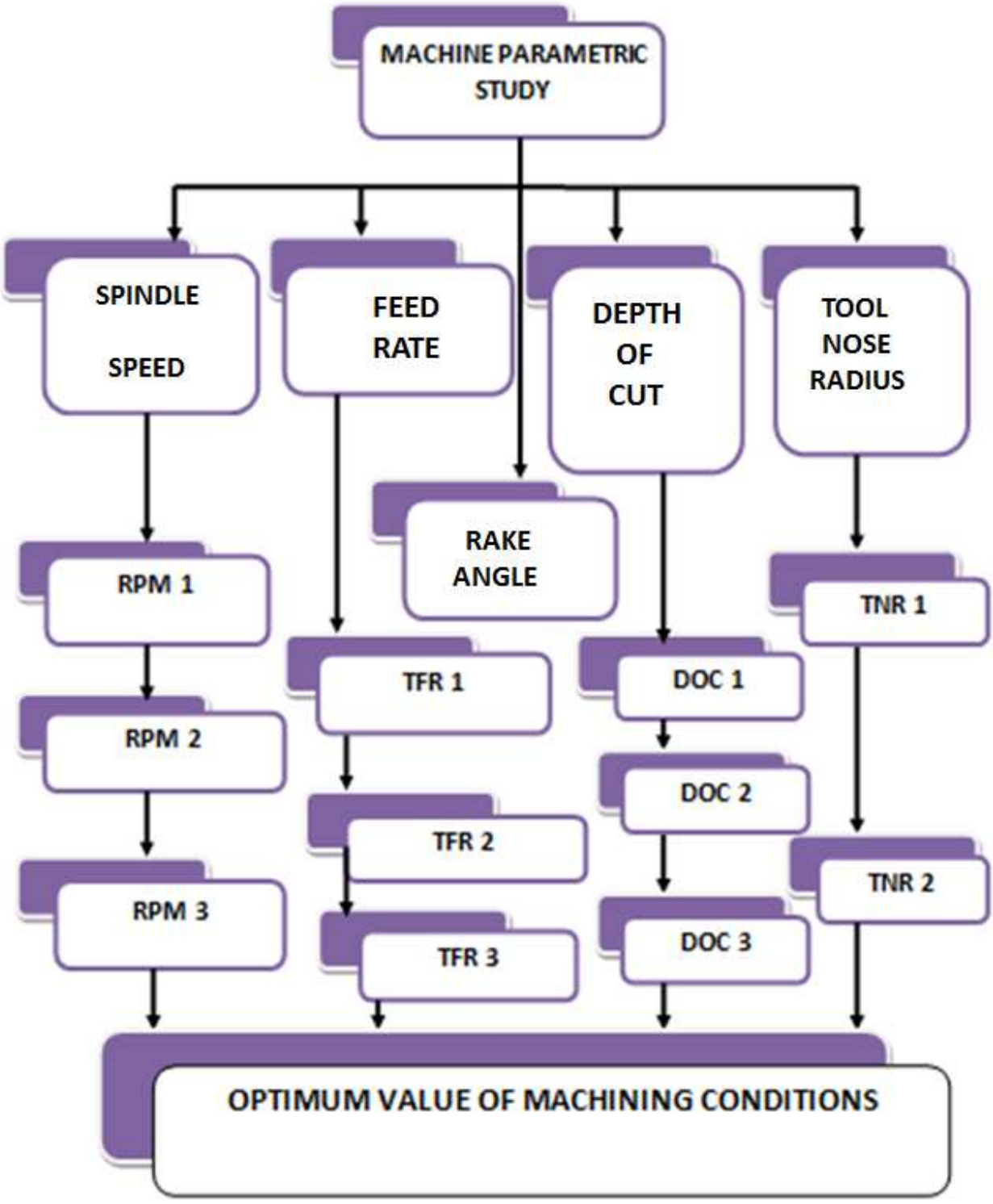

Fig.3.2 (b): Process flow of the SPDT exercise

3.4 METHODOLOGY

The methodology of the dissertation is represented as flow diagram in Fig.3.3.

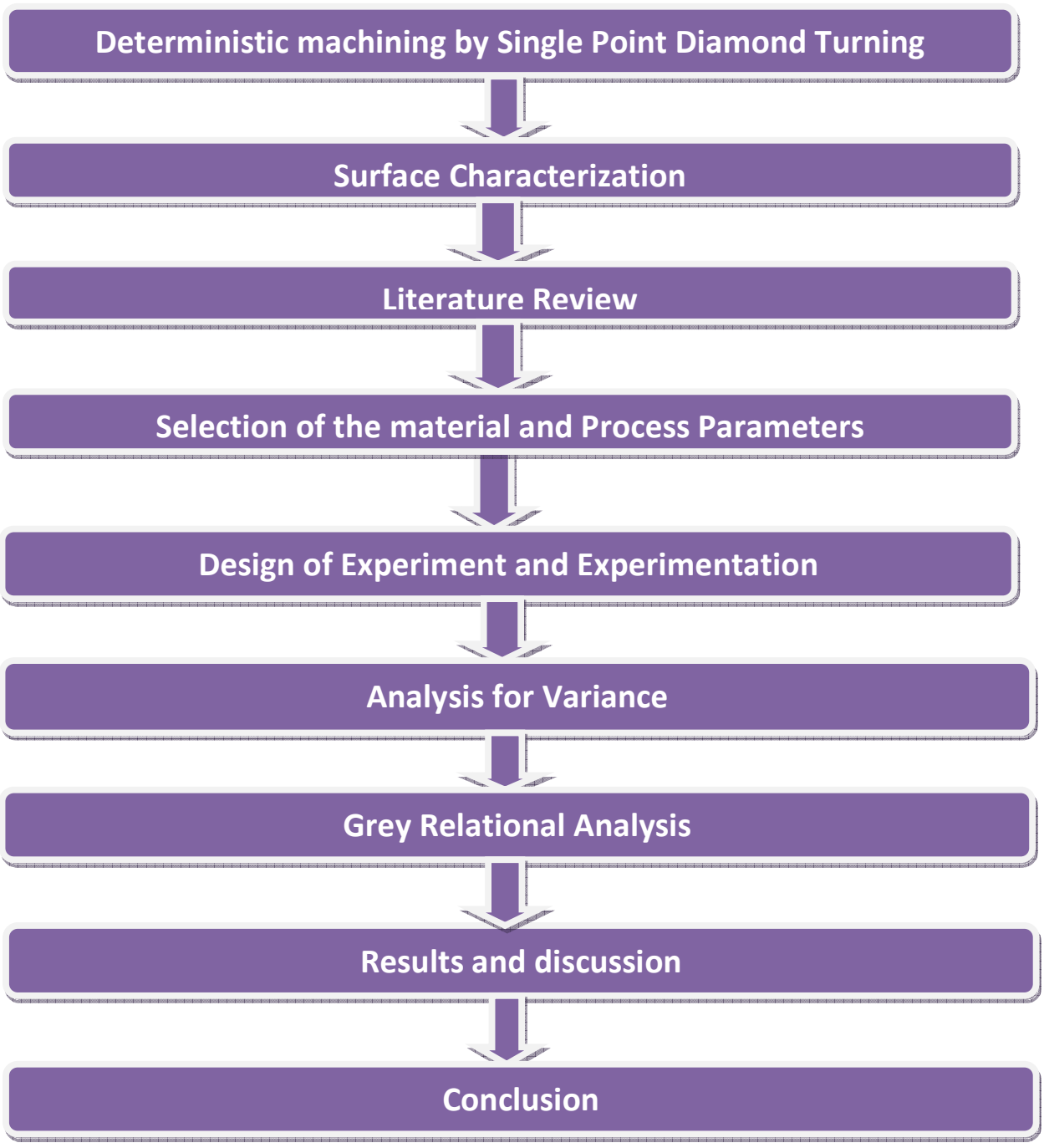

Fig.3.3: Methodology of the Project

3.5 EXPERIMENTAL SETUP

3.5.1 MACHINE TOOLS

Nanoform-250 at CSIR-CSIO, Chandigarh is a versatile, two axis machine with real-time operating system designed for single point diamond turning, grinding and precision machining. The machine makes use of vacuum chuck to hold the work piece. It consists of very stiff and stable (vibration isolated) machine base on which the required number of components can be placed. Machine support system provides isolation of the machine form external mechanical variations transmitted through the ground. Technical specifications along with fabrication capability of Nanoform-250 are provided in Table 3.1.

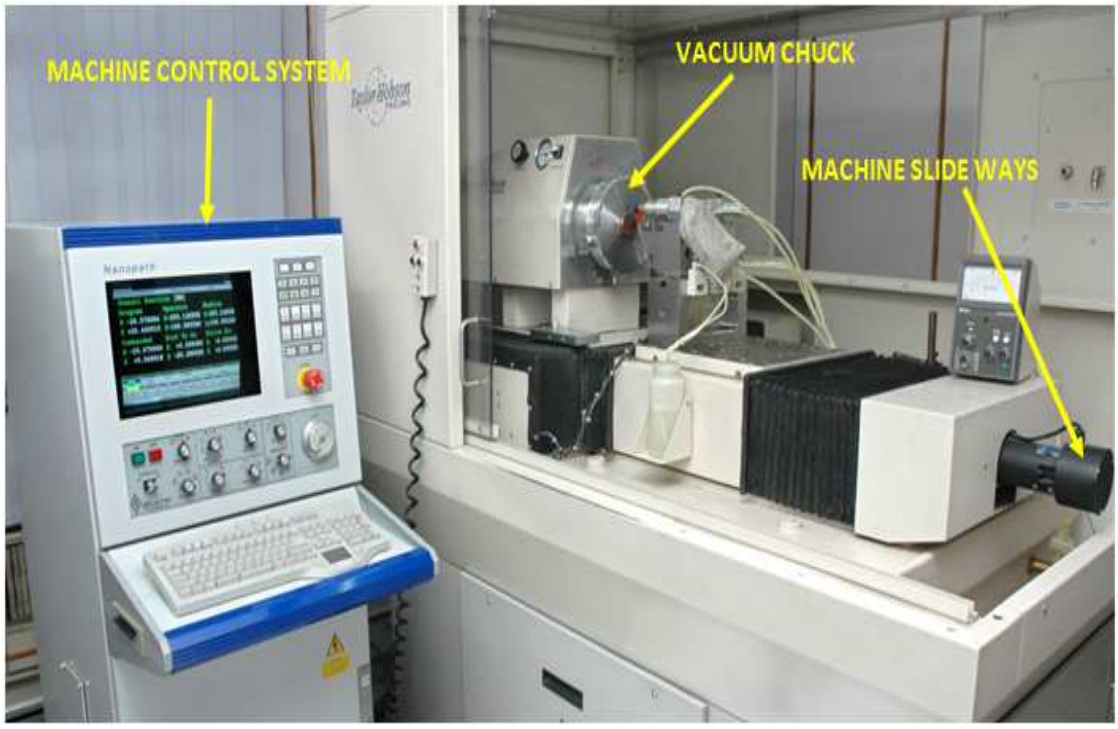

Fig.3.4: Nanoform-250 Diamond Turning Equipment (CSIR-CSIO, Chandigarh)

LVDT TOOL SET STATION

The LVDT tool setting station is used to adjust the height of the diamond tool as well as its X and Z positions relative to the spindle centerline. The vertical LVDT air bearing probe diameter is used to accurately set diamond tool height. The horizontal LVDT air-

bearing probe is used to automatically calculate the diamond tools nose radius and relative X and Z positions, in relation to spindle's centerline.

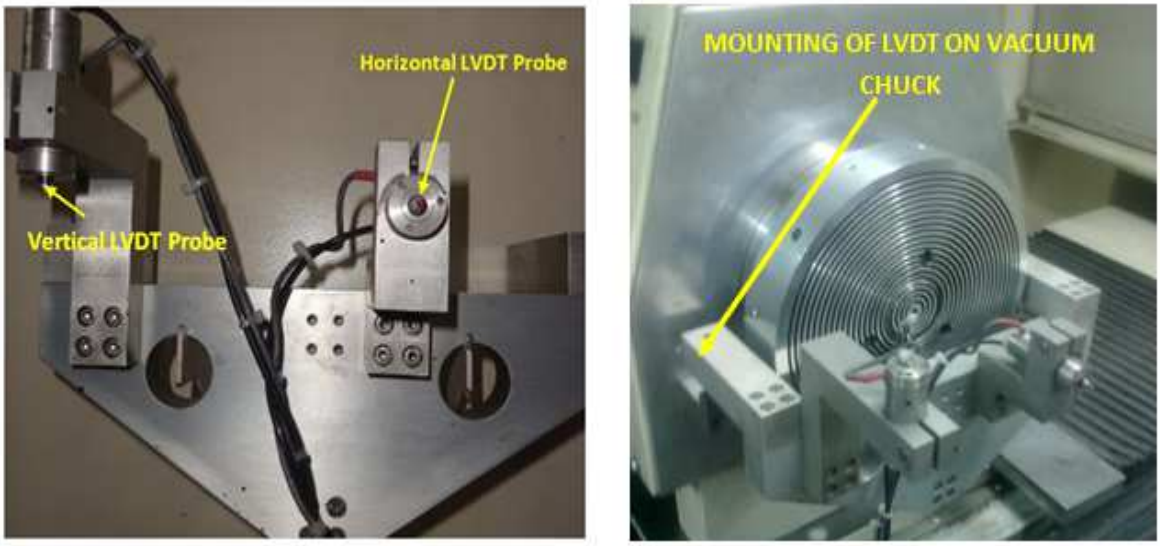

Fig.3.5: LVDT (Linear Variable Differential Transformer) (CSIR-CSIO, Chandigarh)

3.5.2 SPECIFICATION OF SPDT EQUIPMENT

Table 3.1: Specification of Machine

Technical Specifications of Nanoform-250	
X-axis move	350 mm
z-axis move	250 mm
Horizontal straightness in X-axis	0.5µm full travel (350 mm)
Horizontal straightness in y axis	0.3µm full travel (250 mm)
Side ways	Hydrostatic oil bearings
Feedback resolution	3.60 nm
Radial motion error	<0.05µm
Axial motion error	<0.05µm
Maximum spindle speed	5000 rev/min
Fabrication Capabilities of Nanoform-250	
Max. Job diameter	450 mm
Surface figure error	<0.1-0.3µm PV
Surface finish	<10nm Ra

3.5.3 FEATURES OF NANOFORM-250

Nano form -250 is capable of diamond turning optical quality form and finish in a wide range of non-ferrous, crystals and polymers. It works on the basis software assisted aspheric tool path with online diagnosis and analysis. Hydrostatic slides for job and tool axis (250mm travel on each axis). It consist of centering accessory to align job tool with in 0.1µm.

3.5.4 TYPICAL SPDT SETUP

A typical SPDT setup is given in the Fig.3.6:-

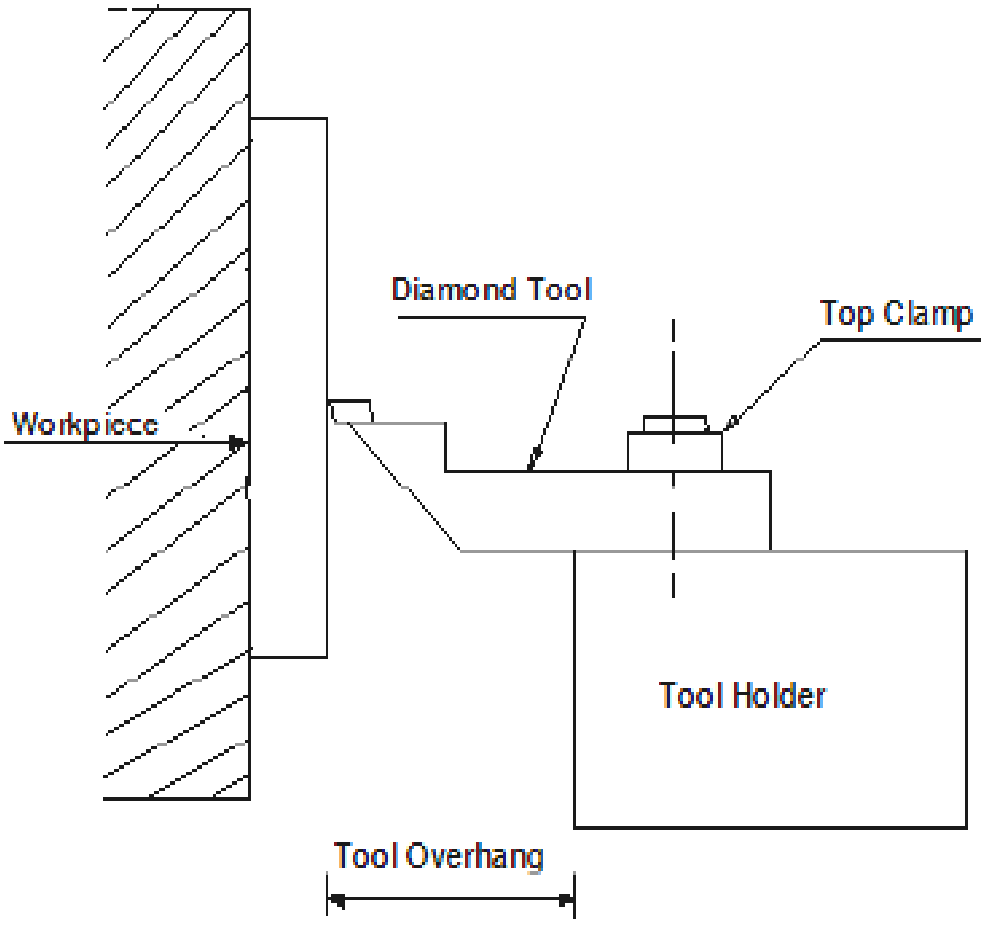

Fig.3.6: Arrangement of tool and work piece

3.6 MEASUREMENT EQUIPMENTS

Characterization is an integral part of precision surface generation in diamond turning operations. Accurate control of position, distance, and measuring speed is essential for stable and repeatable results. Two types of instruments are used for measurements in this work, viz: mechanical profiler and optical profiler. Profilers are instruments that are used to measure surface finish, surface roughness, and the geometry of small features on an object.

3.6.1 CONTACT MECHANICAL PROFILER PGI 120

The Form Talysurf PGI 120 is a contact type mechanical profiler, uses conical stylus diamond tip which record height variation of surface along a straight line at a time being in contact with surface. The profile meter is mounted on epoxy granite construction on anti-vibration mounts and provides a firm support for the column and work piece.

The stylus moves over the surface at a constant speed, and an electrical signal is produced by the Transformer. The stylus is provided with a diamond tip with a cone angle of 60˚ or 90˚ & a tip radius in the range of 1-10µm. These electrical signals are amplified and undergo analog-to-digital conversion. The resulting digital profile is stored in the computer & can be analyzed subsequently for roughness or waviness parameter. Figure 3.7 shows the schematic diagram of stylus instrument. This instrument offers dimensional, form and texture measurements simultaneously with high instrument offers dimensional, form and texture measurements simultaneously with high accuracies and gauge repeatability.

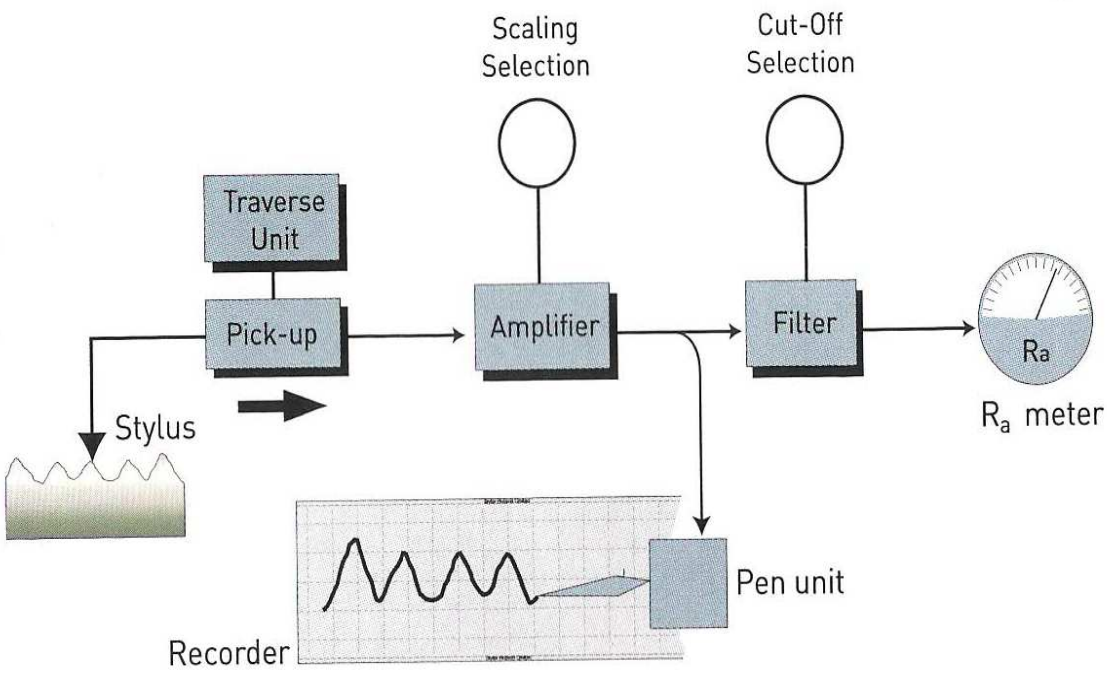

Fig.3.7: Schematic Diagram of Stylus Instrument (CSIR-CSIO, Chandigarh)

Table 3.2: Technical specifications of PGI-120 mechanical profiler

Technical specifications of PGI -120 mechanical profiler	
Traverse length	120 mm
Measuring speed	1mm and 0.5 mm/sec
Traverse speed	Up to 5 mm/sec
Gauge type	Phase grating interferometer
Measuring range	10mm
Technical specifications of PGI -120 mechanical profiler	
Resolution	12.8nm at 10mm range
Range to resolution ratio	780,000:1
Straightness accuracy	0.5µm over 120mm traverse
Data resolution	0.25µm
Dimensions(LxDxH)	396x127x195 mm
Measurement capabilities Of PGI-120	
Compatible	With aspheric surface generator and polisher
Analysis	Form, figure and finish
Job diameter	120mm
Roughness accuracy	~10-15nm at 10mm
Figure accuracy	~0.1µm/ 20mm and ~0.5µm/120mm

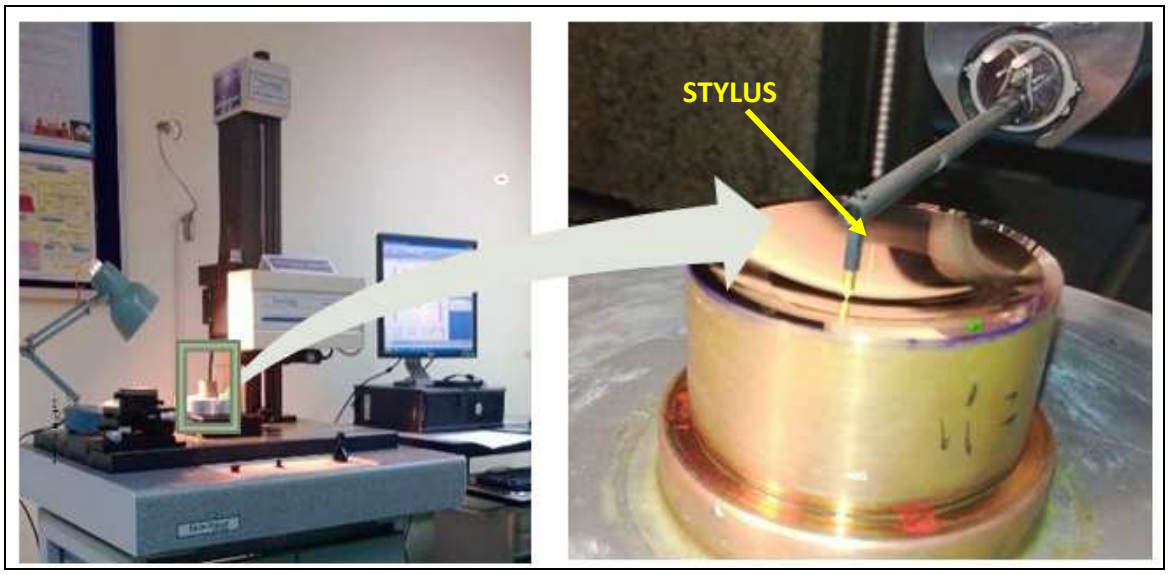

Fig.3.8: Measurement of Concave Profile of Copper alloy by Contact Type Profiler (CSIR-CSIO)

3.6.2 Coherence Correlation Interferometer – CCI 6000 Non-Contact Profiler

The Talysurf CCI is a non contact optical profiler. It makes use of coherence correlation algorithm and a high resolution digital camera array to measure the surface. A three dimensional image of the surface is generated by scanning the surface in a 'Z' direction by measuring the fringes. The information obtained by fringe measurement is processed by a dedicated software, which transforms this fringe data into a quantitatively three dimensional image.

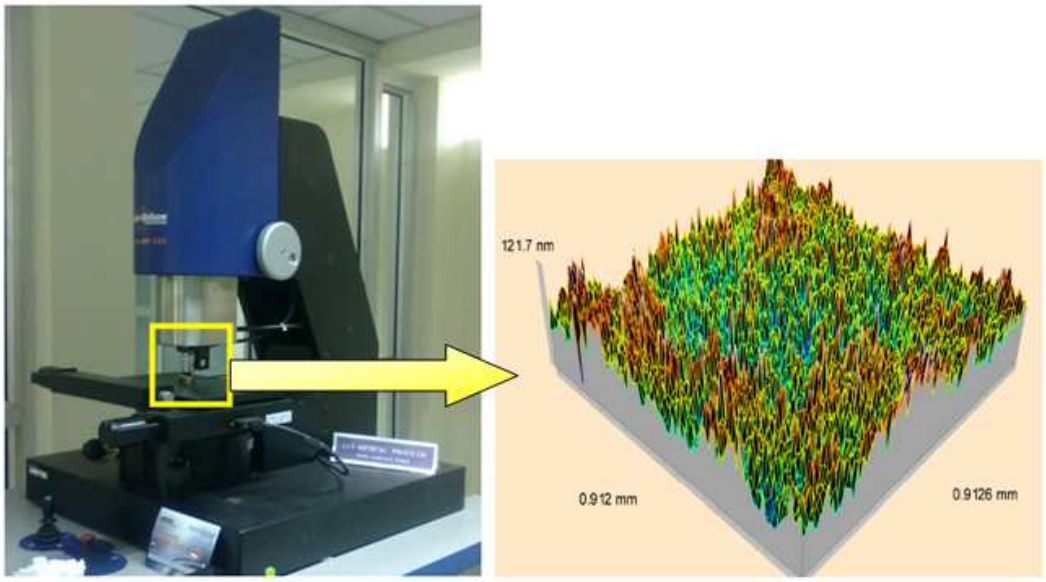

Fig.3.9: Working of CCI and wireframe output (CSIR-CSIO, Chandigarh)

Table 3.3: Technical specifications of CCI-6000

Technical specifications of CCI 6000 optical profiler	
Measurement technique	Coherence correlation interferometry
Vertical range(Z)	100µm (400µm optional)
Vertical resolution	0.1nm [1.0Å] (over full 100µm range)
Measurement area (X,Y)	0.36 mm^2 – 1.8 mm^2
Optical resolution (X,Y)	0.4 – 0.6µm (surface dependent)
Surface reflectivity	0.5% -100%
Measurement time	5-20 seconds (typical)
Measurement capabilities of CCI 6000	
Measurable Material	Glass, Metals, Polymers, Photo-Resist, Liquid Inks, Pastes
Evaluation parameters	Roughness, shape deviations, step height, critical dimensions.

3.7 PILOT EXPERIMENTATION

The effects of various input parameters i.e. spindle speed, tool feed rate, tool nose radius, depth of cut and rake angle are investigated through the pilot experimentation. In this study, rake angle is kept constant. Two responses are selected for pilot experimentation namely surface roughness (Ra) and profile error (Pt). The assignment of factors is carried out using statistical software MINITAB. Typical diamond micro turning parameters for copper material are shown in Table 3.4. All the factors are varied at three levels except the tool nose radius, which is varied at two levels. The degree of freedom required for the experiment is calculated to be 7, thus the orthogonal array that can be used should have degree of freedom (dof) greater than 7. L18 which can accommodate a combination of 2-level and 3-level factors is used for conduct of experiments to measure two response values namely, Ra and Pt.

Table 3.4: Typical diamond micromachining parameters (Geough Mc 2002)

Material	Spindle speed (rpm)	Coolant	Roughing		Finishing	
			Depth of cut (µm)	Feed rate (µm/rev.)	Depth of cut (µm)	Feed rate (µm/rev.)
Copper	800	Light oil	50	15-31.5	2.5	3.1

Table 3.4 (a): Process parameters and there levels of Pilot Experimentation

S No.	Contribution Factors	Units	Level 1	Level 2	Level 3
1	Tool nose radius	mm	0.5	1.0	---
2	Tool feed rate	µm/rev.	1	3	5
3	Depth of cut	µm	2	5	8
4	Spindle speed	rpm	1000	1500	2000

Based on the above experiment it is observed that feed rate is the most significant factor for the response Profile error (Pt) but the same factors are insignificant for the other response of the experiment i.e. surface roughness (Ra). In view of the insignificant result the experiment, its factors, procedure including measurement procedure are reviewed and

it is observes that this result might be arrived due to choosen of narrow range factors. So, to achieve the clear result for both profiles and response, four factors are varied at 3-level for the SPDT. Hence four factors are taken up for the detailed Taguchi experiment. Taguchi design has been used for the design of experiments, because it reduces the number of iterations and used to optimize the known parameters. It is worked out that while doing SPDT machining process on C18000 copper alloy the values of different parameters should be given in Table 3.4.

Table 3.4(b): Process parameters there levels and specification of work piece in Current study

SL. No.	CUTTING CONDITIONS	DESCRIPTION
1.	Work Piece	C18000 Cu-Cr-Si Nickel
2.	Profile	Flat & Spherical
3.	Cutting Tool Material	Diamond
4.	Diameter of Work piece	29.5 mm
5.	Thickness of Work piece	10 mm
6.	Hardness	15 HRC
7.	Cutting Speed	1000, 1500, 2000 rpm
8.	Feed	4, 12, 20µm/rev
9.	DOC	5, 10, 15µm
10.	Rake Angle	0^0 (Constant)
11.	Cutting Environment	Clearsol

3.8 PROCEDURE OF EXPERIMENTAL DESIGN

In the present research work tool nose radius, tool feed rate, depth of cut and the spindle speed have been considered as the control factors affecting surface finish. The average surface roughness (Ra) and profile error (Pt) are chosen as the response variable. The absolute average roughness over the sampling length of the surface is given by the Ra value. The distance between maximum peak and lowest valley over the sampling length of the surface is given by Pt value. The surface roughness and profile error are measured in three different positions by rotating the work piece at (0^0, 60^0, 120^0). The whole procedure of Taguchi method is as under.

1. Establishment of objective functions.
2. Selection of factors to be evaluated.
3. Identification of uncontrollable factors and test conditions.
4. Selection of number of levels for the controllable and uncontrollable factors.
5. Calculation of total degree of freedom needed.
6. Select the appropriate Orthogonal Array(OA)
7. Assignment of factors to columns
8. Execution of experiments according to trial conditions
9. Analyze results
10. Confirmation experiments.

3.8.1 EXPERIMENTAL OBJECTIVE

To study the surface roughness (Ra), Profile error in SPDT, it is necessary to identify and understand the factors affecting the responses. The factors affecting the responses have been studies by conducting series of machining experiments using C18000 Copper alloy as work-piece. C18000 have several properties like its high tensile strength which offers ready machinability. Schematic diagram of SPDT is shown in Fig.3.10. The effect of the different process parameters such as tool nose radius, tool feed rate, depth of cut and spindle speed has been studies and has been reported in the following chapters:

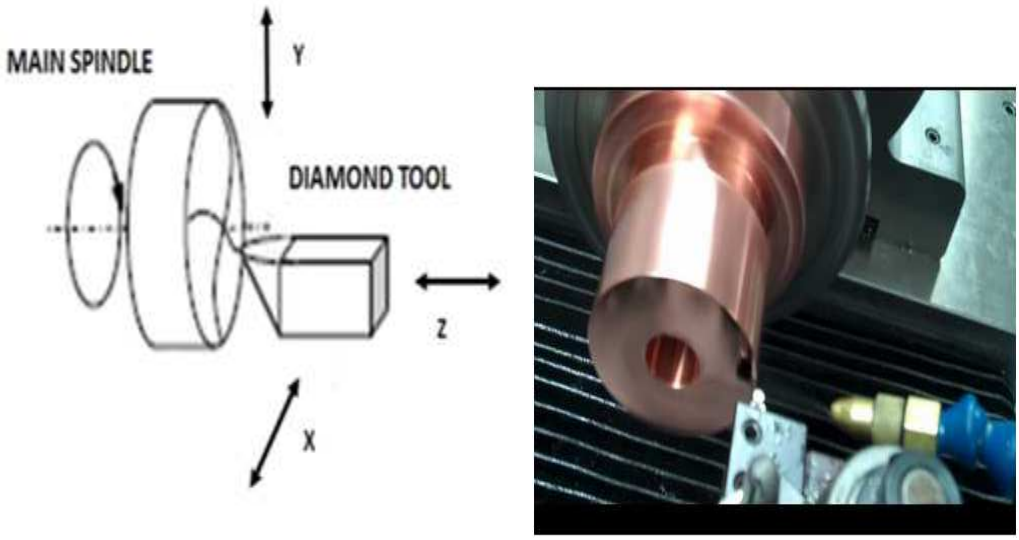

Fig.3.10: Schematic Diagram of SPDT (Lei *et al* 2000)

3.8.2 DESIGN OF THE PROFILES GENERATED

In the present work two profiles (i.e. spherical and flat) are generated on C18000 Copper alloy using single point diamond turning machining process. The designs of both the flat and spherical profiles are generated on solid works software is shown in Fig.3.11-13.

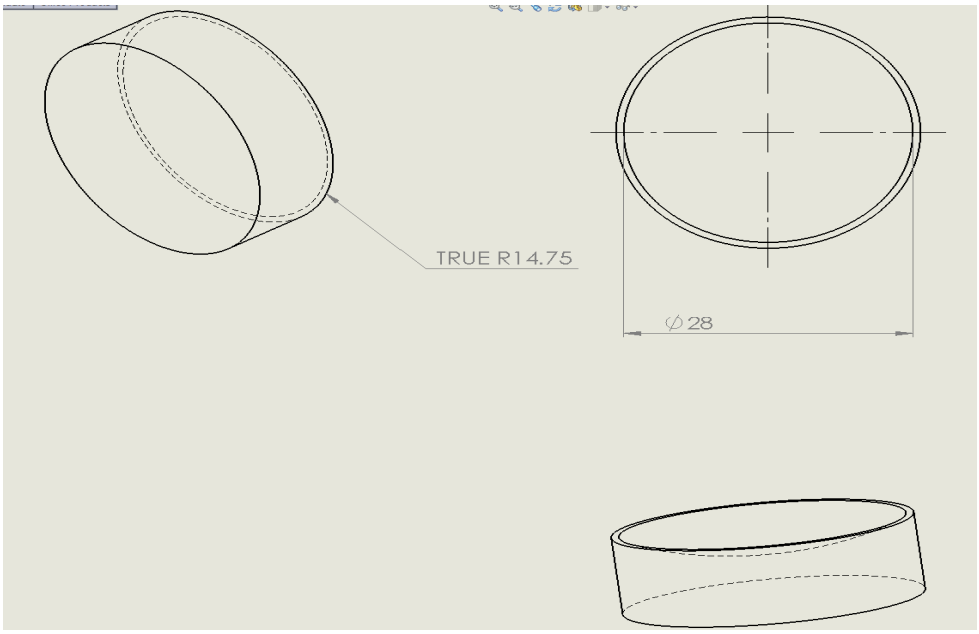

Fig.3.11: Spherical Profile design (Chromium Silicon Nickel Copper C18000)

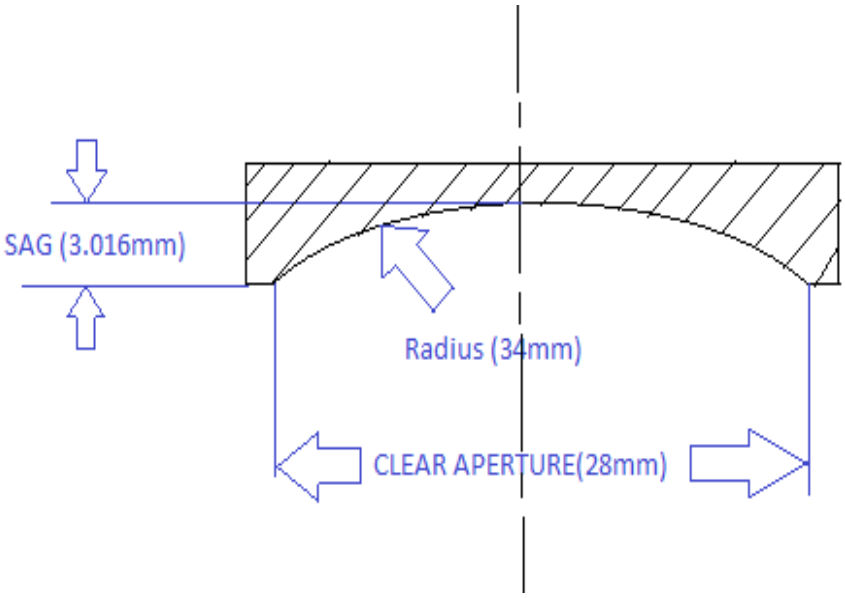

Fig.3.12: Parameters for Spherical Profile

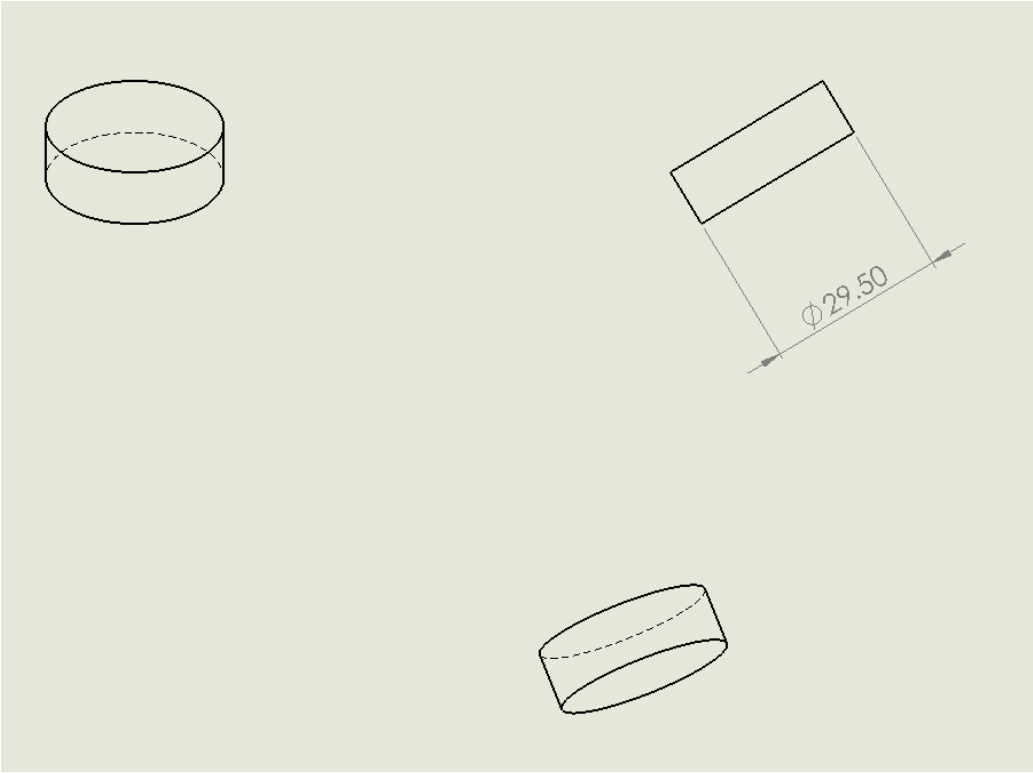

Fig.3.13: Flat Profile design

3.8.3 DEGREE OF FREEDOM (dof)

The number of factors and the level for factors determine the total degree of freedom required for the entire experiment. The degree of freedom for each factor is given by the number of levels minus one. dof for each factor: k-1; where k is the number of level for each factors.

In the present experimental setup, there are four 3-level factors. The rake angle is kept constant. The number of dof for factors A, B, C, D are two. The total dof for the experiment is given in Table 3.6. As the dof required for the experiment is 8, the orthogonal array (OA) to be used should have more than or equal to 8 dof. The most suitable orthogonal array that can be used for this experiment are L9 or L27 but due to wide scope of work i.e. flat profile and spherical profile generation, in view of the other ongoing R&D work of CSIR-CSIO the orthogonal array of L9 was chosen, which has 8 dof assigned to its various columns.

Table 3.5: Degree of freedom

Factor	A	B	C	D	Total
Degree of Freedom	2	2	2	2	8

3.9 SELECTION OF FACTORS

Determination of which factors to investigate depends on the responses of interest. The factors affecting the responses are identified using the pilot experimentation, brainstorming and literature survey done on the copper material. Lists of factors studies with their levels are shown in Table 3.5.

Table 3.6: Factors interested and their levels

CUTTING CONDITIONS					
Factors **Level**	**Spindle Speed (r. p. m)** **(A)**	**Feed Rate (µm/rev)** **(B)**	**DOC (µm)** **(C)**	**Tool Nose radius (mm)** **(D)**	**Rake Angle (Deg)** **(E)**
I	1000	4	5	0.5	0
II	1500	12	10	1	0
III	2000	20	15	1.5	0

3.10 ORTHOGONAL ARRAY

OA plays a critical part in achieving the high efficiency of the Taguchi method. To select an appropriate orthogonal array for experiments, the total degree of freedom needs to be computed. The degree of freedom are defined as the number of comparison between process parameters that need to be made to determine which level is better and specifically how much better it is. In the present study, there are eight degrees of freedom owing to the four cutting parameters in machining operations. Once the degrees of freedom are known, the next step is to select an appropriate orthogonal array to fit the specific task. The degrees of freedom for the orthogonal array should be greater than, or at least equal to, those for the process parameters. Basically, the degree of freedom for the

orthogonal array should be greater than or at least equal to those for the process parameters. In this study, an L_9 orthogonal array with four columns and nine rows are used. Once the appropriate orthogonal array has been selected, the factors can be assigned to the various columns.

Table 3.7: L9 Experimental design

Trial No.	TNR (mm)	TFR (µm/rev.)	DOC (µm)	SS (rpm)
1	0.5	4	5	1000
Trial No.	**TNR (mm)**	**TFR (µm/rev.)**	**DOC (µm)**	**SS (rpm)**
2	0.5	12	10	1500
3	0.5	20	15	2000
4	1.0	4	10	2000
5	1.0	12	15	1000
6	1.0	20	5	1500
7	1.5	4	15	1500
8	1.5	12	5	2000
9	1.5	20	10	1000

3.11 EXPERIMENTAL PROCEDURE

The diamond turned material, nickel silicon chromium copper alloy is composed by weight of 2.0% to 3.0% Nickel, 0.4% to 0.8% Silicon, 0.1% to 0.5% Chromium, and the balance Copper. The micro-hardness of the material is 180-210 HV. In addition to its high strength and excellent thermal conductivity, the alloy has a good thermal stability at relatively high temperatures and excellent resistance to softening at elevated temperatures. Pure copper is considered as a soft material that is easily machinable; however, with the addition of chromium and copper becomes hard and its machining may be accompanied with a number of difficulties related to form error and subsequently final surface finish. The position feedback resolution of the machine is 3.6 nm. Three levels of cutting speeds 1000, 1500 and 2000rpm are selected for the test. The cutting speeds are tried at three values of feed rate: 4, 12, and 20µm/rev; depth of cut is varied at 5, 10, 15µm. Therefore, three different tool nose radii 0.5, 1.0, 1.5mm diamond tool inserts are employed in this study. An aluminum 6061 fixture is used to hold the work piece and

fixture directly mounted on the vacuum chuck of the machine. When performing the ultra-precision turning tests, a bigger depth of cut (10–20µm) is first used for 2-3 times to get rid-off the plastic deformation layer and other damages induced by former turning process conducted on the normal precision lathe. The X and Y axes are controlled to produce a high precision flat mirror on a C18000 work piece of 30mm diameter. In the machining tests, non-controlled waviness single-crystal natural diamond inserts are mounted on a tool holder. The diamond inserts had a rake angle of 0^0 and clearance angle of 10^0. The inserts are manufactured by Apex Company. The machining tests are performed using a coolant in the form of odourless Clearsol mist. The practice using coolant in diamond turning is that the nozzle is usually directed in the way shown in Fig.3.14. We kept this direction unchanged for the experiments. The positioning of the nozzle in this way may help to drive the chip away from the cutting zone and reduce chip tangling effect.

The diamond turned surface is cleaned with alcohole and surface roughness is measured immediately when a turning test has been done. Surface roughness measurements are conducted on a Form Talysurf–120 surface analysis instrument with a 2µm radius stylus. Spacing, cut off length and assessment length are set as 0.8mm, 0.0025mm and 28.5mm, respectively.

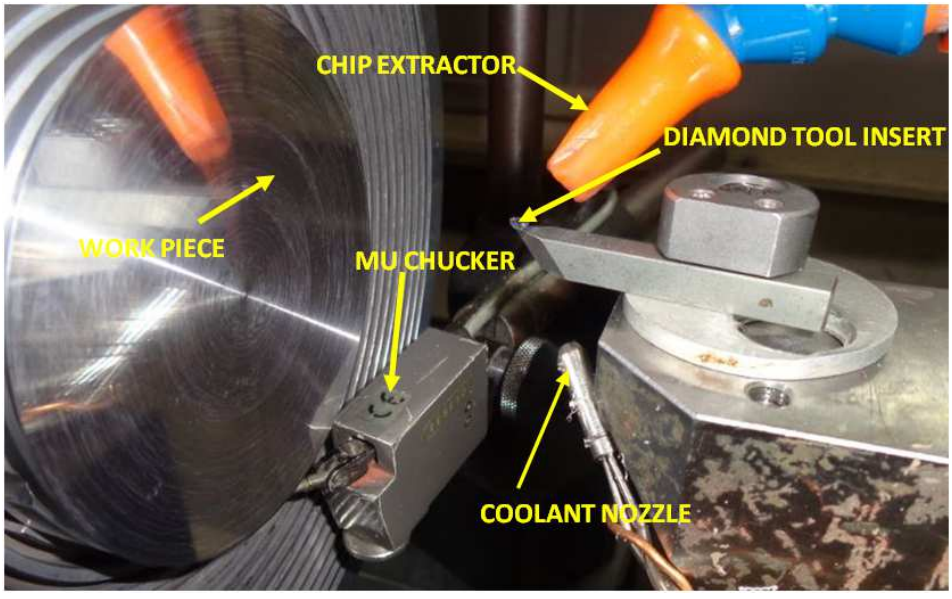

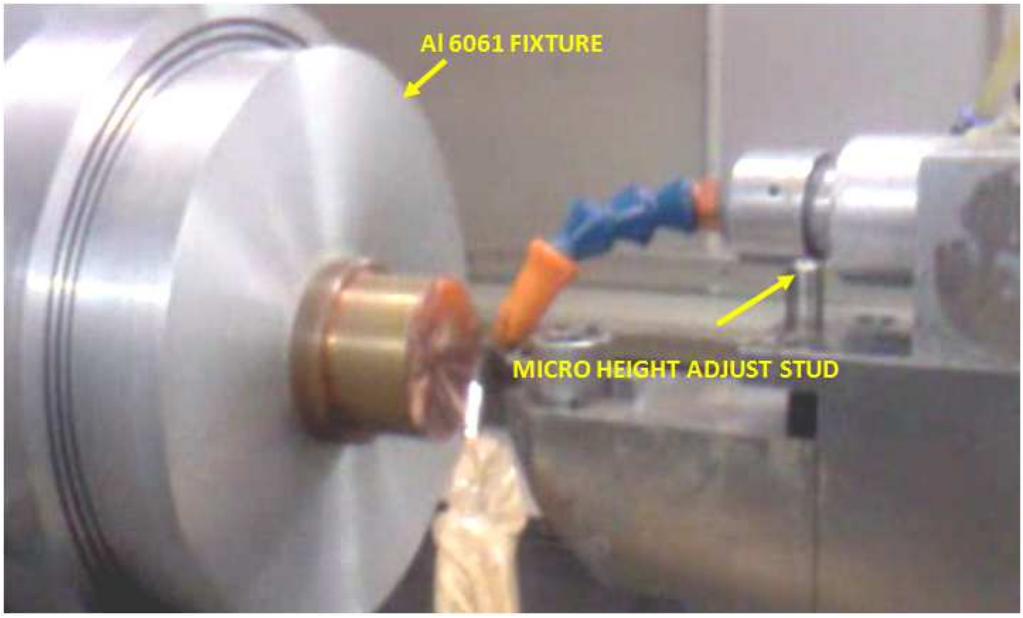

Fig.3.14: The work piece and tool setup (CSIR-CSIO, Chandigarh)

3.11.1 PREPARATION OF BLANK

First of all the blanks with extra thickness of 100µm are prepared. These blank are prepared on low precision machine which has accuracy around 100µm. To achieve the form accuracies in sub-micron region these blanks are again turned with SPDT. A contour shape HSS tool with required radius is made on the grinding machine to give the disc spherical shape as shown in Fig.3.15.

(a)Spherical Profile

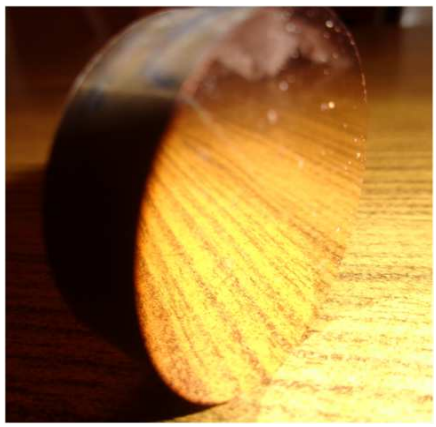

(b) Flat Profile

Fig.3.15: Blank prepared on the conventional lathe machine

3.11.2 PREPARATION ON FIXTURE

Aluminium 6061 which is aluminium alloy material is used as a fixture material. The Design and Fig.3.16 is given below.

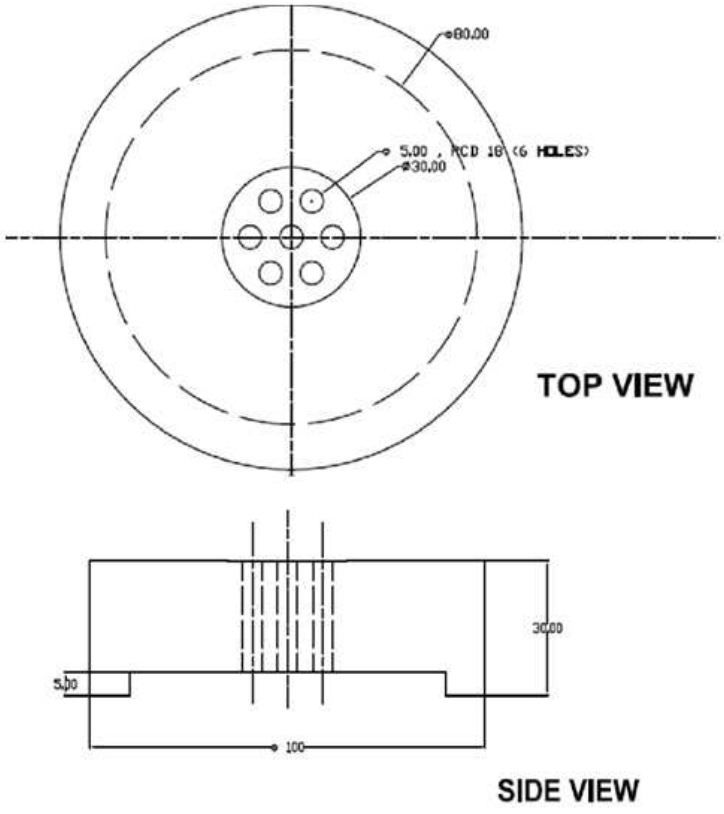

Fig.3.16: Design of Fixture for the mounting of job

3.11.3 LAPPING

Nanoform-250 diamond turning equipment is a high precisions machine. It uses air vacuum chuck because the surface of component is too rough to produce good vacuum during holding, for that reason firstly, the components and the fixtures are lapped with loose abrasive grinding to get smooth surface.

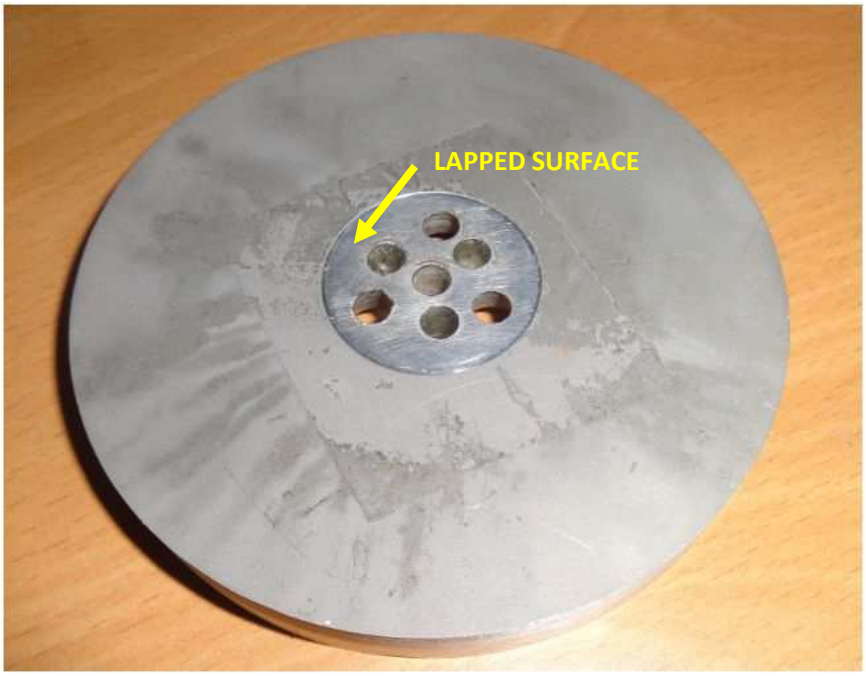

Fig.3.17: Lapping of the Al6061 fixture

3.11.4 SIDE TURNING

The side surface of the blank is quite tough which limits the centering of job. To achieve the centering or job within 1 to 2 micron, side surface of components are turned with SPDT.

3.11.5 FACE TURNING

After prefacing the blanks on low precision lathe, there might be a wedge between back and front surfaces. To remove this tilt, blanks are again faced with diamond turning. This may take few cycles of face turning depending upon wedge present.

3.11.6 MEASURING TOOL RADIUS

Whenever a curved surface is required to be turned, the tool radius has to be given to the CNC program. If the tool radius given to the program is not accurate, then surface profile will be different from the intending one. The measurement of tool radius is done by LVDT in which a ruby crystal ball contacts the tool on three different points for 2-3 times repetitively and gives best fit radius. This process has to be done each time when a new tool is used.

3.11.7 TOOL PATH GENERATION

Single point diamond turning (NanoForm-250) machine works based on computer numerically controlled (CNC) program. The CNC program consists of two parts: one is .NC program and another is .SUB file. First part deals with machining parameters and commands for running the machine. The .SUB file gives path of the tool and it is generated by Diffsys software. The Diffsys software is used to generate the tool path. DIFFSYS generates X-axis vs. Z-axis values (tool path), derived as per spherical design. These values are then given to SPDT.

3.12 WORK MATERIAL

A solid bar of C18000 Copper Chromium Nickel Silicon with 29.5mm diameter, 10mm thickness and of ~15 HRC is used as work piece Fig.3.18.

3.12.1 REASON FOR CHOOSING THE MATERIAL

Copper Chromium Nickel Silicon Alloys, which also called Beryllium Free Copper alloy. This material finds its wide applications in many fields. Nickel Silicon Chromium copper is one of the suitable candidates for both machining and molding point of view. It is an excellent and unique copper alloy with high electrical conductivity, hardness, and ductility, moderate strength, and excellent resistance to softening at elevated temperatures. It offers very good surface finish.

Copper is widely used material in making moulds for developing high quality lenses used in precision optics for production. The moulds surface texture replicates the lens quality, so very fine smooth mould surface are of great interest in the present scenario.

C18000 alloy is an excellent substitute for copper beryllium alloys C17500 and C17510 in terms of many applications. Typical Application for C18000 copper chromium nickel silicon alloy: Industry: Heat Sink Inserts in Steel Plastic Molds, Core & Ejector Pins for Injection Molds.

Fig.3.18: C18000 Copper Alloy rod

Table 3.8: The chemical composition of C18000 Copper Chromium Nickel Silicon in percentage by weight (Reference: www.mipalloy.com)

Alloy	Nickel	Silicon	Chromium	Copper
UNS C18000	1.8-3.0	0.4-0.8	0.1-0.8	Balance

PHYSICAL PROPERTIES (Reference: www.mipalloy.com)

Elastic modulus	Melting Point (Solidus)	Density	Thermal Expansion	Thermal Conductivity (100^0C)	Heat Capacity (100^0C)
18,500 Ksi	~ 1900F	0.318 lb/in^3	9.72 x 10^{-6} in/in^{0}F	130 BTU/hr.ft.^{0}F	0.095 BTU/lb.^{0}F
130GPa	~1040^{0}C	8.81g/cm^3	17.5 x 10^{-6} ^{0}C^{-1}	225W/m.K	0.398 J/g.K

MECHANICAL PROPERTIES (Reference: www.mipalloy.com)

0.2% offset yield Strength	Ultimate Tensile Strength	Elongation	Hardness
75 Ksi 520MPa	95 Ksi 655 MPa	14%	92 HRB HV 180-210

3.13 CUTTING TOOLS

Diamond tools with different geometry are chosen for this experimental work.

Fig.3.19 (a) Dimaond tools

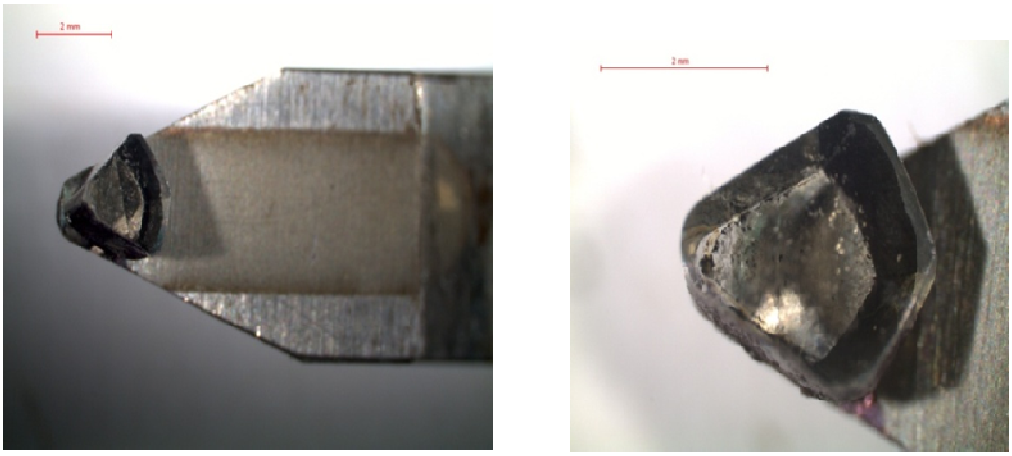

Fig.3.19 (b): Tool images from Optical Microscope

3.13.1 TOOL GEOMETRY

Table 3.9: Tool geometry

Tool	I	II	III
Name of the Company	**APEX**	**APEX**	**APEX**
Top Rake (Deg)	0	0	0
Front Clearance(Deg)	10	10	10
Radius(mm)	0.544	1.056	1.543

3.14 ANALYSIS OF RESULTS

3.14.1 SIGNAL-TO-NOISE RATIO

The parameters that influence the output can be categorized into two classes, namely controllable (or design) factors and uncontrollable (or noise) factors. Controllable factors are those factors whose values can be set and easily adjusted by the designer. Uncontrollable factors are the sources of variation often adjusted with operational environment **(Ross PJ 1996)**. The best settings of control factors as they influence the output parameters are determined through experiments. From the analysis point of view, there are three possible categories of the responses characteristics explained below.

r is the number of tests in a trial (noise of repetitions regardless of noise levels)

$\sum_{i=1}^{r} y_j^{\,2}$ = summation of all responses values under each trial

MSD = Mean square deviation

$y_{j\,=\,observes}$ value of the response characteristic

$y_{o\,=}$ nominal or target value of the results

The three different response characteristics are given by the following.

1) **Higher is Better.** The S/N for higher the better is given by:

$(S/N)_{HB} = -10\ log\ (MSD_{HB})$

(Equation..3.1)

Where $MSD_{HB} = \frac{1}{r}\sum_{j=1}^{r}\left(\frac{1}{y_j^2}\right)$

(Equation..3.2)

2) **Nominal is Better.** The S/N for nominal the better is given by:

$(S/N)_{NB} = -10\ log\ (MSD_{NB})$

(Equation..3.3)

Where $MSD_{NB} = \frac{1}{r}\sum_{j=1}^{r}(y_j - y_o)^2$

(Equation..3.4)

3) **Lower is Better.** The S/N for lower the better is given by:

$(S/N)_{LB} = -10\ log\ (MSD_{LB})$

(Equation..3.5)

Where $MSD_{LB} = \frac{1}{r}\sum_{j=1}^{r}(y_j^2)$

(Equation..3.6)

For this experimental work, response characteristics have given in the Table 3.10.

Table 3.10: Response Characteristics

Response Name	Response Type	Units
Surface Roughness (Ra)	Lower the better	nm
Profile error (Pt)	Lower the better	µm

3.14.2 ANALYSIS OF VARIANCE (ANOVA)

ANOVA is a statistical technique which can infer some important conclusions based on analysis of the experimental data **(Ross PJ 1996)**. The method is very useful for revealing the level of significance of influence of factor(s) or interaction of factors on a particular response. It separates the total variability of the response (sum of squared deviations about the grand mean) into contributions rendered by each of the parameter/ factor and the error. Thus

$\mathbf{SS_T = SS_F + SS_E}$

Where, $SS_T = \sum_{J=1}^{p} (\gamma_j - \gamma_m)^2$

Where, SS_T = Total sum of squared deviations about the mean.

γ_j = Mean response for j^{th} experiment.

γ_m = Grand mean of the response.

SS_F = Sum of squared deviations due to each factor.

SS_E = Sum of squared deviations due to error.

In the ANOVA table mean square deviation is defined as:

MS = Mean Square

$$\mathbf{MS} = \frac{\mathbf{SS\ (Sum\ of\ squared\ division)}}{\mathbf{DOF\ (Degree\ of\ Freedom)}}$$

F-value of Fisher's F ratio (Variance ratio) is defined as:

$$\mathbf{F} = \frac{\mathbf{MS\ for\ a\ term}}{\mathbf{MS\ for\ the\ error\ term}}$$

Depending on F value, P-value (probability of significance) is then calculated. If P-value for a term appears less than 0.05 (For 95% confidence level) then it can be concluded that the effect of the factors / interaction of factors is significant on the selected response. Significance of all the dependent variables has been completed using statistical software MINITAB15.

CHAPTER 4 DATA ANALYSIS AND RESULT

4.1 EXPERIMENTAL RESULTS AND DATA ANALYSIS

The objective of experiment is to optimize the Diamond turning parameters to get better (i.e. low value) surface roughness and Profile error values; the smaller the better characteristics are used. For studying which factor is more significant and optimization of single response Pareto ANOVA and S/N response method are used, and further for the optimization of multiple responses Grey Relational Analysis is used.

4.2 SIGNAL TO NOISE (S/N) RESPONSE ANALYSIS

Taguchi used the S/N ratio as the quality characteristic of choice to analyze the data **(Zhang *et al.* 2007)** S/N ratio is used as a measurable value instead of standard deviation due to the fact that as the mean decreases, the standard deviation also decreases and vice versa. The methods for calculating the S/ N ratio are classified into three main categories, depending on whether the desired quality characteristics are smaller the better, larger the better or nominal the better. In the case of surface roughness and profile error, the smaller values are always preferred. The equation for calculating the S/N ratio for smaller the better characteristics (in decibel) is as follows **(Kurniawan *et al.* 2010):**

$$\frac{S}{N} = -10\log\frac{1}{n}(\sum Y_i^2) \qquad (1)$$

Where, Y_i is the individual measured surface roughness or profile error in first, second, and third columns in Table 4.1 and Table 4.4, and n is the number of the individual measured. In this case, n=3. For each type of the characteristics, the higher the S/N ratio the better is the result.

Furthermore, the S/N response data of the profile error and surface roughness are calculated and summarized in Tables 4.2, 4.3, 4.5, 4.6 respectively.

Table 4.1: Experimental Result Matrix for Flat Profile

Trial No	TNR (mm)	TFR (µm/rev.)	DOC (µm)	RPM (rpm)	Ra 1 (nm) (0^0)	Ra 2 (nm) (60^0)	Ra3 (nm) (120^0)	SN Ra	Pt 1 (µm) (0^0)	Pt 2 (µm) (60^0)	Pt3 (µm) (120^0)	SN Pt
1	0.5	4	5	1000	14.5	16.1	14.2	-23.502	0.837	0.772	0.662	2.375
2	0.5	12	10	1500	26.8	26.7	25.7	-28.433	0.436	0.542	0.517	6.007
3	0.5	20	15	2000	45.7	46.1	45.8	-33.230	0.480	0.486	0.434	6.603
4	1.0	4	10	2000	13.6	14.9	14.7	-23.174	0.659	0.666	0.501	4.237
5	1.0	12	5	1000	13.5	14.1	13.3	-22.694	0.432	0.407	0.554	6.578
6	1.0	20	5	1500	19.3	18.0	20.1	-25.644	0.364	0.366	0.408	8.396
7	1.5	4	15	1500	14.6	17.3	19.2	-24.679	0.836	0.650	0.562	3.187
8	1.5	12	5	2000	18.7	19.3	19.2	-25.606	0.383	0.413	0.305	8.632
9	1.5	20	10	1000	22.1	22.0	22.2	-26.887	0.253	0.324	0.508	8.459

Table 4.2 S/N ratio response data of resultant Surface roughness (Ra) for Flat Profile

FACTORS		A_i (TNR)	B_i (TFR)	C_i (DOC)	D_i (RPM)
LEVEL	**1**	-85.1658	-71.3553	-74.753	-73.084
Summation at the input parameters	**2**	-71.593	-76.734	-78.495	-78.757
	3	-77.173	-85.762	-80.603	-82.01
Delta = (Max – Min)		13.5728	14.4067	5.85	8.926
Rank		**2**	**1**	**4**	**3**

Table 4.3 S/N ratio response data of resultant Profile error (Pt) for Flat Profile

FACTORS		A_i (TNR)	B_i (TFR)	C_i (DOC)	D_i (RPM)
LEVEL	**1**	14.98624	9.8003	19.40395	17.41411
Summation at the input parameters	**2**	19.21224	21.21819	18.70398	17.59102
	3	20.27959	23.45958	16.37014	19.47294

FACTORS	A_i (TNR)	B_i (TFR)	C_i (DOC)	D_i (RPM)
Delta = (Max – Min)	5.29335	13.65928	3.03381	2.05883
Rank	**2**	**1**	**3**	**4**

Table 4.4 Experimental Result Matrix for Spherical Profile

TRIAL NO	TNR (mm)	TFR (µm/rev.)	DOC (µm)	RPM	Ra 1 (nm)	Ra 2 (nm)	Ra3 (nm)	SN Ra	Pt 1 (µm)	Pt 2 (µm)	Pt3 (µm)	SN Pt
1	0.5	4	5	1000	18.5	17.6	18.4	-25.188	0.467	0.382	0.215	8.641
2	0.5	12	10	1500	39.2	41	39.4	-32.014	0.206	0.417	0.415	8.877
3	0.5	20	15	2000	42	41.8	44.5	-32.626	0.284	0.495	0.384	8.022
4	1	4	10	2000	14.9	13.7	14.1	-23.071	0.455	0.545	0.256	7.216
5	1	12	15	1000	13.5	14	13.9	-22.799	0.654	0.482	0.357	5.806
6	1	20	5	1500	18.2	19.6	19.4	-25.610	0.554	0.407	0.432	6.579
7	1.5	4	15	1500	18.9	16.2	17.4	-24.878	0.628	0.633	0.555	4.349
8	1.5	12	5	2000	14.2	14.3	19	-24.077	0.578	0.638	0.704	3.849
9	1.5	20	10	1000	16.1	13.4	13.9	-23.236	0.537	0.785	0.730	3.200

Table 4.5 S/N ratio response data of resultant Surface roughness (Ra) for Spherical Profile

FACTORS		A_i (TNR)	B_i (TFR)	C_i (DOC)	D_i (RPM)
LEVEL	**1**	-89.8273	-73.1371	-74.8752	-71.222
Summation at the input parameters	**2**	-71.4802	-78.8901	-78.3213	-82.5021
	3	-72.1913	-81.4716	-80.3023	-79.7747
Delta = (Max – Min)		18.3471	8.3345	5.4271	11.2801
Rank		**1**	**3**	**4**	**2**

Table 4.6 S/N ratio response data of resultant Profile error (Pt) for Spherical Profile

FACTORS		A_i (TNR)	B_i (TFR)	C_i (DOC)	D_i (RPM)
LEVEL	**1**	25.5397	20.2053	19.0689	17.646
Summation at the input parameters	**2**	19.6004	18.5317	19.2925	19.8045
	3	11.3982	17.8012	18.1768	19.086

FACTORS	A_i (TNR)	B_i (TFR)	C_i (DOC)	D_i (RPM)
Delta = (Max – Min)	14.1415	2.4041	1.1157	2.1585
Rank	**1**	**2**	**4**	**3**

The desired "smaller the better" criteria implies that the lowest surface roughness would be the ideal result, while the largest S/N ratio response would reflect the best response which results in the lowest noise. This is the criteria employed in this study to determine the optimal machining parameters. The S/N ratio graphs of the resultant profile error and surface roughness for selecting the best combination levels for minimum surface roughness are shown in Fig.4.1, 4.2, 4.3 and 4.4.

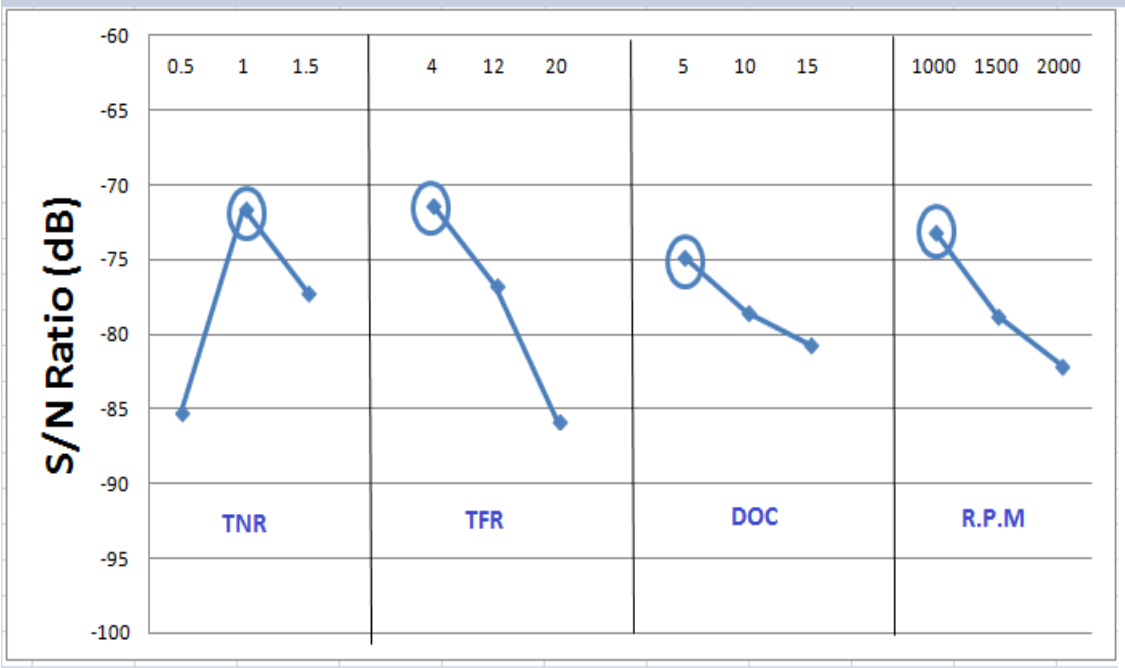

Fig.4.1 S/N ratio response graph of resultant Surface Roughness Flat Profile

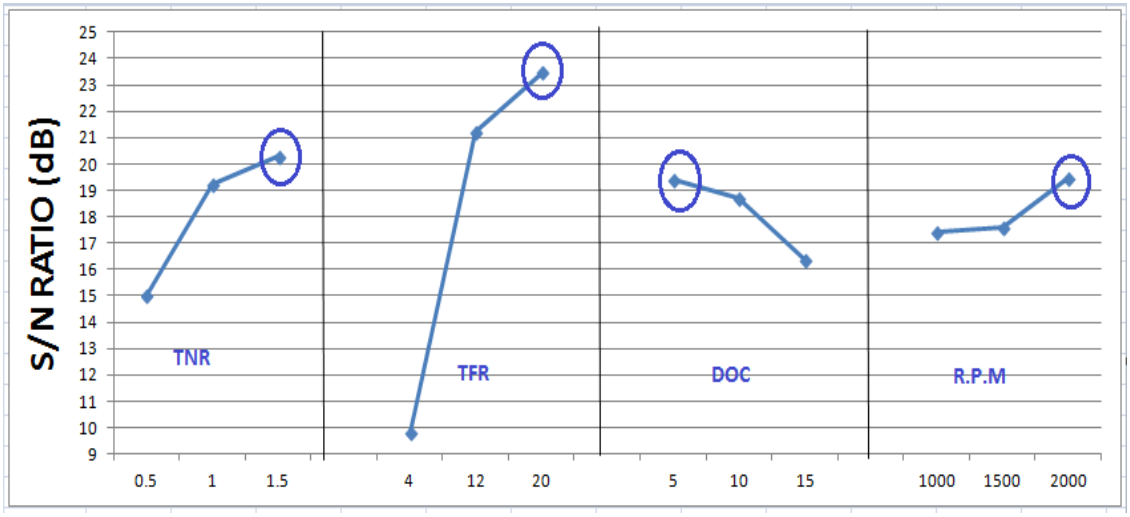

Fig.4.2 S/N ratio response graph of resultant Profile Error (Pt) Flat Profile

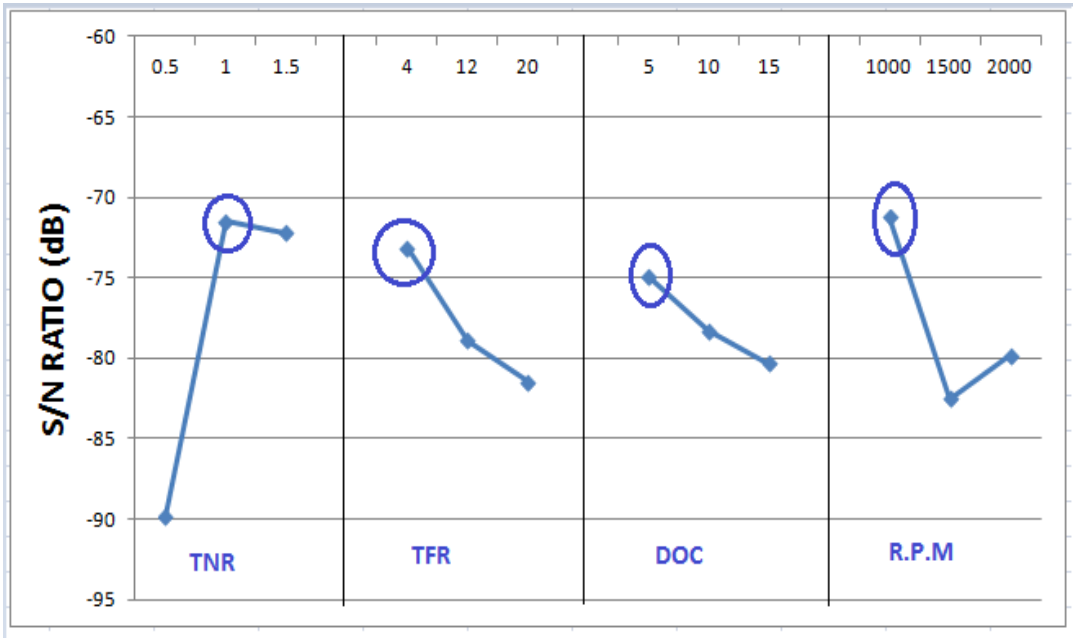

Fig.4.3 S/N ratio response graph of resultant Surface Roughness Spherical Profile

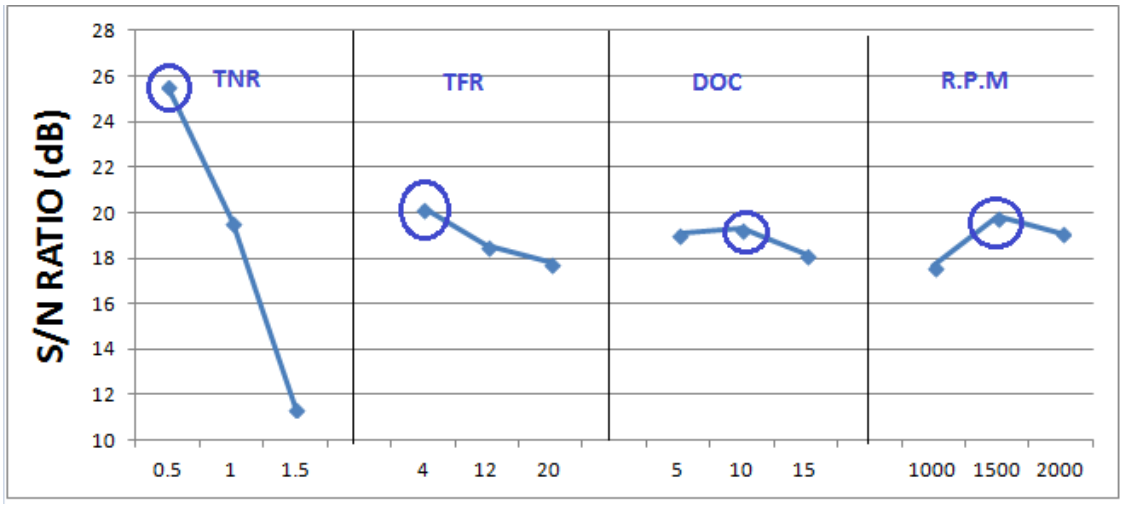

Fig.4.4 S/N ratio response graph of resultant Profile Error (Pt) Spherical Profile

For the surface roughness, Fig.4.1 shows that the tool feed rate (factor B) is found to be more significant followed by the tool nose radius (factor A) and the spindle speed (rpm) (factor D). Consequently, the intermediate value of tool nose radius (A2, 1.0 mm), with the lowest feed rate (B1, 4µm/rev.), lowest depth of cut (C1, 5µm), and the spindle speed (rpm) (D1) is suggested as optimal parameters in order to obtain better surface roughness value. Therefore, the optimal parameters combination is set as (A2 B1 C1 D1).

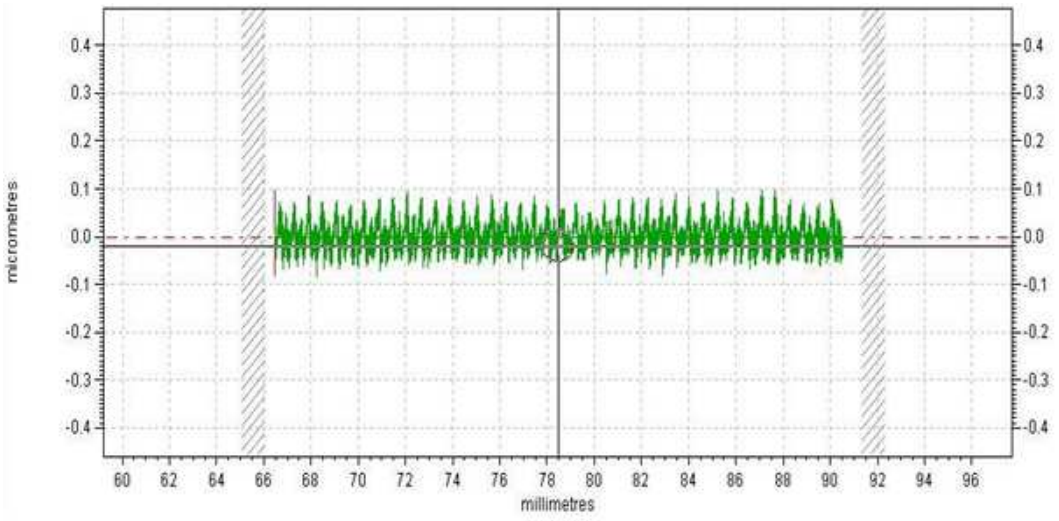

Fig.4.5 Results from Contact Type Profiler with (1.0mm, 4µm/rev., 5µm, 1000rpm) Ra = 12.5nm

For the Profile error (Pt), As seen in Fig.4.2, and based on the higher the S/N ratio the better is the result, the feed rate (factor B) is found to be more significant followed by the tool nose radius (factor A), the depth of cut (factor C), and spindle speed (rpm) (factor D). Consequently, the intermediate value of tool nose radius (A3, 1.5mm), the highest value of the feed rate (B3, 20µm/rev.), the lowest value of the depth of cut (C1, 5µm) and highest spindle speed (rpm) is suggested as optimal parameters in order to obtain better surface roughness (A3 B3 C1 D3).

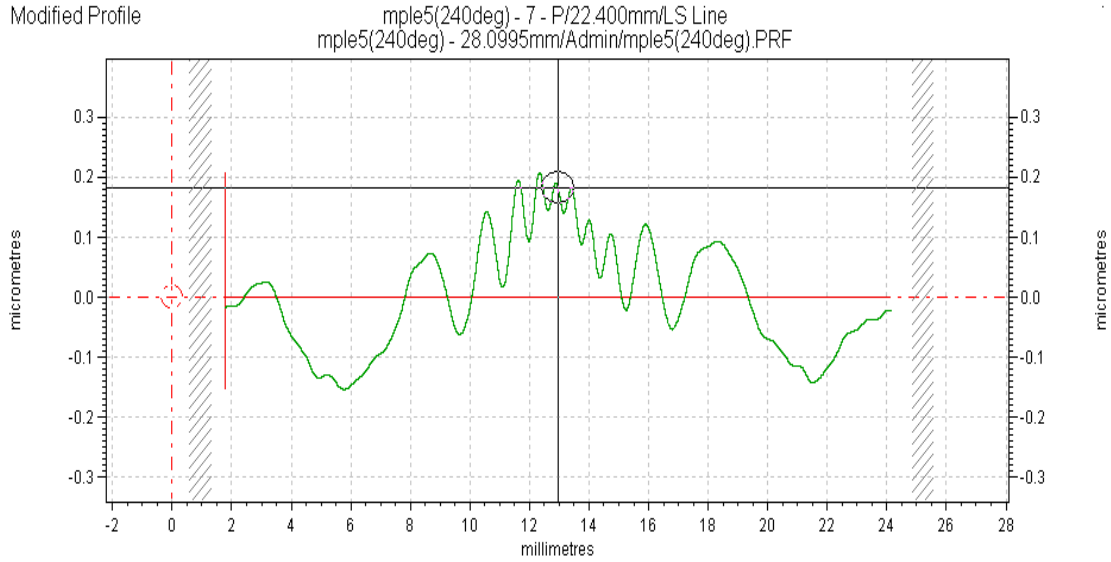

Fig.4.6 Results from Contact Type Profiler with (1.5mm, 20µm/rev., 5µm, 2000rpm) Pt =0.3265µm

For Spherical profile the surface roughness, Fig.4.3 shows that the tool nose radius (factor A) is found to be more significant followed by the spindle speed (rpm) (factor D) and tool feed rate (factor B). Consequently, the intermediate value of tool nose radius (A2, 1.0 mm), with the lowest feed rate (B1, 4µm/rev.), lowest depth of cut (C1, 5µm), and the spindle speed (rpm) (D1) is suggested as optimal parameters in order to obtain better surface roughness value. Therefore, the optimal parameters combination is set as (A2 B1 C1 D1).

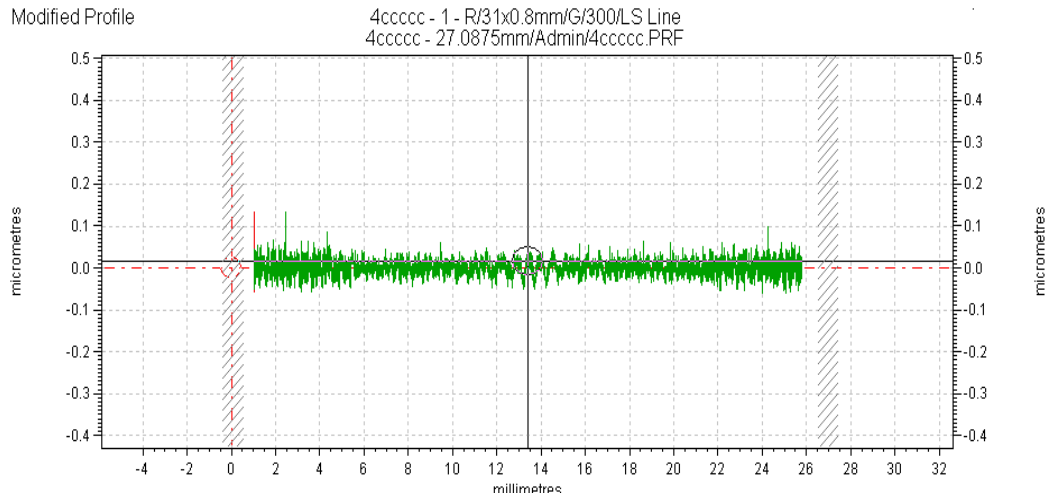

Fig.4.7 Results from Contact Type Profiler with (1.0mm, 4µm/rev., 5µm, 1000r.p.m) Ra = 12.8nm

For Spherical profile the Profile error, Fig.4.4 shows that the tool nose radius (factor A) is more significant followed by the tool feed rate (factor B) and spindle speed (factor D). Consequently, the intermediate value of tool nose radius (A1, 0.5 mm), with the lowest feed rate (B1, 4µm/rev.), depth of cut (C2, 10µm), and spindle speed (D2) is suggested as optimal parameters in order to obtain better surface roughness value. Hence, the optimal parameters combination is set as (A1 B1 C2 D2).

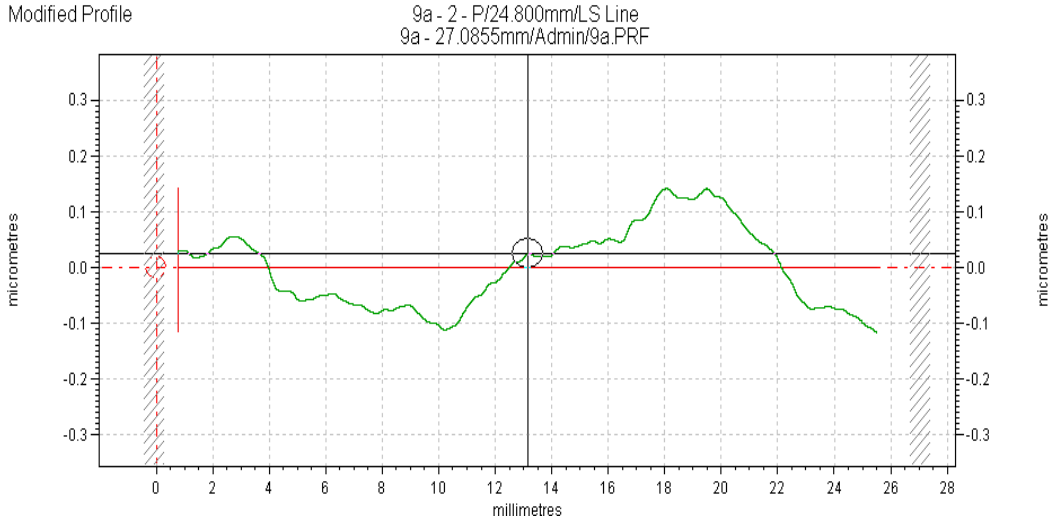

Fig.4.8 Results from Contact Type Profiler (0.5mm, 4µm/rev., 10µm, 15 1500r.p.m) Pt = 0.2597µm

4.3 PARETO ANOVA: AN ALTERNATIVE ANALYSIS

One of the methods to analyze data for process optimization is the use of Pareto ANOVA **(Park 1996)**. Pareto ANOVA is a simplified ANOVA method which uses Pareto principles. It is a quick and easy method to analyze results of parameter design. It does not require an ANOVA table and therefore does not use *F*-tests. It exhibits the percentage of factor influence for each parameter in a very simple way **(Zhang *et al* 2007)** The Pareto ANOVA technique of analysis has been performed, which requires least knowledge about ANOVA method and suitable for engineers and industrial practitioners. Pareto ANOVA for resultant surface roughness and profile error are constructed in Tables 4.7-10, respectively, the summation of squares of differences (S) for each control factor is calculated such that, for example, S_a can be obtained by the following equation:

$$S_a = (A1 - A_2)^2 + (A1 - A_3)^2 + (A2 - A_3)^2 \qquad (2)$$

S_b, S_c, and S_d are similarly calculated. The contribution ratio for each factor is obtained as the percentage of the summation of squares of differences for each factor to the total of summation of squares of differences. The Pareto diagram is plotted organizing the factors in order such that the one has higher contribution comes first followed by the others. The significant factors or parameters are chosen from the left-hand side of the Pareto diagram, which cumulatively contribute up to 90%.

In Table 4.7, the feed rate (factor B, percentage of 41.17 %), tool nose radius (factor A, percentage of 36.15 %), and cutting speed (factor D, percentage of 15.84%) give prominent effect on the Surface roughness. However, the depth of Cut (factor C, percentage of 6.81%) is found to be statistically insignificant. The best combination for lower resultant Surface roughness is A2 B1 C1 D1. This result is found to be similar to the result obtained by S/N ratio response analysis.

In Table 4.8, the Profile error data is similarly calculated. It is suggested that the tool feed rate (factor B, percentage of 82.14 %) is the prominent factor affecting the profile error followed by tool nose radius (factor A, percentage of 11.98 %) and axial depth of cut (factor C, percentage of 3.86%). Similarly, the spindle speed (factor D, percentage of

1.99%), both depth of cut and spindle speed is found to be statistically insignificant. The recommended optimal parameter combination for better profile error is A3 B3 C1 D3. This result is also found to be similar to the results obtained from S/N ratio response analysis. In Table 4.9, the tool nose radius (factor A, percentage of 64.14 %), spindle speed (rpm) (factor D, percentage of 20.6 %), and tool feed rate (factor B, percentage of 10.8 %) give prominent effect on the Surface roughness. However, the Depth of Cut (factor C, percentage of 4.5%) is found to be statistically insignificant. The best combination for lower resultant Surface roughness is A2 B1 C1 D1. This result is found to be similar to the result obtained by S/N ratio response analysis. In Table 4.10, the Profile error data is similarly calculated. It is suggested that the tool nose (factor A, percentage of 94.25 %) is the prominent factor affecting the profile error followed by tool feed rate (factor A, percentage of 2.83 %) and cutting speed (factor D, percentage of 2.254 %). Similarly, the depth of cut (factor C, percentage of 0.7 %), tool feed rate, depth of cut and spindle speed is found to be statistically insignificant. The recommended optimal parameter combination for better profile error is A1 B1 C2 D2. This result is also found to be similar to the results obtained from S/N ratio response analysis.

Table 4.7 Pareto ANOVA Analysis for Surface Roughness Flat Profile

FACTOR		Ai (TNR)	Bi (TFR)	Ci (DOC)	Di (R.P.M)
LEVEL	1	-85.1658	-71.3553	-74.753	-73.084
Summation at the	2	-71.593	-76.734	-78.495	-78.757
input parameter	3	-77.173	-85.762	-80.603	-82.01
Total of summation at factor level		-233.931	-233.851	-233.851	-233.851
Summation of square of Differences		S_a=279.236	S_b=317.99	S_c= 52.66	S_d= 122.35
Total of Summation of square Differences		$S_t = S_a + S_b + S_c + S_d$			
		772.236			
Contribution %		36.15	41.17	6.81	15.84
Pareto Diagram		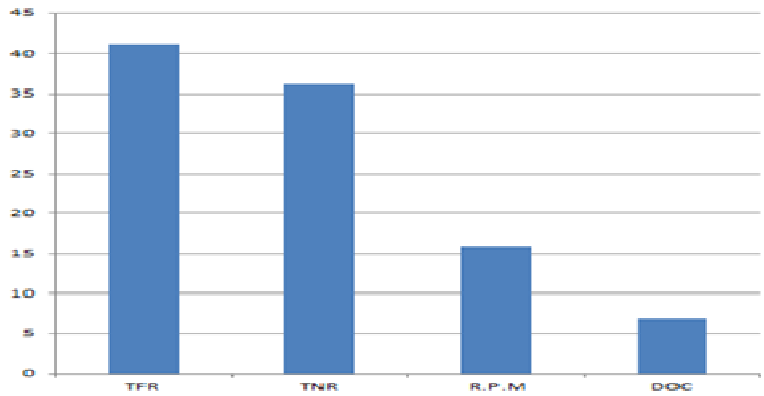			
Cumulative Contribution Ratio		41.17	77.32	93.16	100
Optimum Combination		B 1*	A 2*	D 1*	C 1
The significant factors are chosen from the left hand side in the above Pareto Diagram, which Cumulatively Contributes up to 90%					
Overall optimum condition for all factors		A2 B1 C1 D1			

Table 4.8 Pareto ANOVA analysis for Profile Error (Pt) Flat Profile

FACTOR		A_i (TNR)	B_i (TFR)	C_i (DOC)	D_i (RPM)
LEVEL	**1**	14.98624	9.8003	19.40395	17.41411
Summation at the	**2**	19.21224	21.21819	18.70398	17.59102
input parameter	**3**	20.27959	23.45958	16.37014	19.47294
Total of summation at factor Level		54.47807	54.47807	54.47807	54.47807
Summation of square of Differences		S_a = 47.0178	S_b= 322.1823	S_c= 15.14	S_d= 7.81167
Total of Summation of square Differences		$S_t = S_a + S_b + S_c + S_d$			
		392.15177			
Contribution %		11.998	82.147	3.863	1.99
Pareto Diagram		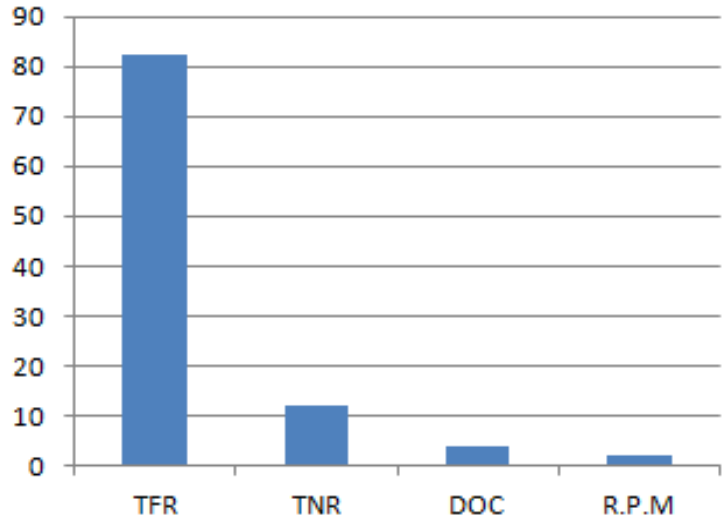			
Cumulative Contribution Ratio		82.147	94.145	98.008	100
Optimum Combination		**B 3** *	**A 3** *	C 1	D 3
The significant factors are chosen from the left hand side in the above Pareto Diagram, which Cumulatively contribute up to 90%					
Overall optimum conditions for all factors		A3 B3 C1 D3			

Table 4.9 Pareto ANOVA analysis for Surface Roughness Spherical Profile

FACTOR		A_i (TNR)	B_i (TFR)	C_i (DOC)	D_i (RPM)
LEVEL	1	-89.8273	-73.1371	-74.8752	-71.222
Summation at the	2	-71.4802	-78.8901	-78.3213	-82.5021
input parameter	3	-72.1913	-81.4716	-80.3023	-79.7747
Total of summation at factor level		-233.498	-233.498	-233.498	-233.498
Summation of square of Differences		S_a=648.149	S_b=109.224	S_c= 45.252	S_d= 207.826
Total of Summation of square Differences		$S_t = S_a + S_b + S_c + S_d$ 1010.457			
Contribution %		64.14	10.8	4.5	20.6
Pareto Diagram		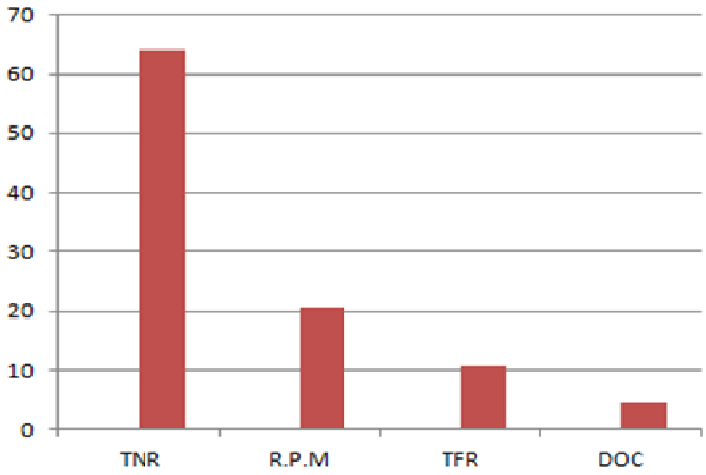			
Cumulative Contribution Ratio		64.14	84.74	95.54	100
Optimum Combination		**A 2**	**D 1**	**B 1**	C 1
The significant factors are chosen from the left hand side in the above Pareto Diagram, which cumulatively contributes up to 90%					
Overall Optimum Condition for all Factors		A2, B1, C1, D1			

Table 4.10 Pareto ANOVA analysis for Profile Error (Pt) Spherical Profile

FACTOR		A_i (TNR)	B_i (TFR)	C_i (DOC)	D_i (RPM)
LEVEL	**1**	25.5397	20.2053	19.0689	17.646
Summation at the	**2**	19.6004	18.5317	19.2925	19.8045
input parameter	**3**	11.3982	17.8012	18.1768	19.086
Total of summation at factor level		56.538	56.538	56.538	56.536
Summation of square of Differences		S_a=302.533	S_b=9.103	S_c= 2.087	S_d= 7.236
Total of Summation of square Differences		$S_t = S_a + S_b + S_c + S_d$			
		320.959			
Contribution %		94.25	2.83	0.7	2.254
Pareto Diagram		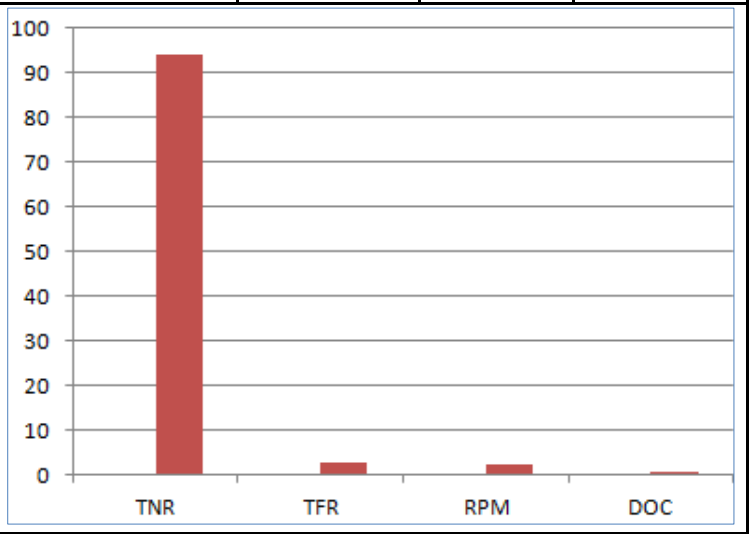			
Cumulative Contribution Ratio		94.25	97.08	99.4	100
Optimum Combination		**A1** *	B1	D2	C2

The significant factors are chosen from the left hand side in the above Pareto Diagram, which Cumulatively Contributes up to 90%

Overall Optimum Condition for all Factors	A1, B1, C2, D2

4.4 DISCUSSION FOR THE FLAT & SPHERICAL PROFILE

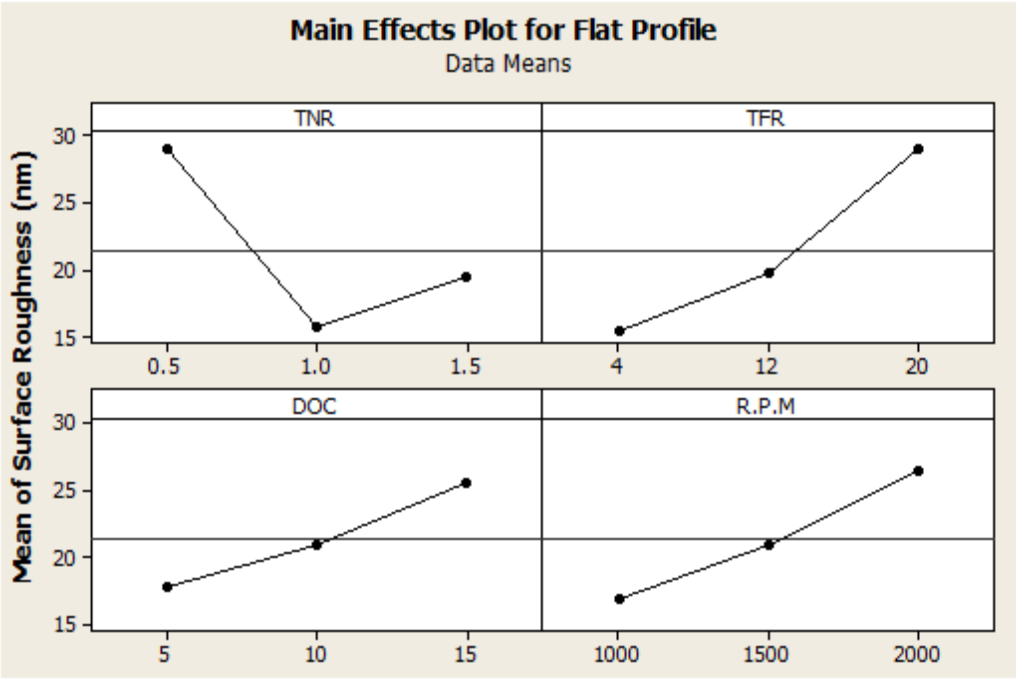

Fig.4.9 Main Effects Plot for Ra (Surface roughness), Flat Profile

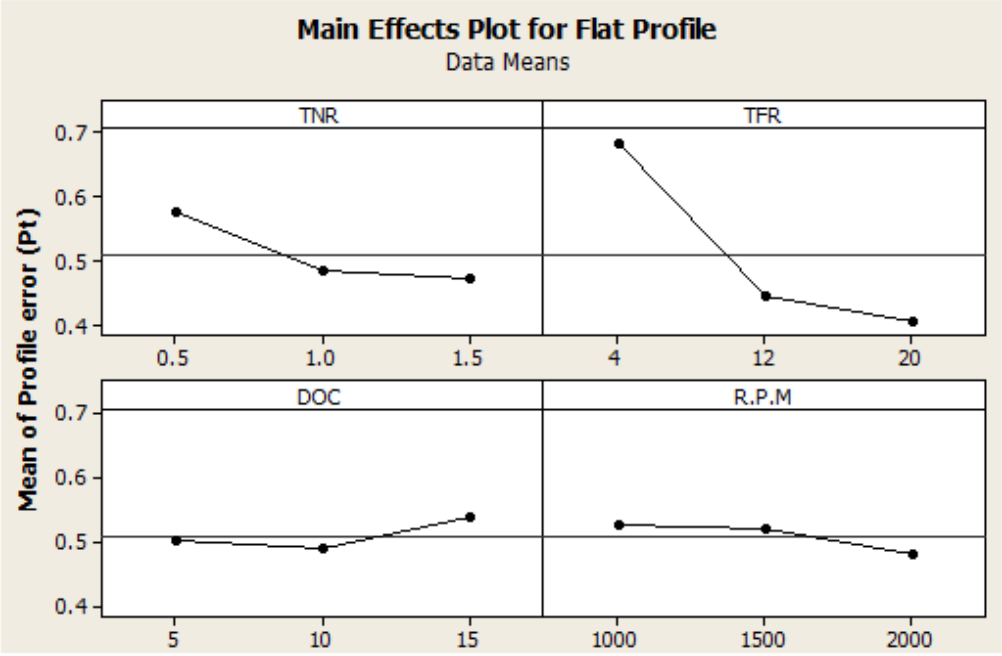

Fig.4.10 Main Effects Plot for Pt (Profile Error), Flat Profile

For surface roughness the feed rate is found to be the most prominent factor influencing the Surface roughness for single point diamond turning followed by tool nose radius. As can be seen from Figs.4.9-4.10, surface roughness increases with increasing feed rate and spindle speed, while lower values of tool feed rate and spindle speed are recommended for better surface roughness. As feed rate increases, the time available for plastic deformation in the surface layer of the work material is reduced and this might in turn leads to less swelling of the work materials. The Surface roughness decreases with increasing tool nose radius at small radius and increases at large radius. This is different from the theoretical prediction which suggests a decrease in surface roughness with increasing tool nose radius. Here the depth of cut is found to be insignificant factor.

For profile error (Pt) the feed rate is found to be the most prominent factor for single point diamond turning followed by tool nose radius, which is same as that of surface roughness (Ra). As the feed rate and tool nose radius increases the Pt value decreases. Depth of cut and spindle speed is found to be insignificant. It is found that the profile error decreases with increasing spindle speed.

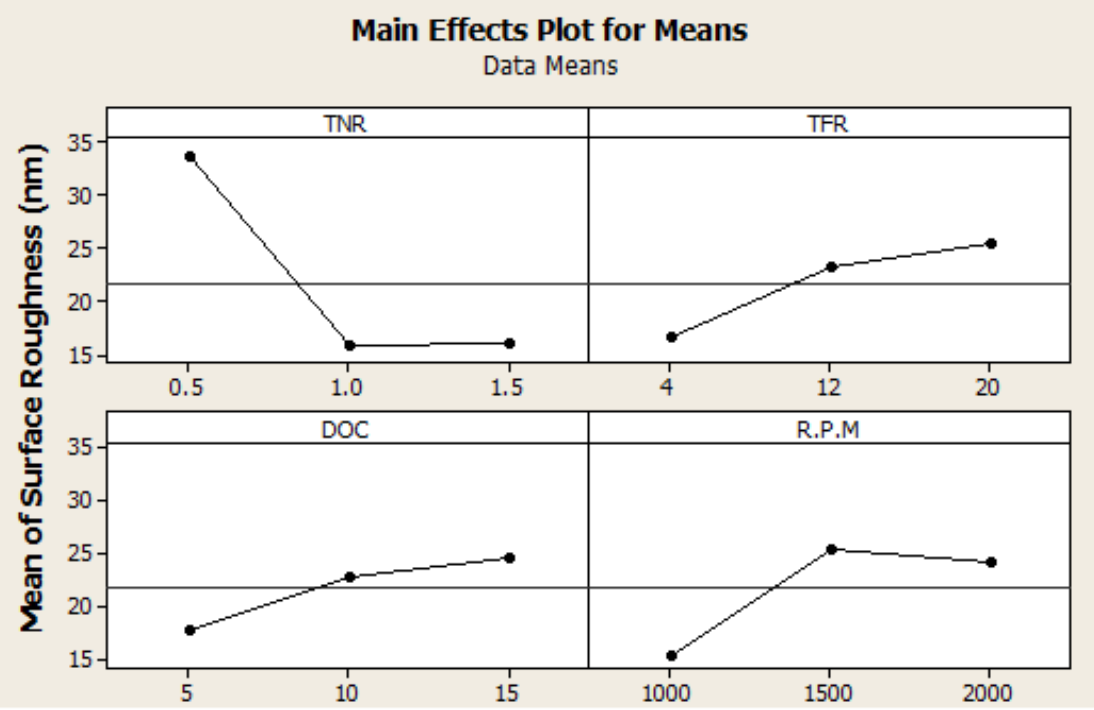

Fig.4.11 Main Effects Plot for Ra (Surface roughness), Spherical Profile

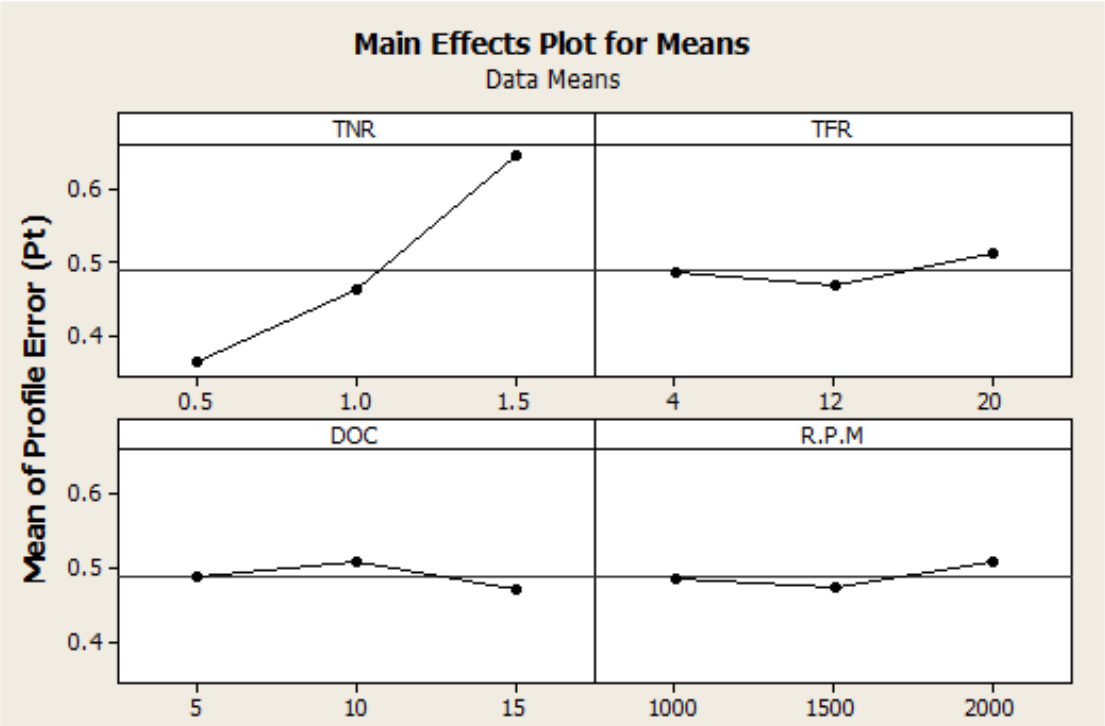

Fig.4.12 Main Effects Plot for Pt (Profile Error), Spherical Profile

For surface roughness the tool nose radius is found to be the most prominent factor influencing the Surface roughness for single point diamond turning followed by tool feed rate. As can be seen from Figs.4.11-4.12, the surface roughness increases with increasing feed rate, while lower values of tool feed rate and spindle speed are recommended for better surface roughness. As feed rate increases, the time available for plastic deformation in the surface layer of the work material is reduced and this might in turn leads to less swelling of the work materials. The Surface roughness decreases with increasing tool nose radius at small radius and increases at large radius. This is different from the theoretical prediction which suggests a decrease in surface roughness with increasing tool nose radius. Depth of cut is found to be insignificant.

For profile error (Pt) the tool nose radius is found to be the most prominent factor for single point diamond turning, which is same as that of the surface roughness (Ra). As the tool nose radius increases the Profile error increases, same results for the tool feed rate. Feed rate, depth of cut and spindle speed is found to be insignificant.

4.5 MULTI RESPONSE OPTIMIZATION USING ORTHOGONAL ARRAY WITH GREY RELATIONAL ANALYSIS

4.5.1 THEORY OF GREY RELATIONAL ANALYSIS

Taguchi methods mainly deal with only single response optimization problems. That is, only one dependent variable (response) is considered and the optimal levels for the parameters are determined on the mean response/maximum of the mean S/N ratio. Taguchi method cannot be used directly to optimize the multi-response problems. However, one can collect the observed data for each response using Taguchi design and the data can be analyzed by different methods developed by various researchers.

Multi-response problems try to determine the optimal levels for the factors based on one response at a time; we may get different set of optimal levels for each response. And it will be difficult to select the best set. Usually, the general approach in these problems is to combine the multiple responses into a single statistic (response) and then obtain optimal levels.

Grey relational analysis is used for solving interrelationships among the multiple responses. In this approach a grey relational grade is obtained for analyzing the relational degree of multiple responses. **(Lin *et al.* 2002)** have attempted grey relational based approach to solve multi-response problems the Taguchi methods. This method converts a multiple response process optimization problem into a single response optimization problem with the objective function of overall grey relational grade Grey relational analysis, experimental data i.e., measured features of quality characteristics are first normalized ranging from zero to one. This process is known as Grey relational generation. Next, based on normalized experimental data, Grey relational coefficient is calculated to represent the correlation between the desired and actual experimental data. Then overall Grey relational grade is determined by averaging the Grey relational coefficient corresponding to selected responses. The overall performance characteristic of the multiple response process depends on the calculated Grey relational grade. This approach converts a multiple response process optimization problem into a single response optimization situation with the objective function is overall Grey relational

grade. The optimal parametric combination is then evaluated which would result highest Grey relational grade. The optimal factor setting for maximizing overall Grey relational grade can be performed by Taguchi method.

Optimization steps in grey relational analysis

Step 1: Transform the original response data into S/N ratio (Y_{ij}) using appropriate formulae depending on the type of quality characteristics.

Step2: Normalize Y_{ij} as Z_{ij} ($0 \leq Z_{ij} \leq 1$) by the following formulae to avoid the effect of using different units and to reduce variability. Normalization is a transformation performed on a single input to distribute the data and scale it into acceptable range for further analysis.

Zij = Normalized value for ith experiment/trial for jth dependant variable/response

$$Z_{ij} = \frac{y_{ij} - \min\ (y_{ij}, i=1,2,\ldots n)}{\max(y_{ij}, i-1,2,\ldots n) - \min(y_{ij}, i-1,2,\ldots n)} \quad (1)$$

(to be used for S/N ratio with Larger –the better case)

$$Z_{ij} = \frac{\max(y_{ij}, i=1,2,\ldots n) - y_{ij}}{\max(y_{ij}, i=1,2,\ldots n) - \min(y_{ij}, i=1,2,\ldots n)} \quad (2)$$

(to be used for S/N ratio with Smaller –the better case)

$$Zij = \frac{(|y_{ij} - T|) - \min(y_{ij} - T, i=1,2,\ldots n)}{\max(y_{ij} - T, i=1,2,\ldots n) - \min(y_{ij} - T, i=1,2,\ldots n)} \quad (3)$$

(to be used for S/N ratio with nominal –the better case)

Step 3: Compute the grey relational coefficient (GC) for the normalized S/N ratio values.

$$GC_{ij} = \frac{\Delta \min + \mu \Delta max}{\Delta ij + \mu \Delta max}$$

i= 1, 2…n----experiments

j= 1, 2…n----responses (4)

GC_{ij}= grey relational coefficient for the ith experiment/trial and jth dependant variable / response.

Δ= absolute difference between Y_{oj} & Y_{ij}, a deviation from target value and can be treated as quality loss.

Y_{oj}= optimum performance value or the ideal normalized value of jth response.

Y_{ij} = the ith normalized value of the jth response /dependant variable.

Δmin= minimum value of Δ

Δmax = maximum value of Δ

μ is the distinguishing coefficient which is defined in the range 0≤ μ≤1 (the value may be adjusted on the practical needs of the system.

Step 4: Compute the grey relational grade (Gi)

$$Gi = \frac{1}{m} \sum GC_{ij} \quad (5)$$

Where m is the number of responses

Step 5: Use response graph method or ANOVA and select optimal levels for the factors based on maximum average Gi value.

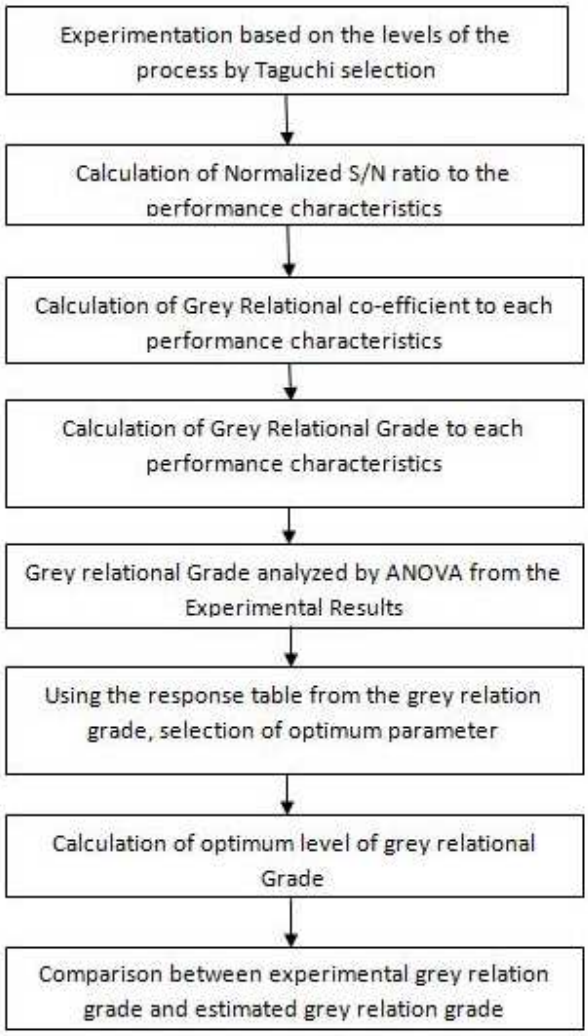

Fig.4.13: Flow chart Of Grey Relational Analysis (Lin *et al.* 2002)

Table 4.11 Orthogonal array L_9 (3^4) of the experimental runs and results of Flat Profile

Trial No.	A	B	C	D	Ra (nm)	Pt (nm)
1	1	1	1	1	14.9	0.7573
2	1	2	2	2	26.4	0.4987
3	1	3	3	3	45.8	0.4669
4	2	1	2	3	14.4	0.6092
5	2	2	3	1	13.6	0.4644

Trial No.	A	B	C	D	Ra (nm)	Pt (nm)
6	2	3	1	2	19.1	0.3798
7	3	1	3	2	17.0	0.6833
8	3	2	1	3	19.0	0.3673
9	3	3	2	1	22.1	0.3619

Table 4.12 Sequence after data pre processing of Flat Profile

Comparability Sequence	Reference Sequence	
	Ra	**Pt**
	1.000	**1.000**
No.1	0.0406	1.000
No.2	0.3960	0.3459
No.3	1.0000	0.2655
No.4	0.0237	0.6254
No.5	0.0000	0.2592
No.6	0.1706	0.0452
No.7	0.1054	0.8128
No.8	0.1685	0.0136
No.9	0.2626	0.0000

Table 4.13 Computed grey relational coefficient & Grey relational grade for nine comparability sequences of Flat Profile

Experimental run (comparability sequences)	Orthogonal array $L_9(3^4)$				Grey Relational coefficient		Grey Relational Grade	
	A	B	C	D	Ra (nm)	Pt (nm)	Grade	Rank
1	1	1	1	1	0.9248	0.3333	0.629081	6
2	1	2	2	2	0.5579	0.5910	0.574512	8

Experimental run (comparability sequences)	Orthogonal array $L_9(3^4)$				Grey Relational coefficient		Grey Relational Grade	
	A	B	C	D	Ra (nm)	Pt (nm)	Grade	Rank
3	1	3	3	3	0.3333	0.6531	0.493228	9
4	2	1	2	3	0.9545	0.4442	0.699429	5
5	2	2	3	1	1.0000	0.6585	0.82928	3
6	2	3	1	2	0.7455	0.9169	0.831271	2
7	3	1	3	2	0.8257	0.3808	0.603321	7
8	3	2	1	3	0.7478	0.9734	0.860642	1
9	3	3	2	1	0.6555	1.000	0.827796	4

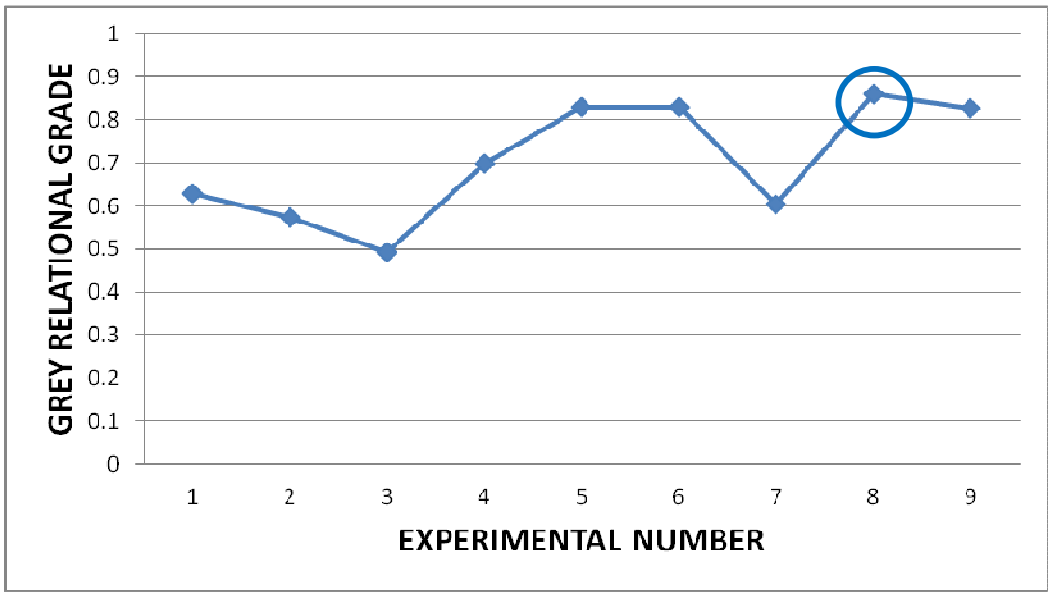

Fig.4.14: Grey Relational Grade for Flat Profile

Table 4.14 The response table for Grey relational of Flat Profile

Symbol	Machining Parameters	Grey Relational Grade			
		Level I	Level II	Level III	Max – Min
A	TNR	0.565607	0.78666*	0.76391	0.221053

Symbol	Machining Parameters	Grey Relational Grade			
		Level I	Level II	Level III	Max – Min
B	**TFR**	0.64394	0.75481*	0.71743	0.11087
C	**DOC**	0.77366*	0.70057	0.641943	0.131717
D	**RPM**	0.76205*	0.66970	0.684433	0.09235
Total Mean Value of the Grey Relational Grade =0.70539					

4.5.2 ANALYSIS OF VARIANCE FOR MEANS FOR FLAT PROFILE

The purpose of ANOVA is to identify which turning parameters significantly affect the multi responses. The ANOVA has been carried out taking data of grey relational grade and shown in Table 4.15 Tool nose radius is found to be the most significant factor from ANOVA study considering surface roughness and Profile error simultaneously into account as their P-value is less than 0.05.

Table 4.15 ANOVA Flat Profile

Factors	Degree of freedom, DF	Sum of square, SS	Mean square, MS	Contribution (%)
Tool Nose Radius	**2**	0.088709	0.044355	59.6
Tool Feed Rate	**2**	0.019089	0.009545	12.8
Depth of Cut	**2**	0.026130	0.013065	17.5
Spindle Speed	**2**	0.014770	0.007385	9.9
Residual Error	**0**			
Total	**8**	0.148700		

ANOVA result of the multiple performance characteristics is given in Table 4.15. The analyses are made for the level of confidence 95% (the level significance is 5%). Tool nose radius, Tool feed rate, Cutting speed and depth of cut influenced the multiple performance characteristics by 59.6%, 12.8%, 17.5% and 9.9%, respectively (Table 12). From the analysis of this table, it could be concluded that Tool nose radius, Tool feed rate and depth of cut are three dominant parameters that affect grey relational grade.

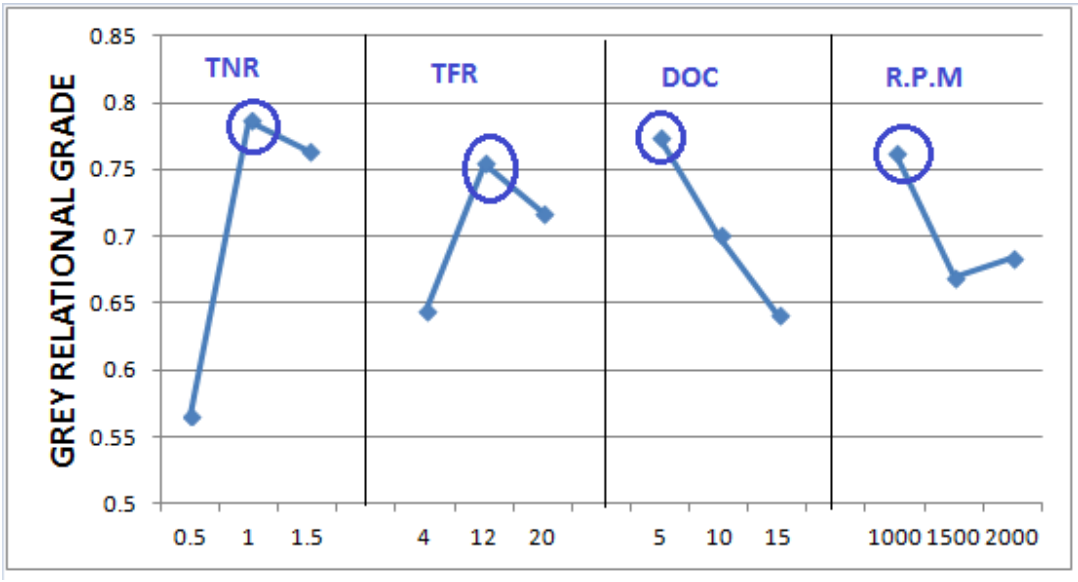

Fig.4.15 Mean of Grey relational grade of Flat Profile

4.5.3 CONFIRMATION TEST FOR FLAT PROFILE

Confirmation test has been carried out to verify the improvement of performance characteristics in diamond turning of Copper alloy C18000 using Single point diamond turning. Optimum parameters are selected for confirmation test Table 4.16. Estimated GRG $Y_{predicted}$ using optimal level of machining parameters can be calculated as

$$Ypredicted = Ym + \sum_{i=1}^{q} (Yi - Ym) \quad (6)$$

=0.70539+ (0.78666- 0.70539) + (0.75481 - 0.70539) + (0.77366 - 0.70539)

=0.70539+0.08127+0.04942+0.06827=**0.90435**

Where Ym is total mean of GRG, Yi is mean of GRG at optimal level, and q is number of machining parameters that significantly affect multiple-performance characteristics.

Table 4.16 Improvements in grey relational grade (GRG) with optimized SPDT machining parameters for flat profile

	Initial Machining Parameters	Optimal Machining Parameters	
		Prediction	Experiment
Setting Level	A1 B1 C1 D1	A2 B2 C1 D1	A2 B2 C1 D1
Surface Roughness (Ra)	15	**0.90435**	14.2
Profile Error (Pt)	0.7573		0.3875
Grey Relational Grade	**0.629081**		**0.9383**
Percentage of improvement of the grey relational grade=49.15%			

Experimental result of the optimal machining parameters from the contact types of profiler are shown in Fig. 4.16 and Fig. 4.17.Figure 4.18 shows the 3D image of the flat profile from CCI. The interferometric representation for the flat profile shows that the Profile error is 0.1217µm/rev. and surface roughness comes out to be 6.14nm.

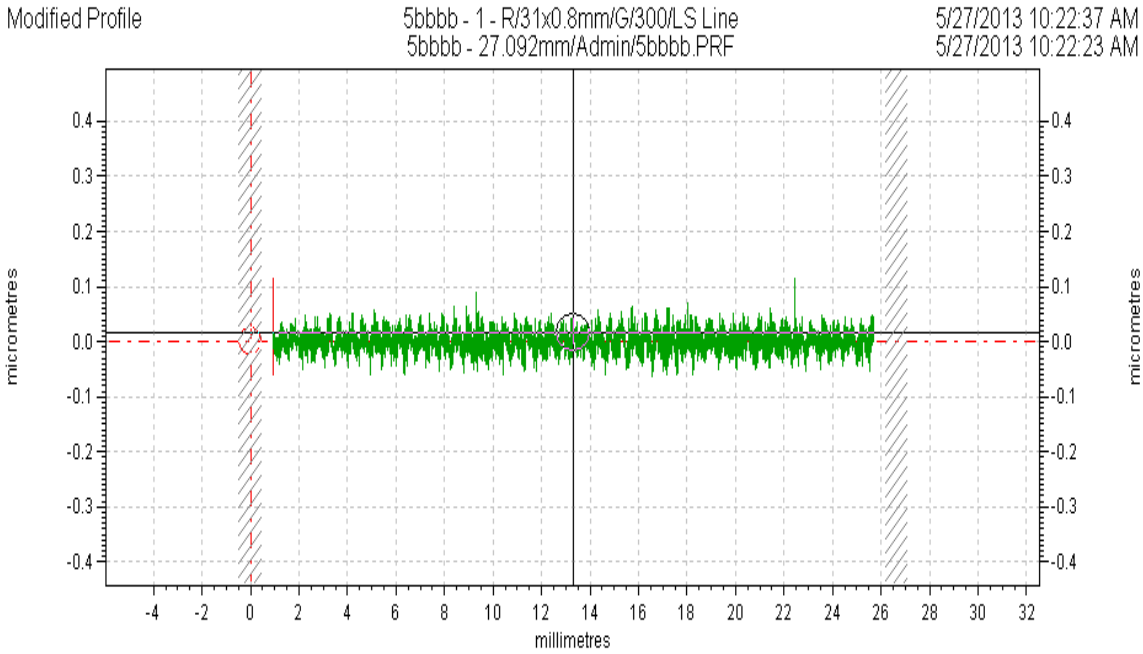

Fig.4.16 Results for Surface Roughness (Ra) by Contact Type Profiler (1.0mm, 12µm/rev., 5µm, 1000r.p.m)

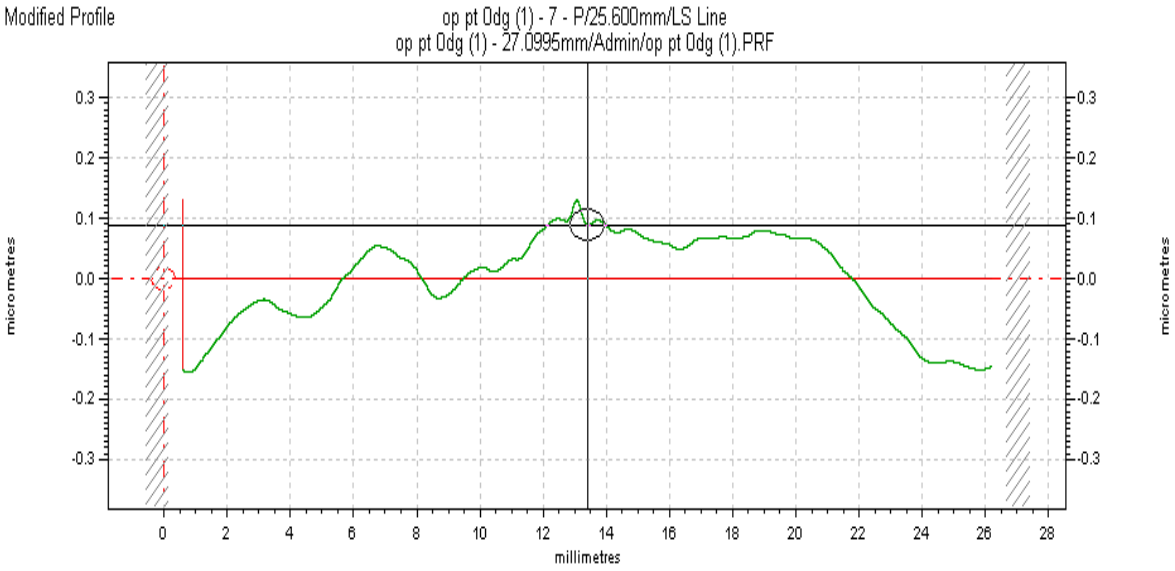

Fig.4.17 Results for Profile error (Pt) from Contact Type Profiler with (1.0mm, 12µm/rev., 5µm, 1000r.p.m)

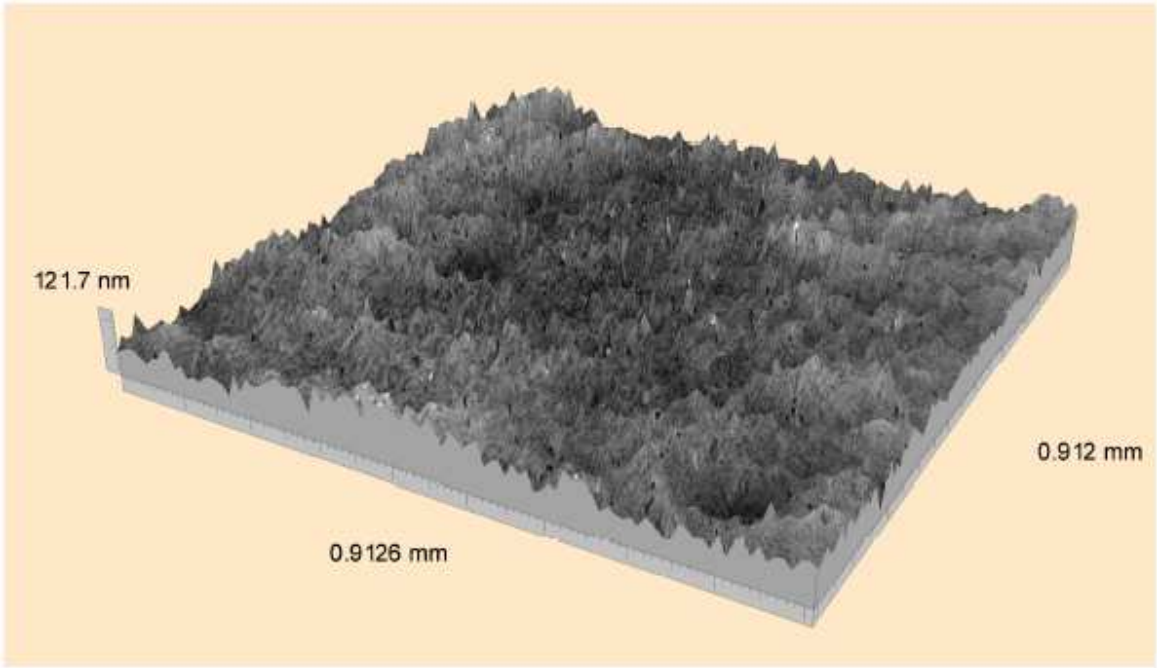

Fig.4.18 Results for Profile error (Pt) from CCI with (1.0mm, 12µm/rev., 5µm, 1000r.p.m)

Using Eq. (6), predicted Ra Surface roughness , Pt profile error and GRG for optimal machining parameters are obtained Table 4.16, which shows comparison of experimental results using initial (A1 B1 C1 D1) and optimal (Grey theory prediction

design, A2 B2 C1 D1) machining parameters. Surface roughness (Ra) is improved from 15nm to 14.2nm and Profile error (Pt) is also reduced from 0.7573µm to 0.3875µm. Corresponding improvement in Ra is 5.6% and Profile error 95.43% respectively. It is clearly shown that multiple performance characteristics in SPDT process are greatly improved through this study.

Table 4.17 Orthogonal array L_9 (3^4) of the experimental runs and results of Spherical Profile

Trial No.	A	B	C	D	Ra (nm)	Pt (nm)
1	1	1	1	1	18.1	0.355
2	1	2	2	2	39.8	0.346
3	1	3	3	3	42.7	0.388
4	2	1	2	3	14.2	0.419
5	2	2	3	1	13.8	0.498
6	2	3	1	2	19	0.464
7	3	1	3	2	17.5	0.605
8	3	2	1	3	15.8	0.640
9	3	3	2	1	14.4	0.684

Table 4.18 The sequence after data pre processing of Spherical Profile

Comparability Sequence	Reference Sequence	
	Ra	Pt
	1.000	**1.000**
No.1	0.1487	0.0266
No.2	0.8996	0.0000
No.3	1.0000	0.1242
No.4	0.0138	0.2159

Comparability Sequence	Reference Sequence	
	Ra	**Pt**
	1.000	**1.000**
No.5	0.0000	0.4497
No.6	0.1799	0.3491
No.7	0.1280	0.7662
No.8	0.0692	0.8698
No.9	0.0207	1.0000

Table 4.19 Computed grey relational coefficient & Grey relational grade for nine comparability sequences of Spherical Profile

Experimental run (comparability sequences)	Orthogonal array L_9 (3^4)				Grey Relational coefficient		Grey Relational Grade	
	A	**B**	**C**	**D**	**Ra (nm)**	**Pt (nm)**	**Grade**	**Rank**
1	1	1	1	1	0.7706	0.9494	0.8600	1
2	1	2	2	2	0.3572	1.0000	0.6786	4
3	1	3	3	3	0.3333	0.8009	0.5671	9
4	2	1	2	3	0.9730	0.6983	0.8357	2
5	2	2	3	1	1.0000	0.5264	0.7632	3
6	2	3	1	2	0.7353	0.5888	0.6620	5
7	3	1	3	2	0.7961	0.3948	0.5954	8
8	3	2	1	3	0.8784	0.3650	0.6217	7
9	3	3	2	1	0.9601	0.3333	0.6467	6

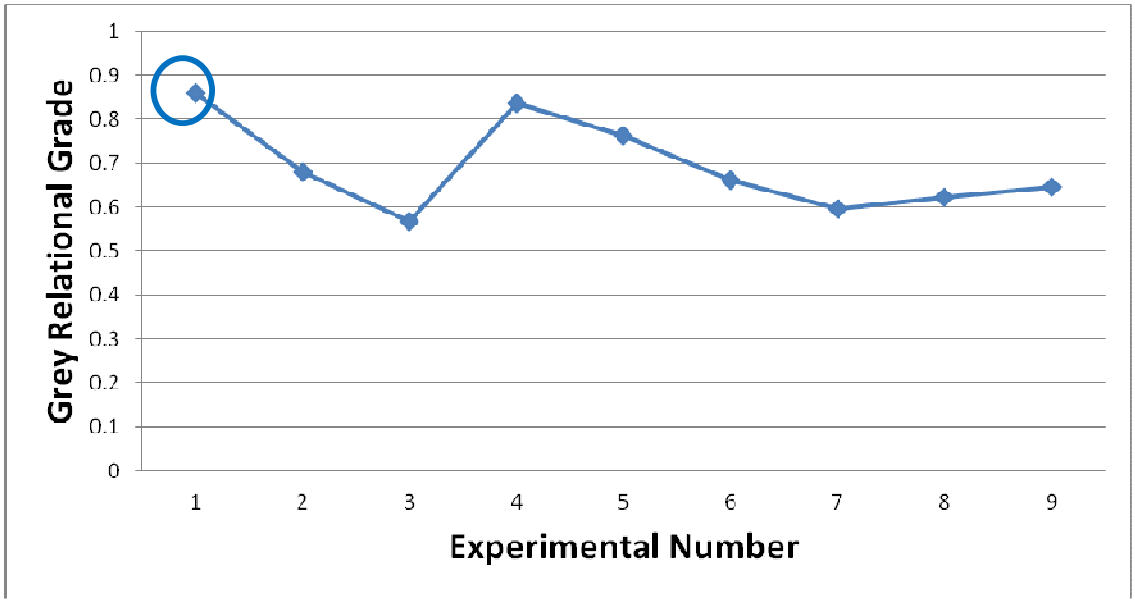

Fig.4.19 Grey Relational Grades for Spherical Profile

Table 4.20 Response data for Grey relational of Spherical Profile

Symbol	Machining Parameters	Grey Relational Grade			
		Level I	Level II	Level III	Max – Min
A	**TNR**	0.7019	0.7526*	0.6213	0.1313
B	**TFR**	0.7637*	0.6878	0.6253	0.1384
C	**DOC**	0.7146	0.7203*	0.6419	0.0784
D	**RPM**	0.7566*	0.6454	0.6784	0.1112
Total Mean Value of the Grey Relational Grade =0.692302					

ANALYSIS OF VARIANCE FOR MEANS FOR SPHERICAL PROFILE

The purpose of ANOVA is to identify which turning parameters significantly affect the multi responses. The ANOVA has been carried out taking data of grey relational grade and shown in Table 4.21. Tool feed rate is found to be the most significant factor from ANOVA study considering surface roughness and Profile error simultaneously into account as their P-value is less than 0.05.

Table 4.21 ANOVA Spherical Profile

Factors	Degree of freedom, DF	Sum of square, SS	Mean square, MS	Contribution (%)
Tool Nose Radius	2	0.026701	0.013351	30.7
Tool Feed Rate	**2**	0.028838	0.014419	33.17
Depth of Cut	**2**	0.011458	0.005729	13.17
Spindle Speed	2	0.019939	0.009970	22.93
Residual Error	**0**			
Total	**8**	0.086936		

ANOVA result of the multiple performance characteristics is given in Table 4.21. The analyses are made for the level of confidence 95% (the level significance is 5%). Tool nose radius, Tool feed rate, Cutting speed and depth of cut influenced the multiple performance characteristics by 30.7%, 33.2%, 22.93% and 13.2%, respectively (Table 12). From the analysis of this table, it could be concluded that Tool nose radius, Tool feed rate and spindle speed are three dominant parameters that affect grey relational grade.

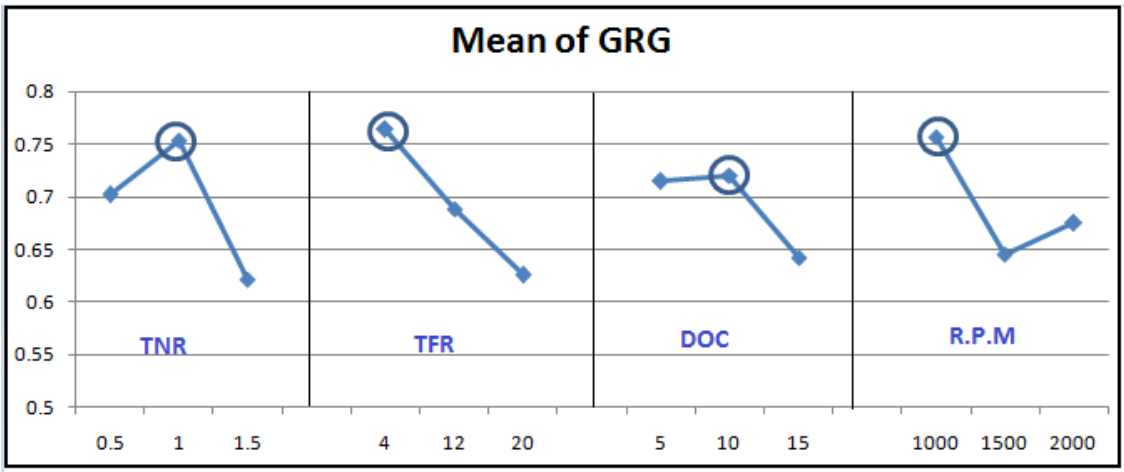

Fig.4.20 Mean of Grey relational grade of Spherical Profile

CONFIRMATION TEST FOR SPHERICAL PROFILE

Confirmation test has been carried out to verify the improvement of performance characteristics in diamond turning of Copper alloy C18000 using Single point diamond turning. Optimum parameters are selected for confirmation test Table 4.22. Estimated GRG $Y_{predicted}$ using optimal level of machining parameters can be calculated as

$$Ypredicted = Ym + \sum_{i=1}^{q} (Yi - Ym)$$

0.692302 + (0.75267 - 0.692302) + (0.76374 - 0.692302) + (0.75666 - 0.692302)

=0.064358+0.071438+0.060368+0.692302= **0.888466**

OPTIMUM PARAMETER 1.0mm, 4µm/rev, 10µm, 1000r.p.m

Where Ym is total mean of GRG, Yi is mean of GRG at optimal level, and q is number of machining parameters that significantly affect multiple-performance characteristics.

Table 4.22 Improvements in grey relational grade (GRG) with optimized SPDT machining parameters for Spherical profile

	Initial Machining Parameters	**Optimal Machining Parameters**	
		Prediction	**Experiment**
Setting Level	A2 B3 C1 D2	A2 B1 C2 D1	A2 B1 C2 D1
Surface Roughness (Ra)	19	**0.888466**	15
Profile Error (Pt)	0.464		0.3547
Grey Relational Grade	**0.662097**		**0.92238**
Percentage of improvement of the grey relational grade=39.31%			

Experimental result of the optimal machining parameters from the contact types of profiler are shown in Fig. 4.21 and Fig. 4.22. Figure 4.23 shows the 3D image of the flat

profile from CCI. The interferometric representation of the spherical profile shows that the Profile error is 0.5396µm/rev. and surface roughness comes out to be 6.34nm.

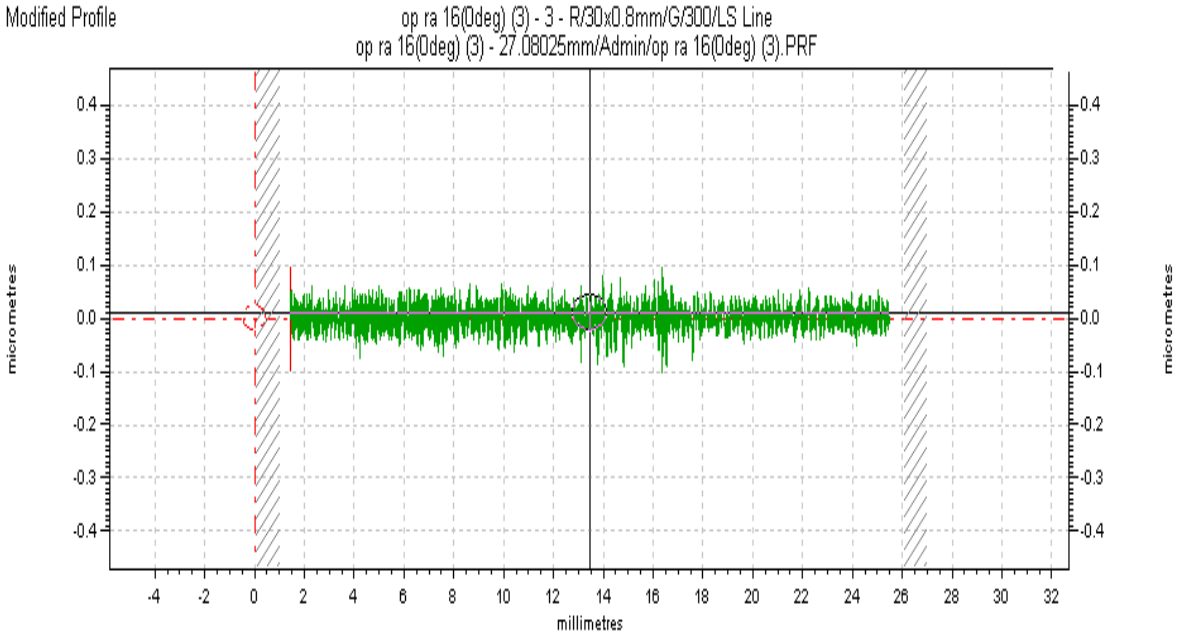

Fig.4.21 Results for Surface Roughness (Ra) by Contact Type Profiler (1.0mm, 4µm/rev., 10µm, 1000r.p.m)

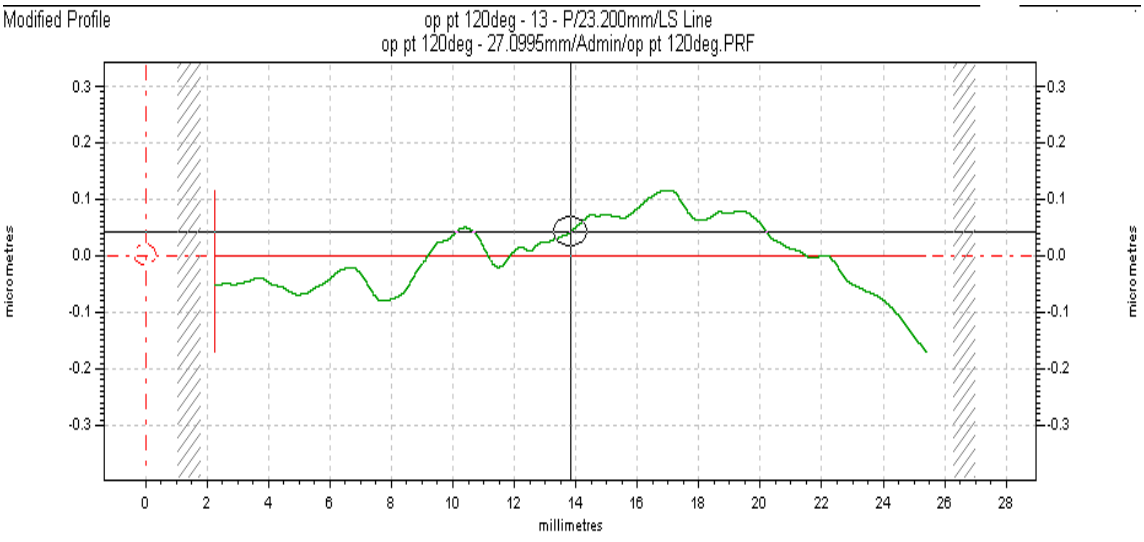

Fig.4.22 Results for Profile error (Pt) by Contact Type Profiler (1.0mm, 4µm/rev., 10µm, 1000rpm)

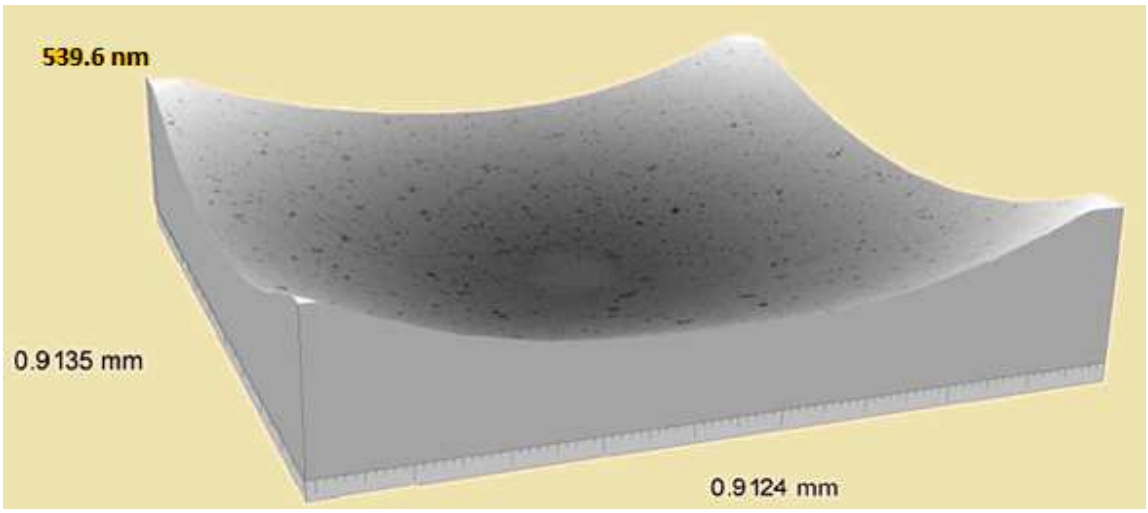

Fig.4.23 Results for Profile error (Pt) by CCI (1.0mm, 4µm/rev., 10µm, 1000r.p.m)

Using Eq. (6), predicted Ra Surface roughness , Pt profile error and GRG for optimal machining parameters are obtained Table 4.22, which shows comparison of experimental results using initial (A2 B3 C1 D2) and optimal (Grey theory prediction design, A2 B2 C1 D1) machining parameters. Surface roughness (Ra) is improved from 19nm to 15nm and Profile error (Pt) is also reduced from 0.464µm to 0.3547µm. Corresponding improvement in Ra is 26.66% and Profile error 30.81% respectively. It is clearly shown that multiple performance characteristics in SPDT process are greatly improved through this study.

CHAPTER 5: CONCLUSION AND FUTURE SCOPE

The present study is carried out to study the effect of machining parameters on surface roughness (Ra) and profile error (Pt) of the C18000 copper alloy component using the single crystal diamond tool during SPDT process. The experiments are conducted under various parameters viz. tool nose radius, tool feed rate, spindle speed and depth of cut. L-9 OA based on Taguchi design is performed for Minitab software is used for analysis the result. From the experimental work conducted and the subsequent analysis, the following conclusions can be drawn:

1. Taguchi's robust design method is suitable to analyze the metal cutting problem as described in this study.
2. The results are analyzed in two different techniques, the conceptual S/N ratio and Pareto ANOVA. However, both techniques delivered similar results.
3. For the flat profile the order of the importance for the controllable factors to the surface roughness (Ra), in sequence, is the tool feed rate, the tool nose radius, the spindle speed and the depth of cut. The order to the profile error (Pt), in sequence, is the tool feed rate, the tool nose radius, the depth of cut and the spindle speed.
4. For the spherical profile the order of the importance for the controllable factors to the surface roughness (Ra), in sequence, is the tool nose radius, the tool feed rate, the spindle speed and the depth of cut. The order to the profile error (Pt), in sequence, is the tool nose radius, the tool feed rate, the spindle speed and the depth of cut.
5. Depth of cut shows minimal effect on both responses surface roughness and profile error compared to other parameters. However, for achieving good optical surface on the copper work piece, lower depth of cut is preferred.
6. The tool feed rate is found to be more significant factor followed by tool nose radius for the flat profile machining. Finally, conformation tests with the optimal levels of all the parameters are carried out to investigate the improvement of the optimization. The result for the Flat Profile machining showed a reduction of

8.08% in the Surface roughness (Ra) and 9.78% improvement on the Profile error performance.

7. The tool nose radius is found to be more significant factor for the Spherical profile machining. Finally, conformation tests with the optimal levels of all the parameters are carried out to investigate the improvement of the optimization. The result for the Flat Profile machining showed a reduction of 7.24% in the Surface roughness (Ra) and 24.94% improvement on the Profile error performance.
8. From the main effect plots, Tool nose radius of 1.0mm and tool feed rate of 4µm gives better surface roughness for both the flat and spherical profiles, increase in the feed rate will lead to increase in the surface roughness.
9. From the main effect plots for the spherical profile it is observes that profile error increases with increase in the tool nose radius.
10. For both the flat and spherical profile it is found that the surface roughness (Ra) decreases with increasing tool nose radius at small radius and increase at larger radius. This is different from the theoretical prediction which suggests a decrease in surface roughness with increasing tool nose radius.
11. A grey relational analysis of the experimental results of surface roughness and Profile error converts multi optimization performance characteristics into single optimization characteristic called the grey relational grade. The optimal parametric combination for flat Profile becomes A2 B2 C1 D1, i.e. Tool nose radius 1.0mm, feed rate 12µm, depth of cut 5µm and cutting speed of 1000rpm.
12. The percentage improvement of grey relational grade from initial parameter combination (A1 B1 C1 D1) to the optimal parameter combination (A2 B2 C1 D1) is found to be 49.15%.
13. From the grey relational analysis, the optimal parametric combination for Spherical Profile becomes A2 B1 C2 D1, i.e. Tool nose radius 1.0mm, feed rate 4µm, depth of cut 10µm and cutting speed of 1000rpm.
14. The percentage improvement of grey relational grade from initial parameter combination (A2 B3 C1 D2) to the optimal parameter combination (A2 B1 C2 D1) is found to be 39.31%.

15. It is clearly shown that the multiple performance characteristics (surface roughness and Profile error) in the Ultra-Precision machining are greatly improved using grey based Taguchi method using single crystal Diamond tool.

FUTURE SCOPE

The future works of the related research may include two fields, the fundamental research on the surface quality of the SPDT and the application of SPDT and micro machining.

For the fundamental research on surface quality, the main aspect is:

1. The material swelling and recovery mechanism and their relationship to the SPDT machining parameters and material property.
2. Effect of tool offset on the profile error on the copper material

REFERENCES

Abhang L. B. and Hameedullah M. (2011), "Modelling and Analysis for Surface roughness in Machining EN-31, using Response Surface Methodology," *International Journal of Applied Research in mechanical engineering*, Vol.1, Issue 1.

Biddut A. Q. , Rahman K. S. N., Sawa M., Maeda Y. (2007), "Performance of single crystal diamond tools with different rake angles during micro-grooving on electro less nickel plated die materials," *International Journal of Advanced Manufacturing Technology*, Vol. 33, pp 891–899.

Blackley W.S. and Scattergood R.O. (1991), "Ductile regime machining model for diamond turning of brittle *materials*," *Precision Engineering*, Vol.13, pp 95-103.

C.Richard, R. Juergens Hamilton Shepard III, (2003) "Simulation of single point diamond turning fabrication process errors", *SPIE* Vol. 93.

Chen H, Dai Y, Zheng Z, Gao H and Li X (2011), " Effect of crystallographic orientation on cutting forces and surface finish in ductile cutting of KDP crystals," *Machining Science and Technology: An International Journal*, Vol.15, No.2, pp 231-242.

Cheung C. F. and Lee W. B. (2000), "Study of Factors Affecting the Surface Quality in Ultra-Precision Diamond Turning," *Materials and Manufacturing Processes*, Vol. 15:4, pp 481-502.

Cheung C. F. and Lee W. B. (2002), "Prediction of the Effect of Tool Interference on Surface Generation in Single-Point Diamond Turning," *International Journal of Advanced Manufacturing Technology*, Vol.19, pp 245–252.

Cheung C.F., To S. and Lee W.B. (2002), "Anistropy of surface roughness in diamond turning of brittle single crystals," *Materials and Manufacturing Processes*, Vol. 17, No.2, pp. 251-267.

Childs T.H.C., Dornfeld D., Lee E., Min S., Sekiya K., Tezuka R., Yamane Y. (2008), "The influence of cutting edge sharpness on surface finish in facing with round nosed cutting tools," Annals-*CIRP Manufacturing Technology*, Vol. 57, pp 89-92.

Corbett J, Keown P.A., Peggs G.N, Whatmore R. (2000), "Nanotechnology: International Developments and Emerging Products," *Annals of the CIRP*, Vol. 49, No.2, pp 523-545.

Davim J. Paulo, Mata F. (2010), "Performance of diamond coated tools (CVD) in machining polyamides," *International Journal Materials and Product Technology*, Vol.37, pp 188-198.

Davim, J.P. (2003), "Design of optimization of cutting parameters for turning metal matrix composites based on the orthogonal arrays," *Journal of Material Processing Technology*, Vol. 132, pp 340-344.

Ding X., Jarfors A.E.W. , Lim G.C., Shaw K.C., Liu Y.C., Tang L.J. (2012) "A study of the cutting performance of poly-crystalline oxygen free copper with single crystalline diamond micro-tools," *Precision Engineering*, Vol. 36, pp 141– 152.

Hocheng H., Hsieh M.L. (2004), "Signal analysis of surface roughness in diamond turning of lens molds," *International Journal of Machine Tools & Manufacture*, Vol. 44, pp 1607–1618

Jacob J., Balasubramaniam R., and Suri V.K (2005), "Some Studies in the signature analysis of machined surfaces," *Precision Engineering*, pp 386-391.

Jain V.K. (2010), “Introduction to Micromachining”; *Narosa Publishing House Pvt. Ltd.*

Jasinevicius R.G., Porto A.J.V., Pizani P.S., Duduch, J.G., Santos, F.J.(2005), “Characterization of structural alteration in diamond turned silicon crystal by means of micro raman spectroscopy and transmission electron microscopy”, *International Journal of Machine Tools & Manufacture* , Vol. 8, No.3, pp 261-268.

Keown P. A., (1987) “The role of precision engineering in manufacturing of the future,” *Annals of CIRP*, Vol. 36, No. 2, pp 495-501.

Kurniawan D, Yusof NM, Sharif S (2010), “Hard machining of stainless steel using wiper coated carbide: tool life and surface integrity,” *Material Manufacturing Processes*, Vol. 25, No.6, pp 370–377.

Lee W.B., Cheung C.F., Chiu W.M. and Leung T.P. (2000) “An investigation of residual form error compensation in the ultra precision machining of aspheric surfaces,” *Journal of Material Processing Technology*, Vol.99, pp 129-134.

Lee W.B., To S. and Cheung C.F. (2000), “Effect of crystallographic orientation in diamond turning of copper single crystals,” *Scripta Mater*, Vol.42, pp 937-945.

Lin, C.L., Lin, J.L. and Ko, T.C., (2002), “Optimization of EDM process based on the orthogonal array with the Fuzzy Logic and Grey relational analysis method,” *International Journal of Advanced Manufacturing Technology*, Vol. 19, pp 271-277.

Liu X.D., Lee L.C, Ding X. and Fang F.Z. (2002), “Ultra precision turning of Aspherical Profiles with deep sag,” *IEEE International Conference*, Vol.02, No.1, pp 1152-1157.

Meng Liu., Jun-ichiro, Takagi., and Akira, (2004), “Effect of tool nose radius and tool wear on the residual stress distribution in turning of bearing steel,” *Journal of Materials Processing Technology*, Vol. 150, pp 234-241.

Mc Geough J.A., (2001), “*Micromachining of Engineering Materials*,” CRC Press.

Mustafa A., and Tanju K. (2011), “Investigation of the machinability of the Al 7075 alloy using DLC coated cutting tools,” *Scientific Research and Essays*, Vol. 6, pp 44-51.

Nalbant, M; Gokkaya,H; Sur, G (2007), “Application of Taguchi method in the optimization of cutting parameters for surface roughness in turning,” *Material & Design* , Vol. 28, pp 1379-1385.

Nes S. , Yaldız S. , Turkes E. (2011), “Optimization of tool geometry parameters for turning operations based on the response surface methodology,” *Measurement*, Vol. 44, pp 580–587.

Osmer J. , Meier A., Glabe R., Riemer O. and Brinksmeier E. (2010), “Ultra Precision Machining of Non-Ferrous Metals and Nitrocarburized Tool Steel,” ; *Advanced Optical Manufacturing technology,* Vol. 447-448, pp 46-50.

Palanikumar K. (2008) “Application of Taguchi and response surface methodologies for surface roughness in machining glass fiber reinforced plastics by PCD tooling,” *International Journal of Advanced Manufacturing Technology,* Vol.36, pp 19–27.

Park SH (1996), “*Robust design and analysis for quality engineering,”* Chapman & Hall, London.

Philippe Revel, Hatem Khanfir and Yves Fillit (2006) “Surface characterization of aluminum alloys after diamond turning,*”* *Journal of Materials Processing Technology*, Vol. 178, pp 154–161.

Pramanik A., Neo K.S., Rahman M., Li X.P., (2003), "Cutting performance of diamond tools during ultra-precision turning of electroless-nickel plated die materials," *Journal of Materials Processing Technology*, Vol.140, pp 308–313

Rahman M., Liu K., Neo K.S and Chan C.C. (2003), "Nano precision measurement of diamond tool edge radius for wafer fabrication," *Journal of Materials Processing Technology*, Vol. 140, pp 358-362.

Ramesh K. Lewis W.G., Veldhuis S.C. and Yui A. (2005), "Redefining the diamond cutting edge: A technique that complements nao-metric surface generation," *Materials and Manufacturing Processes*, Vol. 20, pp 895-903.

Ravindra D. and Patten J. (2011), "Ductile regime single point diamond turning of quartz resulting in an improved and damage-free surface," *Machining Science and Technology*, Vol. 15, pp 357–375.

Ravindra D., Patten J. A., Qu J. (2009), "Single point diamond turning effects on surface quality and subsurface damage in ceramics," *Proceeding of ASME 2009 International Manufacturing science and engineering conference USA.*

Rhorer R L & Evans C J (2010), "*Fabrication of Optics by Diamond Turning*" in Handbook of Optics, edited by Michael Bass, (McGraw-Hill, Inc.), Vol. I, pp 41.1-41.13.

Ross P.J. (1996), "*Taguchi Techniques for Quality Engineering*," 2nd ed.; Mc Graw-Hill.

Riedl M.J. (2001) "Stretching the Optical Envelope; Single-point diamond turning cost effectively increases optical designers' options" *Photonics Spectra*, pp 130-132.

Sarepaka SV (2012), "Optimization of Process Parameters to Achieve Nano Level Surface Quality on Polycarbonate," *Int. Journal of Computer Application*, Vol.48.

Saito T.T. (1978), “Diamond turning of optics: The past, the present and the exciting future,” *Optical Engineering*, Vol. 17, pp 570-573.

Sanger G. M. (1987), “*Precision machining of optics*” Applied Optics and Optical Engineering, edited (Academic Press, Inc.), Vol. 10, pp 251-390.

Sata T., Li M, Takata S., Hiraoka H., Li C.Q., Xing X.Z. and Xiao X.G. (1985), “Analysis of surface roughness Generation in turning operation and its applications,” *Annals of the CIRP*, Vol. 34, No.1, pp 473-476.

Shimada S., Inoue. R., Uchikoshi. J and Ikawa.N (1995), “Molecular dynamics analysis of microstructure of diamond turned surfaces,” *Proceeding SPIE*, 2576, pp 396-405.

Smith k., Winger R., Lettington A.H. and Stillwells P.F.T.C. (1988), “Diamond turning of mirrors and infrared optical components,” *Journal of Applied Physics*, Vol. 21, pp 67-79.

Suleyman Neseli, Suleyman Yaldız and Erol Turkes (2011) “Optimization of tool geometry parameters for turning operations based on the response surface methodolo*gy,” Measurement*, Vol. 44, pp 580–587.

Taniguchi N. (1983), “Current status in, and future trends of ultra precision machining and ultrafine material processing,” *Annals of CIRP*, Vol. 32, No. 2, pp 573-582.

To S., Lee W.B., and Chan C.Y. (1997), “Ultra precision Diamond Turning of Aluminium Single Crystals,” *Journal of Materials Processing Technology*, Vol. 63, pp 157-162.

Uchida F. Moriyama S. and Suzuki Y. (1991), “Fabrication of Aspherical mirrors for a hard X-ray microprobe,” *Journal of the Japan society of Precision Engineering*, Vol. 55, No.2, pp 179-184.

Palanikumar (2008) “Surface roughness parameters optimization in machining A356/sic/20p metal matrix composites by PCD tool using response surface methodology and desirability function,” *Machining Science and Technology*, Vol. 12, pp 529–545.

Weck M., Hartel R. and Modemann K. (1988), “Performance assessment in ultra precision machining,” *Annals of CIRP*, Vol. 37/1, pp 499-502.

Whitehouse D J (1988), “Comparison Between Stylus and Optical Methods for Measuring Surfaces,” *Annals of CIRP*, Vol. 37, pp 649-653.

Whitehouse D.J. (1994), “*Handbook of surface Metrology, Bristol*, Philadelphia; Institute of Physics Pub.

Wilks J. (1980), “Performance of diamonds as cutting tools for precision machining,” *Precision Engineering*, Vol. 2, pp 57-72.

Yan B.H., Huang F.Y., Chow H.M. (1995), “Study on the turning characteristics of alumina-based ceramics,” *Journal of Material Processing Technology*, Vol. 54, pp 341-347.

Yan J., Tamaki Junichi, Syoji K., Kuriyagawa T. (2004), “Single-point diamond turning of CaF_2 for nanometric surface,” *International Journal of Advanced Manufacturing Technology*, Vol.24, pp 640–646.

Yingfei G., Jiuhua X., Hui Y. (2010), “Diamond tools wear and their applicability when ultra-precision turning of SiCp/2009Al matrix composite,” *Wear*, Vol. 269, pp 699–708.

Zhang JZ, Chen JC, Kirby ED (2007), “Surface roughness optimization in an end-milling operation using the Taguchi design method,” *Journal of Materials Processing Technology*, Vol. 184, pp 233–239.

Zhimin Z., Yuanliang Z. , Xiaoyan L., Huiyuan Z. , and Baoyuan S. (2011), "Influences of Various Cutting Parameters on the Surface Roughness during Turnings Stainless Steel" ; ISSN 17710, *Acoustical Physics*, Vol. 57, pp 114–120.

Zhong Z. W. and Lu Y. G. (2002), "3D characterization of super-smooth surfaces of diamond turned OHFC copper mirrors," *Materials and Manufacturing Processes*, Vol. 17, No.3, pp 387–399.

Zhong Z. W. and Lu Y. G., (2003) "Fractal Roughness Structure of Diamond-Turned Copper Mirrors," *Materials and Manufacturing Processes*, Vol. 18, No.2, pp 219-227.

Zhong Z.W., Leong M.H., Liu X.D. (2011), "The wear rates and performance of three mold insert materials," *Materials and Design*, Vol. 32, pp 643–648.

Zhou M. and Ngoi B. K. A. (2001), "Effect of tool wear and tool setting on the profile accuracy of diamond-turned nonferrous components" *Materials and Manufacturing Processes*, Vol.16:1, pp 79-89.

Zhou M. and Ngoi B.K.A. (2003), "Factors affecting form accuracy in diamond turning of optical components," *Journal of Materials Processing Technology*, Vol. 138, pp 586-589.

Zhou M., Ngoi B. K. A., Zhong Z. W. and Chin C. S. (2001), "Brittle-ductile transition in diamond cutting of silicon single crystals," *Materials and Manufacturing Processes*, Vol.16, No.4, pp 447-460.